Effect of viral early proteins, mutations and IL17F on the transcriptional activity of the Merkel cell polyomavirus promoter in different cell lines

Master Thesis in Medical Biology

MBI-3911

By

Ibrahim Afolabi Abdulsalam

Molecular Inflammation Research Group

Institute of Medical Biology

UiT-The Arctic University of Norway

May 2016

Acknowledgements

The work presented in this thesis was carried out during the period of January 2015 to May 2016 at the Molecular Inflammation Research Group (MIRG), Institute of Medical Biology, UiT- the Arctic University of Norway, under the supervision of Professor Ugo Lionel Moens and co-supervisor, Professor Baldur Sveinbjørnsson.

My profound and unending gratitude goes to the Creator, the Alpha and Omega for HIS oceanic and immeasurable mercies and favors on me right from my birth till present.

I dedicate this thesis to the memory of my late father, AbdulGaniyy A. Abdulsalam, late doctor, Franz Gruber, (your demise has been unforgettable and created a scar in my heart, you have both been inspirations in my life), the less privileged and martyrs who lost their lives while supporting the emancipation of their fellow human beings.

My sincere appreciation goes to my enviable supervisor, Professor Ugo Lionel Frida Anton Moens who has given me groundbreaking trainings, been a mentor and a RARE GEM. You have always been there for me, supporting me academically and morally at all times. Your door has always been opened to me at all times, I am overly grateful. To my co-supervisor supervisor, Professor Baldur Sveinbjørnsson, who has always updated me intellectually, my gratitude is unmeasurable.

I as well would appreciate members of MIRG: Prof. Dag Coucheron, Kashif, (my small Boss), who has been teaching me the basics of all experiments and contributed immensely to the success of this thesis with vital information at all times. Ketil, who inspires me with his motivational smiles and taught me how to use Graph pad prism. Conny and Aelita, who both motivated me at all times with lovely smiles and academism. Maria, who takes her time to make constructive criticism of my figures and poster, enabling me to get close to perfection. To Gianina who kept keeping an eye on my experimental procedures ensuring I strictly adhere to protocols and get best achievable results at all times. Igor, who I run to, for good pieces of advice from his vast range of expertise. Nanan and Brynja, your contributions are well appreciated. I am highly grateful.

I also would mention my fellow master's students, Micheal, Bryan and Betty, thanks for being lovely colleagues. I express gratitude to Prof Ingebryt Sylte, Dr Arinze, Clement Ajayi, Swapnil, Yakubu, Panos Dr Femi, Oluwatosin, Dare, Frank, Annas, Youkay and Elizbeth, your enormous support and contributions are unforgettable and appreciated.

To my Family, my Angelic mother, Mrs B.T Salam, mother in-law, Modinat Komolafe, my lovely siblings: Jubril, Sheriff, Moshood and Abdulrasheed, my uncles: Mr Lanre Tiamiyyu, Alhaj Fatih Salisu., Abdulsalam Tijani, my cousins: Demola, Djfussy, Mojisola, Abimbola, Teejay, Dammy, Ola- Baale, my lovely friends. Kazeem Ganiu, Qamar, Abiona, Basirat, Sherad, Wasii, Alaba, Lebraskee D and to The entire Ajetunmobi and Komolafe Family. Munirat Ololade (My Bae) and Maimunah Agbaje, thank you for all the words of encouragement you gave me all through.

Lastly to my INAMORATA and irreplaceable wife, Moriham Oluwadunmininu A. Abdulsalam, who painstakingly edited all diagrams and tables in this thesis as well as final arrangement of this write-up and the incarnation of my father and son Abdulghaniyy Modupeoluwa Abdulsalam. All the sacrifices you made resulted in attaining the acme of this thesis. You both are my strength and joy, without you two, I am meaningless.

Abdulsalam Ibrahim Afolabi

May, 2016.

Abstract

Merkel cell polyomavirus (MCPyV) is common in the human population with a seropositivity of approximately 60%. The virus is chronically shed from healthy skin, but the genuine host cell remains unknown and a permissive cell culture system is lacking. The viral genome is in an episomal state in cells where MCPyV has been found. The virus is not harmful in healthy individuals, but it is involved in the pathogenesis of Merkel cell carcinoma (MCC) in elderly and immunosuppressed individuals. Approximately 80% of all examined MCC specimens are MCPyV-positive. Two hallmarks of virus-positive MCCs are integrated viral genome and expression of truncated large T-antigen (tLT-ag). The non-coding control region (NCCR), encompassing the origin of replication and the promoter/enhancer controlling the expression of the early and late viral genes, of most MCPyV isolates are quasi identical to the reference strain MCC350. However, the NCCR of MCPyV isolated from healthy skin (strain 16b), feces (strain HB039C), and a Kaposi's sarcoma sample (strain TKS) is ~25 bp longer due to a repeated sequence. In this study the relative MCPyV promoter strength of variants MCC350 and 16b was compared in three different cell lines (HEK 293, MCC13 and C33A). The effect of the early proteins: large T antigen (LT-ag) and small t-antigen (st-ag) on promoter activity was examined. Our result demonstrated that early and late promoter strength of MCPyV16b variant is higher than that of MCC350 in HEK293 and MCC13 cells but similar in C33A cell. MCPyV LT-ag and st-ag regulated the expression of the viral promoter and the differences in promoter architecture affect their effect on transcriptional activity in a cell-dependent manner. Because expression of interleukin-17F (IL-17F), a pro-tumorigenic cytokine, is upregulated in MCPyV-positive MCC compared to MCPyV-negative MCC, we investigated the effect of LT-ag and st-ag on the IL-17F promoter, as well as the effect of IL-17F on the MCPyV promoter activity. MCPyV LT-ag stimulated the expression of IL-17F and vice versa, IL-17F enhanced the MCPyV promoter. In conclusion, mutations in the MCPyV promoter changes its activity and may affect cell tropism and virulence. The reciprocal interaction between IL-17 and MCPyV may contribute to the development of MCC.

Abbreviations

aa	Amino acids
ACT1	Adoptive cells transfer
ALTO	Alternative T antigen open reading frame
Amp	Ampicillin
ATPase	Adenosine triphosphatase
B cells	B lymphocytes
bp	Base pair
CCL	Chemokine ligand with two adjacent cysteines
CD	Cluster of differentiation (cell surface antigen)
cDNA	Complementary DNA
CH_3CO_2K	Potassium acetate
CNS	Central nervous system
COX	Cyclooxygenase
CXC	Chemokine
CXCL	Ligand of chemokine receptor
CXCR	Chemokine receptor
ddNTP	Dideoxynucleotide triphosphate/dideoxynucleotide
DNA	Deoxyribonucleic acid
dNTP	Deoxy nucleotide triphosphate/deoxynucleotide
dsDNA	Double stranded DNA
DTT	Dithiothreitol
EBV	Epstein –Barr virus
EDTA	Ethylene diamine tetraacetic acid
EGFP	Enhanced green fluorescent protein
Elk 1	Ets-like transcription factor 1
Fas-L	Ligand of the Fas death receptor
FBS	Fetal bovine serum
FLT-ag	Full length Large T antigen

Foxo3A	Forkhead box O3 A (transcription factor)
G-CSF	Granulocyte colony-stimulating factor
GM-CSF	Granulocyte macrophage colony stimulating factor
HBV	Hepatitis B virus
HCV	Hepatitis C virus
HHV8	Human Herpesvirus 8
HIF l	Hypoxia-inducible(transcription)factor 1
HPV	Human papillomavirus
HTLV1	Human T-cell lymphotropic virus type 1
IDO	Indoleamine 2,3-dioxygenase
IFN	Interferon
IFNy	Interferon gamma
IL	Interleukin
IκB	Inhibitor of NF-κB
JCPyV	JC polyomavirus
KSHV	Kaposi's sarcoma herpesvirus
LB	Lauria Bertani
LTag	Large Tumor antigen
MCC	Merkel cell carcinoma
MCPyV	Merkel cell polyomavirus
MDSC	Myeloid-derived suppressor cell
MHC	Major histocompatibility complex
MIRG	Molecular inflammation research group
miRNA	Micro RNA
MMP	Matrix metalloproteinase
mTOR	Mammalian target of rapamycin
NaOH	Sodium hydroxide
NCCR	Non-coding control region
NEMO	NF-κB essential modulator

NF-κB	Nuclear factor-kappa B
NK	Natural killer (Lymphocyte)
NKG2D	Natural killer group 2 member D
NOD	Nucleotide-binding oligomerization domain
p53	Tumor protein p53
PBS	Phosphate buffer Saline
PCR	Polymerase chain reaction
PD1	Programmed death1
PDL1	Programmed death ligand1
PIK3CD	Phosphatidylinositol 4,5-bisphosphate 3-kinase catalytic subunit delta isoform
pRB	Retinoblastoma protein
PSB	Protein solving Buffer
PSME3	Proteasome activator complex subunit3
RA	Rheumatoid arthritis
RAE1	Retinoic acid early inducible gamma 1 reading frame
RNA	Ribonucleic acid
SCF	Stem cell factor
SDS	Sodium dodecyl sulphate
SEFIR	Similar expression to fibroblast growth factor genes and IL-17Rs
SLE	Systemic lupus erythematosus
ssDNA	Single stranded DNA
ssRNA	Single stranded RNA
St-ag	Small tumor antigen
STAT3	Signal transducer and activator of transcription
T-cell	T lymphocytes
TGF	Tumor growth factor
TGFβ	Transforming growth factor beta
T_H17	T helper 17
TIL	Tumor infiltrating lymphocyte

TIM	Tumor infiltrating macrophages
Tim3	T cell immunoglobulin and mucin domain 3
TIR	Toll-interleukin receptor
TLR	Toll like receptor
tLTag	Truncated Large T antigen
TNF-α	Tumor necrosis factor alpha
TRAF-6	TNF receptor-associated factor 6
T-regs	Regulatory T cells
VEGF	Vascular endothelial growth factor

Table of Contents

1. INTRODUCTION

Cancer, is a major public health problem in many parts of the world and thus, a pandemic disease. Globally, cancers have been figured by the World health organization among the prominent causes of morbidity and mortality, with roughly 14 million recent incidents and 8.2 million deaths related to cancer in 2012. It is anticipated that within the next 2 decades, a rise in cancer incidents from 14 million in 2012 to 22 will occur annually [1].

Approximately 15% of cancer deaths are accounted for by cancer causing viral infections. Viruses associated with human cancer include hepatitis B virus (HBV), hepatitis C virus (HCV), human papillomaviruses (HPV), Epstein-Barr virus (EBV), human T-lymphotropic virus type 1 (HTLV-I), human herpes virus 8 or Kaposi's sarcoma-associated herpes virus (HHV8 or KSHV), and human polyomavirus Merkel cell polyomavirus (MCPyV). While HBV and HCV are associated with hepatocellular carcinoma, HPV is predominantly responsible for genital cancers, EBV for Burkitt's lymphoma and nasopharyngeal cancers, while HHV8 is the etiological factor for Kaposi's sarcoma. MCPyV is associated with approximately 80% of all Merkel cell carcinomas (MCC). Finally, human immunodeficiency virus is an indirect cause to cancer because this virus perturbs the host's immune system, leading to enhanced incidence of cancer [2-6].

1.1 History of Merkel cell polyomavirus

Merkel cells, originally described by Friedrich Sigmund in 1875, were believed to originate from the neural crest [7]. More recently, it was shown that they descended from the epidermal lineage [8, 9]. Merkel cells are found in the basal layer of the skin near the end of axons and the outer root sheet of hair follicles. They are located in touch sensitive areas of the skin epidermis, specifically the epidermal-dermal junction of the skin called stratum basale (Figure 1) [10]. Their function remains incompletely understood, but they act as mechano- or chemoreceptors [11, 12].

In 1972, Toker described an unusual form of skin cancer as trabecular carcinoma of the skin [13]. Later, this rare skin cancer was shown to derive from Merkel cells and this tumor type was renamed Merkel cell carcinoma (MCC) [14]. MCC has its clinical features summarized using the acronym “AEIOU”: **A**symptomatic, **E**xpanding rapidly (approximately 3 months or less), **I**mmune suppression, **O**lder than 50 years of age and **U**V-exposed site on a fair-skinned

person [15]. Using digital transcriptome subtraction, the group of Chang and Moore identified a novel virus present in 80% of all MCC [16].

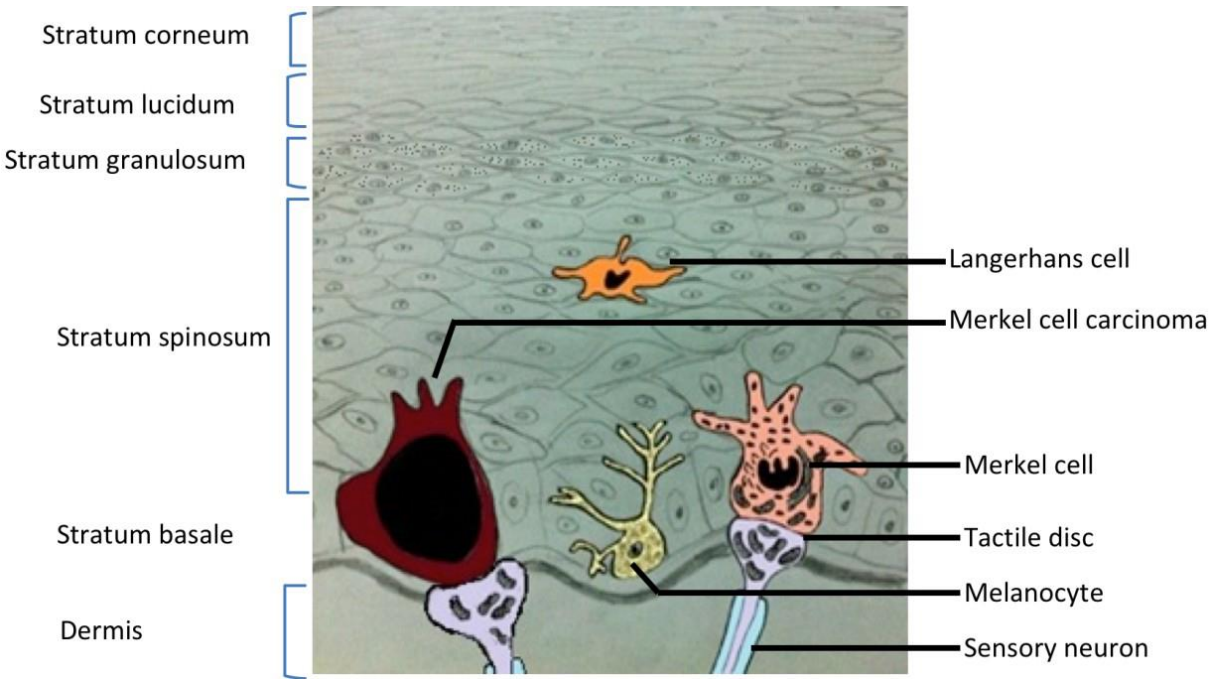

Figure 1. Diagram illustrating a cross-section of the skin with its layers. The skin is mainly composed of the epidermal and dermal layers. The epidermis is made up of Stratum corneum, stratum lucidum, stratum granulosum, stratum spinosum and stratum basale. Found dispersed and resident in the stratum basale include melanocyte and Merkel cell (normal and neoplastic) [10].

The virus was integrated in a clonal pattern, suggesting that integration preceded clonal expansion of the tumor cells. This new virus displayed high homology with other human polyomaviruses and was subsequently referred to a Merkel cell polyomavirus (MCPyV) [16].

1.2 MCPyV Seroprevalence and cell tropism

Serological studies have demonstrated that MCPyV is common in the human population. Anti-MCPyV antibodies have been reported in 37-85% of non MCC adult subjects [17 -19]. Exposure occurs in early childhood with seroprevalence of 20-40% in children aged 1-5 years, but the route of infection and transmission is not known, but virions seems to be continuously shed from the skin [17,20]. Its seropositivity has also been seen to increase with age (Figure 2) [21]. MCPyV does not only infect Merkel cells. Besides its skin tropism, viral DNA and

proteins have also been detected in blood, gall bladder, appendix, liver, lung, tonsils, lymphoid and intestine tissue, and cervical specimens of healthy individuals [reviewed in 22- 25].

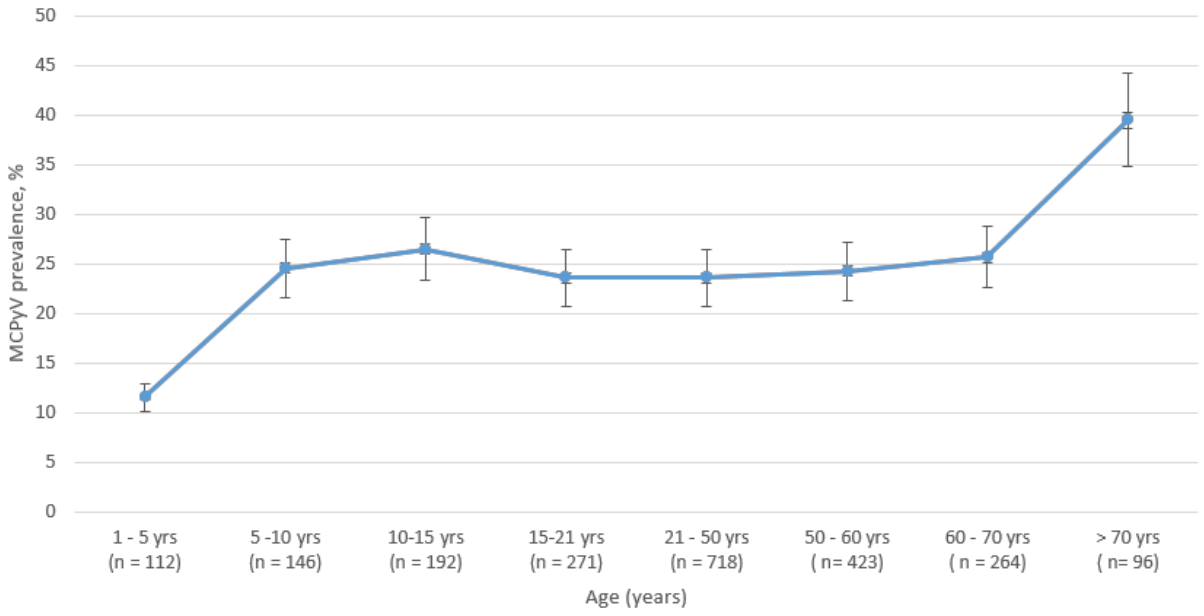

Figure 2. MCC350 MCPyV age-specific seroprevalence in a study population of humans in Denver, USA. Standard error bars are shown. Modified from [21].

1.3 MCPyV and other cancers

Viral sequences have also been found in other tumors, including porocarcinoma (malignant neoplasm from the intraepidermal ductal portion of the eccrine sweat glands) [26], esophageal squamous cell carcinomas [27], oral squamous cell carcinomas [28], tonsillar tumors [25], parotid small cell carcinoma [29], Kaposi's sarcoma [30, 31], CNS tumors [32], non-small cell lung cancer [33], cervical squamous cell carcinomas [23], and chronic lymphocytic leukemia [34]. However, immunohistochemical studies on 1,184 tumor samples of 12 different organs (lung, oral cavity, stomach, colon, bladder, kidney, skin (not MCC), breast, brain, mesothelium, and non-Hodgkin's lymphoma) were all negative for MCPyV proteins [35].

1.4 Molecular biology of MCPyV

MCPyV has the typical characteristics of polyomaviruses. It is a non-enveloped virus with an icosahedral capsid of about 50-55 nm surrounding a circular dsDNA genome [36]. The viral genome can be divided into three functional regions (Figure 3) [10]. The early region is

expressed early in infection and codes for large T-antigen (LT-ag), small t-antigen (st-ag), a 57K protein and an ALTO protein (Figure 4; [37, 38]).

LT-ag regulates viral DNA replication as well as transcription of the viral genes. The former function requires the ATPase/helicase activity of LT-ag, its ability to bind viral DNA, and the interaction with proteins of the cellular DNA replication machinery. The role of st-ag is less understood, but it plays an auxiliary role for LT-ag in viral replication and virion production [39-43]. Both LT-ag and st-ag have oncogenic properties in cell culture and animal models [44-54].

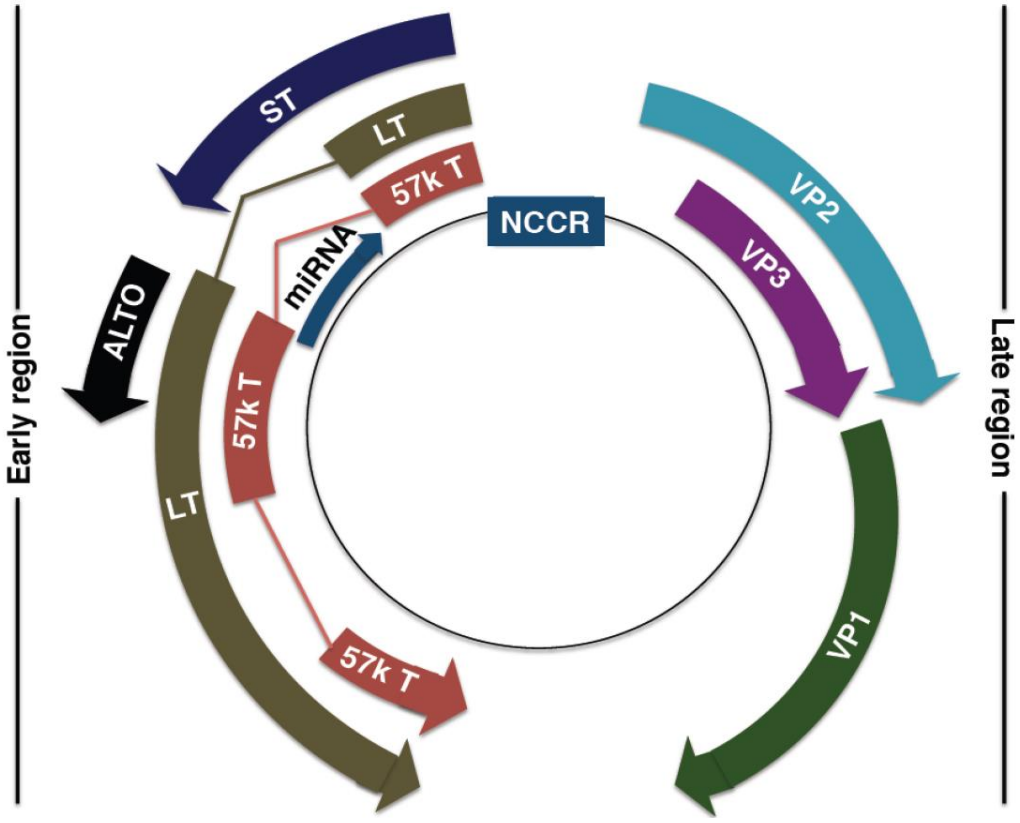

Figure 3. Schematic diagram illustrating the genomic organization of the Merkel polyomavirus. The early region encodes Large T-ag and small t-ag, 57kT antigen (57kT), microRNA (miRNA), alternative T antigen open reading frame (ALTO) while the capsid proteins VP1-3 are encoded by the late region. The bi-directional Non-coding control (NCCR) partitions the early and late regions and serves as the origin of replication and viral gene promoter [10].

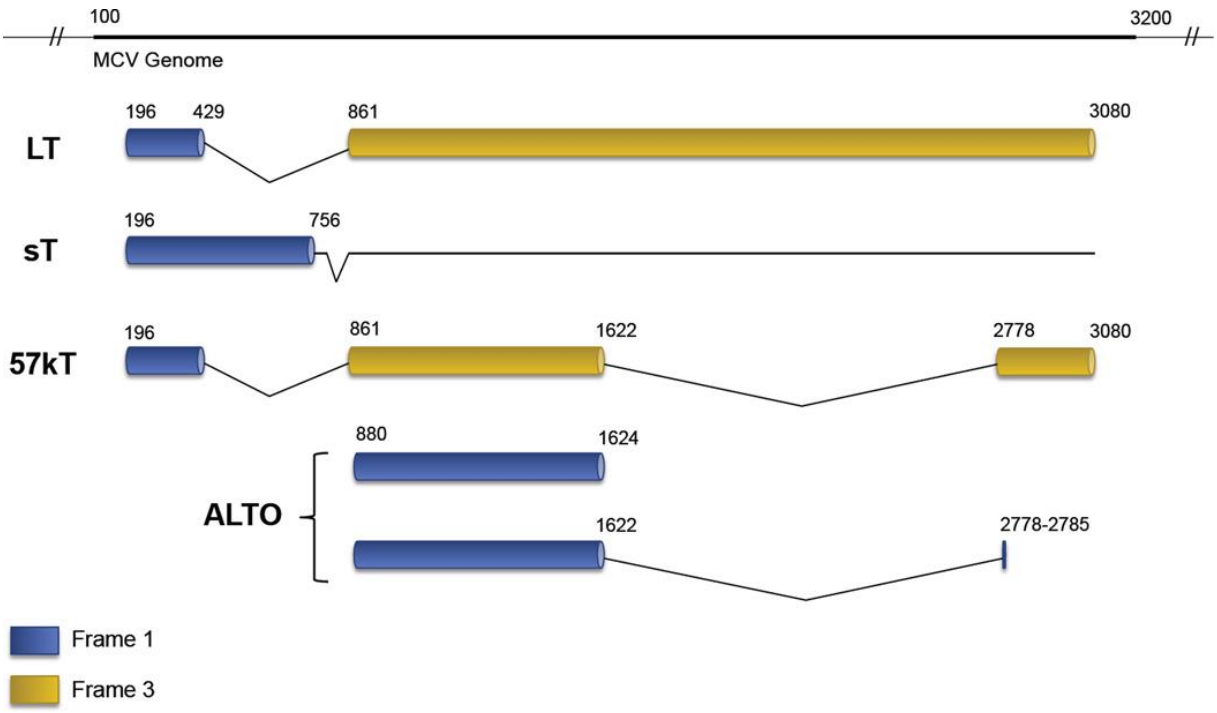

Figure 4. Gene products encoded by the early gene region. Expression of several gene products from the early coding region of the MCPyV genome occurs as a consequence of alternative splicing of RNA transcripts. For each gene product, their respective splicing pattern are illustrated. MCPyV mainly expresses three T antigens represented as LT, sT and 57kT, and among them a common first exon sequence is shared. An alternate frame of the LT open reading frame (ALTO) +1- switched proportionately to the second exon of LT [37, 38].

The LT-ag and st-ag can interact with several cellular proteins and several of these interactions contribute to the oncogenic properties of these viral proteins (Table 1). The function of the 57KT protein remains elusive, while the role of ALTO is incompletely understood, but it does not appear to be essential for viral genome replication because an ALTO deficient mutant replicates with comparable levels as wild-type virus [37].

Table 1.1: Cellular interaction partners of MCPyV LT-ag and st-ag.

cellular protein	Viral protein	Biological relevance	reference
ATM kinase	LT-ag	Ser-816 phosphorylation contributes to a mechanism that inhibits cell proliferation by inducing cell death	[55]
Hsp70	LT-ag, st-ag	Viral DNA replication, disruption pRB-E2F complex	[39] [56]
pRb	LT-ag	S phase cell cycle progression	[57] [49] [58]
hVam6p/Vps39	LT-ag	Viral egress	[59]

			[40]
Brd4	LT-ag	Enhances viral DNA replication	[60]
Cdc20	st-ag	Sustain cap-dependent translation during mitosis	[61]
Cdh1	st-ag	Sustain cap-dependent translation during mitosis	[62]
E4-BP1	st-ag	Sustain cap-dependent translation during mitosis; promote Ser-65 hyperphosphorylation of E4-BP1	[44] [61] [62]
Nemo/IKKγ	st-ag	Inhibit NFκB-mediated transcription	[63]
PP2A	st-ag	Inhibition NFκB signaling; transforming activity	[44] [63] [64]
PP4C	st-ag	Inhibition NFκB signaling	[63]
Fbw7	st-ag	Prevents proteasomal degradation of LT-ag; stimulation of viral replication	[65]
Usp7	LT-ag	Stabilization of LT-ag	[66]
Kap1/TRIM28	LT-ag, st-ag	Restricts MCPyV replication by preventing LT-ag binding to origin of replication	[67]
p53	LT-ag (FLT-ag)	Cell cycle progression and interference with DNA repair,p53-mediated transcription, and apoptosis	[49]

The late region encodes the major capsid protein VP1 and the minor capsid protein VP2, while the other minor protein VP3, which is present in other polyomaviruses, is lacking [68]. The late region also encodes a 22-nucleotide-long microRNA (miRNA), MCV-miR-M1-5p. The miRNA is encoded antisense to the LT-ag coding region and reduces the levels of early gene transcripts [69]. Its role in cellular transformation is not known, but miR-M1-5p can be detected in about half of MCPyV-positive MCC tumors [70]. When present, MCPyV miRNA levels were <0.025% of total miRNA levels [70, 71]. These observations suggest that miR-M1-5p is not involved in development of MCC.

Interspersed between the early and late region lies the non-coding control region (NCCR). This region contains the origin of replication with binding motifs for LT-ag (5'-GAGGC-3') and the transcription control region directing the transcription of the early and late genes [39]. The transcriptional control region contains putative binding sites for cellular transcription factors, but their participation in transcription of the early and late genes remains to be proven.

The MCPyV genome is integrated in Merkel cell carcinoma cells, but episomal in other cell types. Another hallmark of MCPyV positive MCCs is that they express a C-terminal truncated

form of the LT-ag. Truncation removes the p53 binding site, the ATPase and helicase activity, and the DNA binding domain of the protein (Figure 5). This shorter form of LT-ag is unable to support viral replication [57].

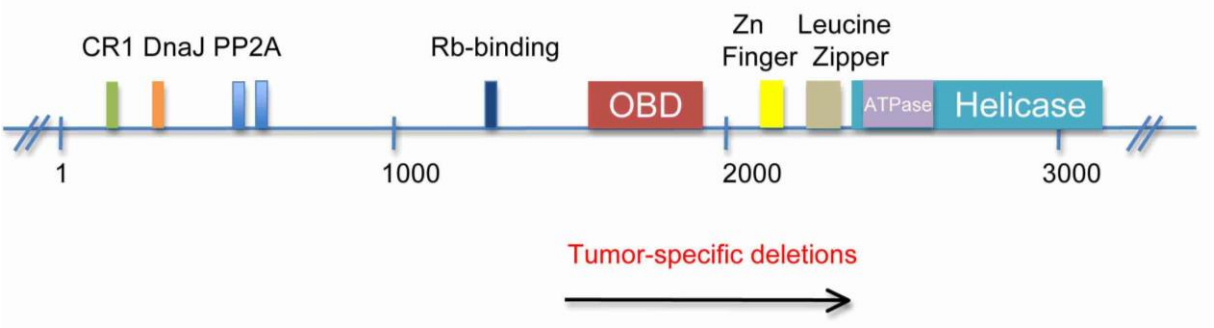

Figure 5. Transcript mapping of the multiple spliced MCPyV T antigen locus. Three T antigens are identified as Large T, small T and 57KT. All four transcripts encode CR1 (green, LXXLL) and DnaJ (orange, HPDKGG) domains. ST proteins contain two PP2A binding motifs (blue, CXCXXC). Rb binding (dark blue, LXCXE) domain are conserved in Large T and 57KT. Large T contains unique domains including origin binding (red), zinc finger (yellow), leucine zipper (blue), and helicase (cyan)/ATPase (purple). [57]

It is not known whether the non-sense mutations generating these truncated forms in MCC occur prior or after integration of the viral DNA in the host cell genome (Figure 6) [10]. It is believed that MCPyV-induced oncogenesis often requires the virus to become replication-defective, allowing cellular proliferation [10, 3].

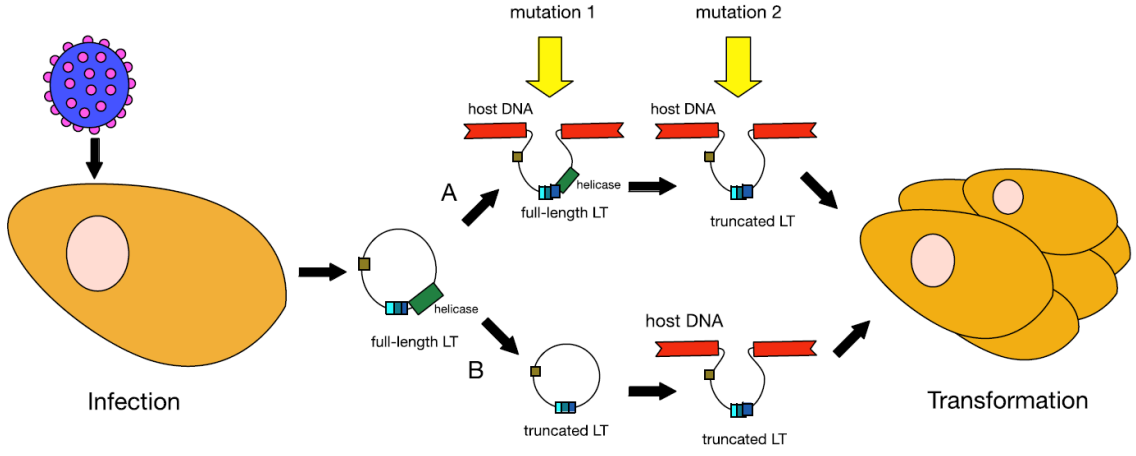

Figure 6. Models for MCPyV-driven MCC oncogenesis. Majority hypothesizes occurrence of early childhood infection by MCPyV. Loss of immunosurveilance enhances viral proliferation and a consequential increased susceptibility to carcinogenesis. Transformation of cells by MCPyV requires two mutations. Model A assumes a Full-length viral genome integration into host DNA to be the first mutation while the LT-ag truncation is the second mutation. LT-ag truncation prior to integration is

presumed in Model B. Both Models lead to transformation and proliferation of cells and tumor respectively [10].

Infectious entry into transformed melanocyte and human skin- derived primary keratinocytes is seen to be exhibited by MCPyV pseudovirions, but in primary melanocytes and primary transformed keratinocytes (HaCaT), MCPyV infection was not permitted. Additionally, of all the 60 human tumor cell lines studied, none expressed tropism for MCPyV. In human embryonic kidney cell-derived cultures (HEK-293), MCPyV propagation is possible and this cell line is currently used in studying MCPyV life cycle [10].

1.5 Inflammation

A basic component of the body's response to external and internal environmental stimuli is formed by inflammation, which typically annihilate the aggressor agent and resuscitate the tissue physiology; serving as a mode of ''counter attack'' [72]. Inflammation is triggered as an adaptive response by noxious stimuli such as tissue injury and infection, and is aimed at restoring homeostasis [73].

A characteristic inflammatory response comprises of four elements, namely; inflammatory inducers, sensors that recognize them, the inflammatory mediators which the sensors induce, and the target tissues on which the inflammatory mediators express their effects (Figure 7) [74]. Each part comes in myriad forms and their aggregation functions in definite inflammatory pathways. The nature of the inflammatory inducer is dependent on the type of pathway initiated under a specific condition [74]. Infection or tissue injury induces acute inflammatory responses which involves a transmission of blood components (leukocytes and plasma) to the sites of injury or infection in a regulated fashion [75, 76]. This response has been well characterized for microbial (specifically bacterial) infection, whereby Toll-like receptors (TLRs) and NOD (nucleotide-binding oligomerization-domain protein) - like receptors (NLRs), which are receptors of the innate immune system, trigger such response [77]. These receptors (TLRs) are expressed on tissue-resident macrophages and initiate the synthesis of chemokines (CCL2 and CXCL8), pro-inflammatory cytokines (TNFα, IL-1, and IL-6) and prostaglandins. On target tissues which include local blood vessels, these inflammatory mediators elicit their actions such as vasodilation, mobilization and infiltration of leukocytes at the site of infection. These recruited leukocytes seek and eradicate invading pathogens [74]. Depending on the pathogen causing infection, (bacterial, viral or parasitic) the sensors, mediators and target tissues differ

in such that the relevant type of inflammatory response is triggered. For instance, virus infected cells produce type-I interferons (IFNα and IFNβ) and cytotoxic lymphocytes are activated as a result of a triggering effect elicited by the viral infection [74].

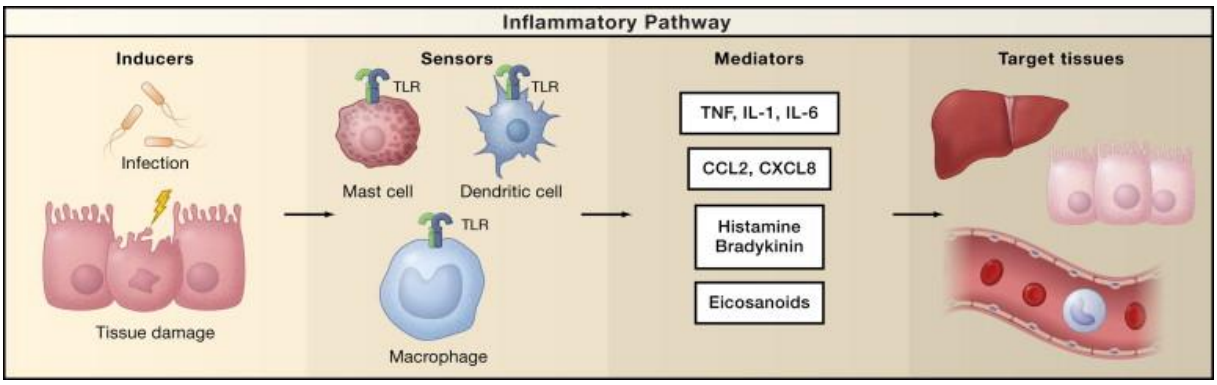

Figure 7. Components of the inflammatory pathway. Inducers, sensors, mediators and target tissues make up the inflammatory pathway. Inflammatory responses are initiated by the inducers. Receptors such as toll-like receptor (TLRs) expressed on macrophages, mast and dendritic cells which are specialized sentinel cells are examples of inflammatory sensors. They trigger the synthesis of mediators such as chemokines, bioactive amines, cytokines, and eicosanoids. On several target tissues these inflammatory mediators act, to evoke changes in their functional state that enhance adaptation to the noxious condition (tissue injury or infection) correlating with the specific inducers that evoked the inflammatory response. The diagram shows a representation of a small sample of the several types of distinct sensors, inducers, mediators and target tissues implicated in the inflammatory response [74]

This acute inflammatory response is maintained for a short period, having therapeutic consequences involving the elimination of the infectious agents which is ensued by a resolution and repair phase. However, if the pathogen and infection persists without being eliminated by the acute inflammatory response, the inflammatory process becomes chronic and acquire new characteristics [72, 73].

1.6 Inflammation and cancer

Chronic inflammation is veritably implicated in various pathologies such as diabetes, rheumatoid arthritis, lung diseases, autoimmune disorders, cardiovascular disease Alzheimer's and cancer [72]. Inflammation enhances tumor cells to acquire other characteristics, because it provides the tumor microenvironments with pro-angiogenic factors, growth factors, enzymes, survival factors, amongst others which are bioactive molecules that contribute to extracellular matrix (ECM) modification [78,79]. Thus, inflammation via its mediators is able to orchestrate

the tumor microenvironment, thereby contributing to cancer progression via angiogenesis, invasion and metastasis, adaptive immune evasion, proliferation, alteration of responses to chemotherapeutic agents and hormones [80].

Inflammatory molecules such as cytokines and chemokines, play essential roles both in the immunopathology associated with several viral diseases and host response to viral infections. Direct stimulation of cells to produce chemokines and cytokines is initiated by interactions between cellular receptors and several glycoproteins. The NF-κB pathway amongst other signaling pathways appears to perform specifically vital functions as far as cytokine and chemokine expression is concerned [81].

1.7 Cytokines as mediators involved in cancer and inflammation

Cytokines comprise of a group of signaling molecules that are central to pivotal inflammatory and immune responses. Cytokines are released in response to injuries caused by inflammation, carcinogens and infection. At inception, their role is to subside the damage and stimulate tissue repair, but in chronic diseases, their incessant secretion will promote the formation and progression of tumor [72]. Stromal and immune cells produce cytokines in response to signals released by neighboring cells, or by the tumor cells themselves, as a component of the inflammatory process and hypoxic states which characterize tumor growth [82, 83].

Cytokines are divided into subgroups, namely: chemokines, interleukins, growth factors, tumor growth factor (TGF), colony stimulating factors, interferon (IFN) and tumor necrosis factor (TNF). They can be further classified as anti-inflammatory and pro-inflammatory. Anti-inflammatory cytokines include, IL-4, IL-10, IL-13, IFNγ, transforming growth factor beta (TGFβ), while the pro-inflammatory cytokines comprise IL-1, IL-6, IL-15, IL-17, IL-23, and TNFα [71]. Many of these cytokines have been implicated in human virus-induced oncogenesis such as human papillomaviruses [84], HBV [85], EBV, HCV and HTLV-1[86].

1.8 Interleukin-17

Interleukin-17 (IL-17) is a pro-inflammatory cytokine that performs vital roles in host defense against infections and inflammation. Nevertheless, excessive secretion of IL-17 promotes chronic inflammation associated with several autoimmune and inflammatory diseases such as psoriasis, rheumatoid arthritis (RA), multiple sclerosis, asthma, and systemic lupus

erythematosus (SLE). Thus, IL-17 elicits a pleiotropic effect on various cell types [87]. The earliest bioactivity of human IL-17 was described in its effect both on synoviocytes from RA patients and on normal skin fibroblasts from RA-free persons, indicating IL-17 could initiate IL-6 and IL-8 production [88]. IL-17 is majorly produced by a lineage of T cells referred to as T helper 17 cells (T_H17 cells) [89]

The IL-17 cytokine family consists of six members and includes IL-17A (frequently referred to as IL-17), IL-17B, IL-17C, IL-17D, IL-17E (also called IL-25) and IL-17F. IL-17A and IL-17F have their biological roles and regulation well understood among other members of the IL-17 family and are the closest members sharing the highest sequence homology. Both are produced as homodimers (IL-17A and IL-17F) and as IL-17A/F heterodimers [87, 90].

IL- 17 cytokines bind to a family of cytokine receptor referred to as IL-17R which consists of five subunits: IL-17RA, IL-17RB, IL-17RC, IL-17RD and IL-17RE. IL-17A and IL-17F homodimers as well as IL-17A/F heterodimer bind the same receptor complex consisting IL-17RA, and IL-17RC subunits [91, 92].

1.9 Interleukin-17 receptor signaling

All Interleukin-17 receptors (IL-17R) possess a sole transmembrane domain and the 17RA/RC complex binding by IL-17A (and/or IL-17F) mobilizes the ubiquitin ligase and adaptor protein ACT1 (also known as TRAF3IP2) via a conserved motif SEF/IL-17R (SEFIR) domain and a homologous TOLL/IL-1R (TIR) domain. [91, 93]. TNF receptor-associated factor 6 (TRAF6) is recruited by ACT1 and this induces the stimulation of NF-κB (Figure 8A) [87, 93] and the mitogen–activated protein kinase pathways [87]. Such stimulation, upregulates expression of several inflammatory genes, specifically the neutrophil specific CXC chemokines [87, 93].

1.10 Interleukin-17 and Inflammation

The action of IL-17A and IL-17F on several isolated human and mice cells such as endothelial cells, fibroblast, osteocytes, macrophages and chondrocytes can upregulate monocytes secretion of pro-inflammatory cytokines (TNFα, IL-6, G-CSF, IL-1β, granulocyte-macrophage colony–stimulating factor (GM-CSF)). IL-17 solely is usually inadequately active, but in synergism with other inflammatory cytokines such as IL-22, GM-CSF, IL-1β, and IFNγ can

result in an enhanced synthesis of inflammatory mediators such as IL-6 and IL-8 [87, 93]. Figures 8A and 8B gives a diagrammatic illustration of IL-17 roles in inflammation.

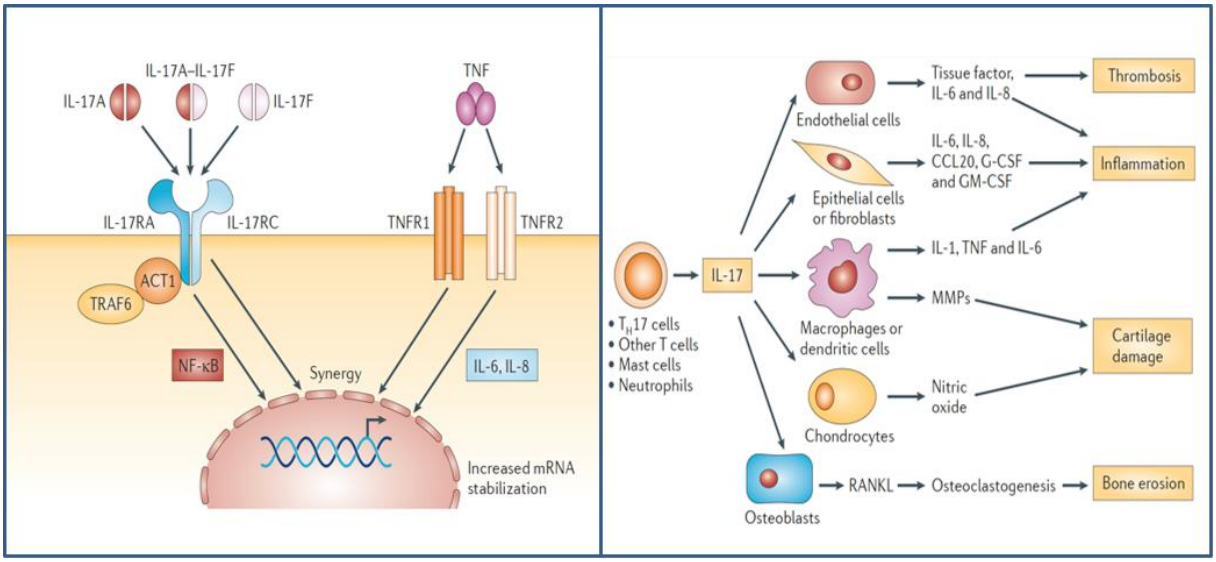

8A **8B**

Figures 8A and 8B

8A. IL-17 structure and interaction with IL-17R. The IL-17R complex which is made up of IL-17RA and IL-17RC subunits are bond to by dimeric ligands formed by IL-17A and IL-17F. ACT1, TRAF6 and NF-κB stimulation is triggered by signals from the receptor, resulting to an enhanced transcription of IL-6 and IL-8 gene. TNF, a homotrimer, elicits its effect on its receptors, TNFR1 and TNFR2. A synergistic activity results from the combination of TNF and IL-17 ligands, which can be partly described by increased stability and overexpression of mRNA and TNFR respectively [93].

8B. IL-17 central functions and its actions in inflammation and matrix annihilation**.** On several cellular targets, IL-17 acts resulting in cell activation. IL-17 action on endothelial cells evokes pro-coagulant activity and inflammation. On epithelial cells and fibroblasts, IL-17 provokes enzyme and cytokine secretion, when acting on monocytes and dendritic cells, it promotes inflammation by enhancing pro-inflammatory cytokine production. In the situation of joint inflammation, a process involving chondrocytes and osteocytes, IL-17 triggers destruction of matrix in bone and cartilage [92].

1.11 Interleukin 17 and cancer

Several studies have convincingly shown that IL-17 plays a complex role in the pathophysiology of cancer, from carcinogenesis, proliferation, angiogenesis and metastasis, to tumor adaptation in its capabilities to bestow upon itself resistance against chemotherapy and immune attack [94]. Figure 9 gives a synopsis of the mechanisms via which IL-17 promotes the aforementioned hallmarks of cancer.

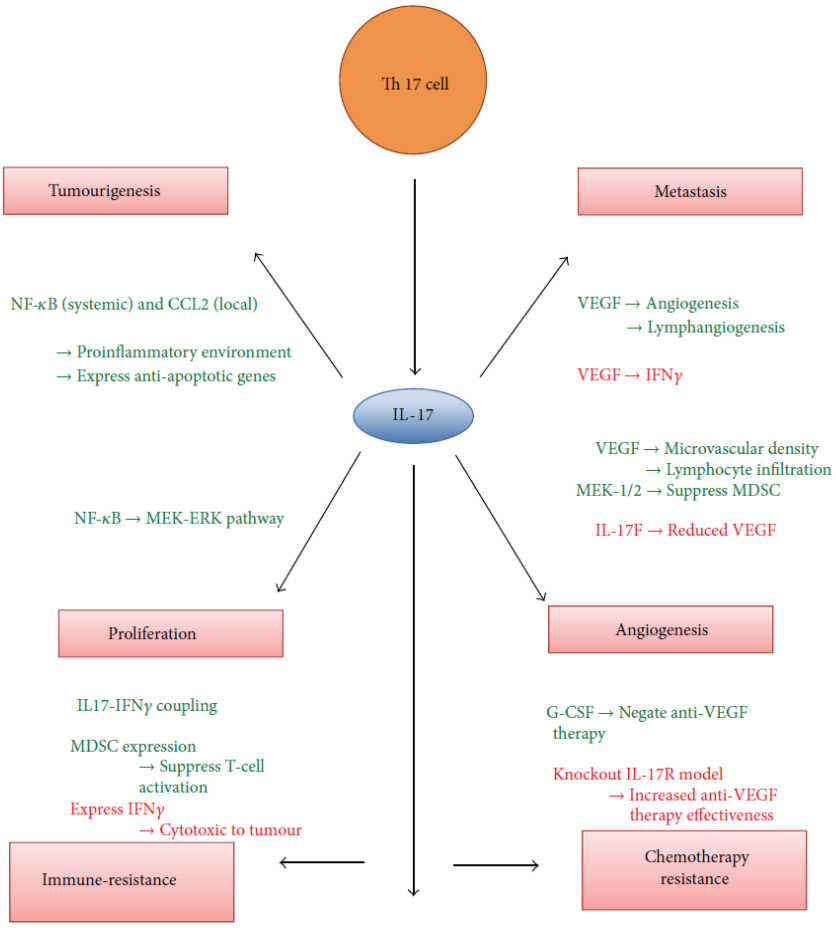

Figure 9. Diagram outlining the investigated mechanisms via which IL17 initiates (green) or downregulates (red) several aspects of cancer pathogenesis. IL-17: interleukin 17; VEGF: vascular endothelial growth factor; NF-κB: nuclear factor kappa-light-chain-enhancer of activated B cells; CCL2: Chemokine (C-C motif) ligand 2; IFNγ: interferons γ; G-CSF: granulocyte colony stimulating factor [94].

Since IL-17 can induce the production of cytokines such as IL-6 and IL-8 [88], it indirectly contributes to cancer progression as these cytokines have been shown to play key roles during carcinogenesis via various pathways [72].

1.12 Inflammation and oncoviruses.

Besides triggering these tumorigenic processes, inflammation may also contribute to virus-induced cancer. Inflammatory molecules may expedite viral infection and debilitate immune defense mechanisms, while viruses, possibly via a prolonged secretion of pro-inflammatory molecules, stimulate inflammation [78, 79].

1.13 Role of inflammation in MCC (virus positive and virus negative)

The interaction between cancer and inflammation has been described to occur via two pathways: an extrinsic, which involves the facilitation of cancer development by inflammatory conditions (by secreting mediators for instance), and an intrinsic pathway, where the inflammatory process is enhanced by genetic modifications/mutations that induce the secretion of inflammatory mediators by tumor cells, hence, promoting the formation of a microenvironments that supports tumorigenesis. As a result, irrespective of the tumor origin, inflammatory cells are also recruited to the tumor, where they continue to support the inflammation milieu and the progressive tumor growth [72, 80]. Figure 10 summarizes the molecular pathways linking inflammation and cancer [80].

An inflammatory microenvironment can be induced in certain types of cancer and chronic inflammation frequently promotes cancer development. This cancer-related inflammation, in addition to enhancing tumor aggressiveness, also promotes cancer immune evasion [72]. This phenomenon is observed in Merkel cell carcinoma (MCC) [95].

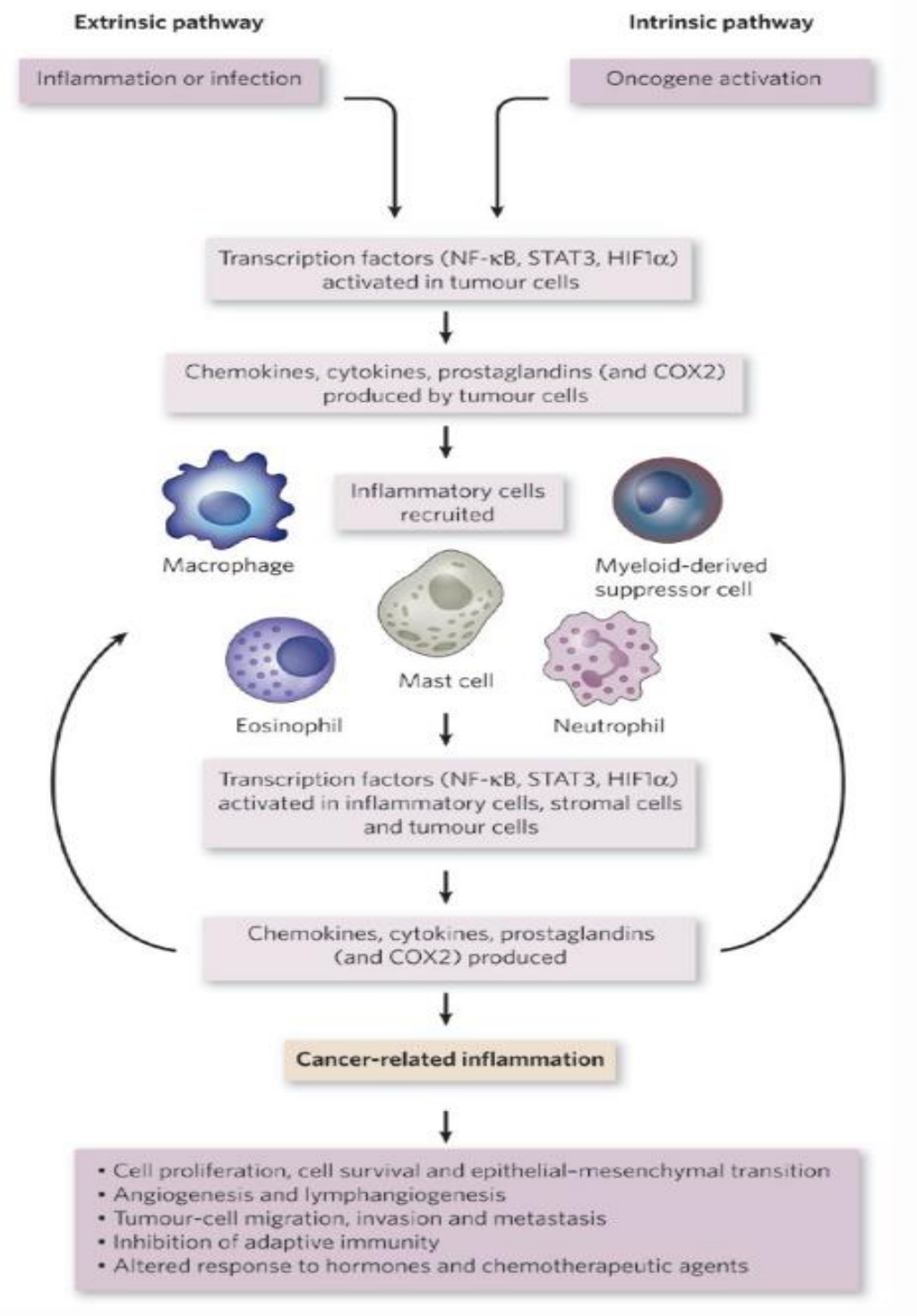

Figure 10. Molecular pathways connecting inflammation and cancer. The intrinsic and extrinsic pathways have been identified as the main affluence to the inflammatory environment: the intrinsic one, involving genetic changes (e.g. oncogenes) initiating neoplastic transformation induces the inflammatory process and the extrinsic pathway where chronic inflammation (e.g. infection, carcinogens and other environmental factors), substantially escalates the risk for different cancer types. The convergence of both pathways leads to the upregulation of transcription factors (e.g. NF-κB, STAT3) which regulate the production of various inflammatory mediators and the stimulation of several leukocytes creating a cancer-related inflammatory micro-environment [80].

1.14 Inflammation promotes MCC tumorigenesis and immune evasion

In MCC, various inflammatory modulators have been identified to be required for immune surveillance evasion by tumors, thus, establishing MCPyV's contribution in tumorigenesis. A number of disparate groups have investigated immune cells and inflammatory mediators associated with virus-positive and virus-negative MCC. Table 2 gives a synopsis of the variations in immune and inflammatory cells, markers and expression of genes investigated in both MCPyV-positive and MCPyV-negative MCC tumors. A higher number of infiltrating CD8+ T-cells, CD16+ natural killer cells, CD3+ T-cells, CD20+ B cells, macrophages (specifically CD68+, CD69+ and CD163+) have been observed in MCPyV-positive MCC relative to MCPyV-negative MCC tumors. In 4/4 LT-ag positive MCC and 3/6 LT-ag negative tumors, FoxP3+ regulatory T-cells were observed to be present and absent respectively [95].

Table 1.2: Immune cells and inflammatory mediators associated with Merkel cell carcinoma (MCPyV-positive and MCPyV-negative MCC) [95].

Component	**MCPyV-positive *versus* MCPyV-negative MCC**
Cells in tumor microenvironment	
-CD3+ T-cells	higher number in MCPyV-positive MCC
-CD4+ T-cells	high number associated with high LT-ag expression
-CD8+ T-cells	higher number in MCPyV-positive MCC
- CD16+ natural killer cell	higher number in MCPyV-positive MCC
-CD20+ B cells	more common in MCPyV-positive MCC; no significant difference between MCPyV-positive and – negative MCC
-CD68+ macrophages	higher number in MCPyV-positive MCC
-CD69+ macrophages	higher number in MCPyV-positive MCC
-FoxP3+ regulatory T-cells	more common in MCPyV-positive MCC
Cell surface markers:	
-CD3D	enrichment of transcripts in MCPyV-positive MCC
-CD3G	enrichment of transcripts in MCPyV-positive MCC
-CXCR3	lacking in CD8+ T-cells

-MHC-I	lower levels in MCPyV-positive MCC
-PD1	higher in MCPyV-positive MCC
-Tim-3	higher in MCPyV-positive MCC
Signal transduction proteins	
-NF-κB levels	lower in MCPyV-positive MCC
-IκB levels	lower in MCPyV-positive MCC
-TANK	reduction in MCPyV st-ag expressing cells MCC13 cells compared to virus-negative cells
- ZAP70	enrichment of transcripts in MCPyV-positive MCC
Cytokines/chemokines	
-CCL20	reduction in MCPyV st-ag expressing cells MCC13 cells compared to virus-negative cells
-CXCL-9	reduction in MCPyV st-ag expressing cells MCC13 cells compared to virus-negative cells
-IL-2	reduction in MCPyV st-ag expressing cells MCC13 cells compared to virus-negative cells
-IL-8	reduction in MCPyV st-ag expressing cells MCC13 cells compared to virus-negative cells
-Prokineticin 1 mRNA	higher in MCPyV-negative MCC
-Prokineticin 2 mRNA	higher in MCPyV-positive MCC
Other differentially expressed proteins	
-granzyme B (role in apoptosis)	Expression was rare in CD8+ cells

1.15 Immune evasion mechanisms in Virus positive-MCC

Several mechanisms via which MCPyV and MCC tumors circumvent attack and recognition by the immune system have been reviewed. The significance of the innate immunity as a shield against microbial invasion is obvious and has been well emphasized, but pathogens are still able to devise several mechanisms aimed at overwhelming it. The responses of the MCPyV in subverting attacks from the host's innate defense mechanism in order to establish a primary and chronic viral infection has been made evident by recent studies [10].

1.15.1 Evasion via expression of MCPyV early and late proteins

The small t-antigen (st-ag) of MCPyV interacts with NF-κB essential modulator (NEMO, also known as IKKγ) to evoke the down-regulation of NF-κB-mediated transcription of NF-κB target genes listed in Table 1 (e,g. IL-2, IL-8, IκB CXCL9, MHC-I) [10, 95]. The expression of MCPyV early proteins (LT-ag and st-ag) negatively regulates toll-like receptor 9, (TLR9) a vital receptor and intracellular viral DNA immune sensor which recognizes viral double-stranded DNA (dsDNA) in epithelial and MCC cells [95]. The consequences of MCPyV early protein expression is a repression of the innate immune response and enabled persistence of the virus in the infected cell [10, 95]. Additionally, PIK3CD/p110δ and PSME3, which are proteins associated with immune functions, have been prognosticated to be hypothetic targets for MCPyV miRNA. PIK3CD expresses a unique function in antigen receptor signaling via B-cell proliferation and T-cells activation, while PSME3 is a proteosomal subunit important for production of peptides presented to MHC I [95].

1.15.2 Evasion via altered expression of cell surface markers on MCC cells

In the tumor environment of polyomavirus-induced tumors, existing tumor-infiltrating macrophages express pro-inflammatory cytokines such as TNF, IL-1α, IL-33, and IL-1β which all inhibit the expression of RAE-1, consequently reducing the susceptibility of these tumors to natural killer (NK) cell-regulated cytotoxicity. The killing of polyomavirus-induced tumor cells by NK cells particularly requires the interaction between RAE-1 and NKG2D, where the latter is an activating receptor expressed on NK cells and the former is a surface expressed NKG2D ligand by tumor cells transformed by polyomaviruses [96].

Expression of the immunosuppressive PDL-1 (programmed death ligand -1) was shown by Evan *et al* in the microenvironment of approximately 50% of virus positive MCC tumors, on various cell types (macrophages, tumor cells, lymphocytes). Furthermore, traits of geographic tumor infiltrating lymphocytes (TIL) and tumor cells expressing PDL-1 co-localizations, indicate that cytokine production by immune cells that are responsive to tumor, possibly enhances the expression of PDL-1 to protect tumor cells from immune attack via a negative feedback loop [97]. It was further observed that T cells specific to MCPyV, co-express T-cell immunoglobulin and mucin domain-3 (Tim-3) and programmed death-1 (PD-1), which are markers of exhaustion, at extremely high levels when compared with that expressed by T cells specific for other prevalent human viruses. Additionally, within the tumor microenvironment of MCC, the MCPyV-specific T cells expressing PD-1 would likely be encountered by the inhibitory receptor ligand, PDL-1, thus inhibiting T-cell response and permitting tumor progression [98]. It has been predicted that IFN-γ may trigger PD-L1 expression without excluding interleukins like IL-6, IL-10, IL-17 and IL-21 [95].

T-cell responses are also inhibited by T-cell immunoglobulin and mucin domain-3 (Tim-3), a cell-surface protein which is positively upregulated on infiltrating T-cells in MCPyV-positive MCC [95]. Simultaneous co-expression of Tim-3 and PD-1 (exhaustion markers) in a higher number of T cells specific for MCPyV in blood and MCC infiltrating lymphocytes, gives a combination that is frequently involved in chronic antigen exposure as well as reversible T-cell malfunction [99, 100]. The expression of these markers signify a characteristic exhaustion of T cells instead of T cell activation, as illustrated by Figure 11. Transmission of inhibitory signals as well as repression of T cell proliferation resulted in interaction between PD-1 receptor and PDL-1 ligand to form the PD-1/PDL-1 inhibitory receptor-ligand complex [101].

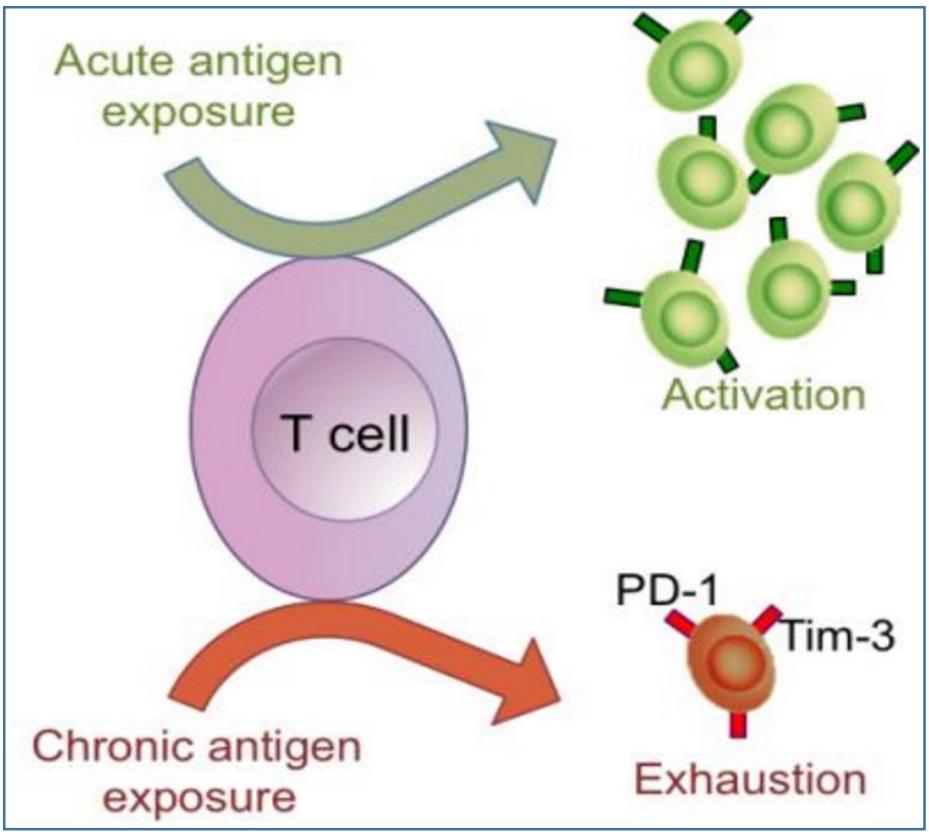

Figure 11. Diagram illustrating effects of acute and chronic exposure of antigen to T-cell. T cells are activated by acute exposure to antigen while PD-1 and Tim-3 which are markers of T cell exhaustion are expressed by T cells on chronic exposure to antigens in MCC tumors. These markers PD-I and Tim-3 exert inhibitory effects on T cells and possibly demonstrates immune escape by the Merkel Cell Cancer [101].

1.15.3 Evasion via establishment of a local immunosuppressive micro-environment by MCC cells

In MCC tumor, excessive production of T-cell response inhibitors like indoleamine 2,3-dioxygenase (IDO) and galectin-1 as well as immunosuppressive cytokines which include IL-10, TGF-β, Fas-L by immunologically transformed cells occur. Pro-inflammatory danger signals could also be suppressed by the tumor via STAT3-activated pathways causing a debilitated maturation of dendritic cells. The production and stimulation of Myeloid-derived suppressor cells (MDSC) and CD4+CD25+ regulatory T cells (T-regs), which are immunosuppressive cells may be facilitated by tumor cells [102].

MCC tumors can impede lymphocyte invasion by evoking an extremely reduced and insignificant infiltration of CD8+ T cells as well as a decline of E-selectin-positive vessels within the tumor microenvironment [95, 103]. Expression of cell-surface MHC-I was revealed

to be significantly lower in MCPyV–positive MCC relative to virus-negative MCC. Negative regulation of MHC-I expression has been observed at a high percentage in MCC, identifying this strategy as an immune evasive mechanism adopted by oncoviruses [95].

All these constitute a dysfunctional systemic immune defense as well as the establishment of a local immunosuppressive micro-environment evoked by the inflammation processes involved in MCC [102].

1.16 Possible production and activation of Interleukin-17 in MCC

Present in the MCC tumor micro-environment are CD8 + T cells, macrophages, NK [95, 102], and MDSC cells [102], which as well as other various cell types have been identified to be sources of IL-17 [87, 104]. In human tumor environment, high levels of CXC-chemokine ligand 12 (CXCL12) and CCL20, which are ligands for CXCR4 and CCR6 respectively are found at high levels. CCL20 is a chemokine particularly present in the MCC microenvironment and its receptor CCR6 together with CXCR4 facilitate the trafficking of IL-17 producing cells (T_H17 cells) to tumors [105].

The release of pro-inflammatory IL-17 can initiate a variety of cytokines such as IL-1β, tumor necrosis factor (TNF)-α, TGF-β and IL-6 and chemokines such as IL-8, and prostaglandins to be produced from endothelial cells, fibroblast, epithelial cells, and macrophages, leading to inflammation and its amplification. The production of IL-6 in an IL-17-mediated fashion, will result in the activation of STAT3 pathway [105] which has been implicated in MCC [102]. Present in MCC microenvironment are STAT3 and transforming growth factor-β [102], which are vital to the differentiation of IL-17 producing cells (T_H17 cells). IL-6 also enhances the differentiation of IL-17 producing cells (T_H17 cells), and the release of IL-6 in the tumor is amplified by interleukin 17 [105].

In MCC tumor, a signal transduction protein component of the tumor microenvironment is NF-κB [95] which has been shown to be involved in IL-17–mediated tumorigenesis [94].

1.17 Possible roles of Interleukin-17 in MCC tumorigenesis

A critical signaling molecule is STAT3 which is implicated in the generation of the tumor microenvironment via downstream regulation of pro-inflammatory cytokines and factors facilitating cancer growth, progression and metastasis. The differentiation and maturation of T_H17 cells to produce IL-17 can be regulated by a constitutively functional phosphorylated STAT3, which via a positive feedback loop enhances STAT3 signaling and trigger IL-17 release. The mobilization and infiltration of MDSCs such as CD11b+Gr1+ cells to the tumor microenvironment is promoted by IL-17, with a reciprocal augmentation of development and function of MDSCs by IL-17. The development of vascular endothelial cells and upregulation of the angiogenic process can be promoted by IL-17 by an elevated release of cytokines such as IL-8, VEGF and TNF-α. IL-17 can also enhance cancer cell invasion via positive regulation and negative regulation of MMP-2 and MMP-9 expression and the expression of tissue inhibitors, MMP-1 and MMP-2 respectively [104].

1.18 Aims of the study

Merkel cell polyomavirus is a dermatotropic virus that is chronically shed from healthy skin [20]. However, viral DNA can be found in cells of other organs and tissues, including liver, lungs, gall bladder, lymphoid and blood cells, intestine, and cervix [22]. Despite the apparent broad *in vivo* cell tropism, so far no cell culture system has been identified that can sustain replication of MCPyV. Previous studies with the human polyomaviruses BK and JC have shown that variations in promoter sequences affect promoter activity, viral protein expression levels, virus propagation, and pathogenic properties [106-111]. Similar studies with MCPyV are lacking and identifying a cell type that strongly supports MCPyV promoter activity may provide an idea of a permissive cell line. For these reasons this study aimed at the following:

-to compare the relative MCPyV promoter strength in different cell lines to provide a basis for identifying a suitable cell line to propagate MCPyV,

-to elucidate the effect of naturally occurring mutations in the MCPyV promoter on the activity,

-to investigate the role of the early proteins LT-ag and st-ag on viral promoter activity,

-to examine whether LT-ag is implicated in the upregulating of IL-17F in MCPyV-positive MCC compared to MCPyV-negative MCC,

-to test whether IL-17F has an effect on MCPyV promoter activity.

2. Materials

Table 2.1: Kits used in this study

Kit	Manufacturer	Purpose
Nucleospin® Plasmid	Macherey Nagel	Plasmid purification, small quantities.
Nucleobond® Xtra Midi	Macherey Nagel	Plasmid purification, medium quantities
QIAmp DNA Mini kit	Qiagen	DNA purification from cultured cells
QIAamp® MinElute® Virus Spin	Qiagen	Viral DNA purification
GFXTM PCR DNA and Gel band purification	GE Healthcare	Purification of DNA from gel or solution
Luciferase kit	Promega	Luciferase assay
Protein quantification assay kit	Macherey Nagel	Protein quantification
Jetprime transfection kit	Polyplus transfection®	Transient transfection
BigDye Teminator v3.1 cycle Sequencing kit	ThermosFisher Scientific	DNA sequencing
QuickChange Site-directed Mutagenesis kit	Agilent Technologies	Site-directed mutagenesis

Table 2.2: Buffers and solutions used in this study

Buffers and solutions	Manufacturer/Contents	Purpose
Blotting buffer	5.8 g Tris base+ 29 g glycin + 200 ml methanol + 800 ml dH_2O	Western blotting
	150 ml PBS + 7.5 g dry milk + 150 µl Tween 20	Western blotting
10x Washing buffer	100 mM Tris HCl pH9.5, 100 mM NaCl, 10 mM $MgCl_2$ and dH_2O up to 1 L. Working dilution 1:10	Western blotting
Tropix® CDP-Star®	Applied Biosystems	Western blotting
CDP star buffer	10 ml DEA + 850 ml ddH_2O. pH 9.5. dH_20	Western blotting
1xTE Buffer (pH 8.0)	100 mM Tris/10 mM EDTA	DNA storage

Protein solving buffer (PSB)	Macherey-Nagel	Protein quantification assay
Bovine serum albumin (BSA)	Macherey-Nagel	Protein quantification assay
Quantification reagent (QR)	Macherey-Nagel	Protein quantification assay
SeaKem LE agarose	Lonza	Agarose gel electrophoresis
96% Ethanol	Sigma-Aldrich	Plasmid DNA purification
Isopropanol	Arcus	Plasmid DNA purification
Tropix® Lysis buffer	Promega	Luciferase assay
10 x cloned PFU reaction buffer	Stratagene	Site directed mutagenesis
Jet prime buffer	Polyplus transfection®	Transient transfection of mammalian cells
Jet prime reagent	Polyplus transfection®	Transient transfection of mammalian cells
Luciferase buffer	Promega	Luciferase assay

Table 2.3: Molecular markers used for agarose and acrylamide gel electrophoresis in this study

Molecular markers	**Manufacturer**	**Purpose**
GelRed™	Biotium	Agarose gel electrophoresis
1 kb Plus DNA ladder	Invitrogen	Agarose gel electrophoresis

SeeBlue® Plus 2 Prestained Standard (1x)	Invitrogen	Western blotting
MagicMarker™ XP Western Standard	Invitrogen	Western blotting

Table 2.4: Primers used in this study

Analysis (Product size)	Primer	Sequence	Source
MKL2 LTag stop (37 kDa)	MKL-2 F	5'-GAAGACCCCTCCTCCATAGTCAAGAAAGCG-3'	This study
	MKL-2 R	5'-CGCTTTCTTGACTATGGAGGAGGGGTCTTC-3'	This Study
MKL-1 LTag stop (50 kDa)	MKL-1 F	5'-GCCATGCTGTGTACAAGTTTTAAACAGTCTCCTGTTTTGC-3'	This Study
	MKL-1 R	5'-GCAAAACAGGAGACTGTTTAAAACTTGTACACAGCATGGC-3'	This Study
MS-1 LTag stop (60 kDa)	MS-1 F	5'-GCCACTGCTAAATTAGGAATTTCAAGAAAAAG-3'	This Study
	MS-1 R	5'-CTTTTTCTTGAAATTCCTAATTTAGCAGTGGC-3'	This Study
CMV primer	CMVprom	5'-GAGCTGGTTTAGTGAACCGTC-3'	This Study
MCPyV LT-ag	LT-ag F	5'TACAAGCACTCCACCAAAGC-3'	This Study
	LT-ag R	5'-TCCAATTACAGCTGGCCTCT-3'	This Study

Table 2.5: Bacterial strains used in this study

Bacterial Strain	Description	Purpose
Escherichia *coli* DH5α	A recombination-deficient, Suppressing, competent strain	Amplification of plasmid vectors

Table 2.6: Plasmids used in this study

Plasmid construct	Size of plasmid	source	properties	purpose
$pcDNA_5$ flag MCPyV st-ag		Andrew Macdonald [63]	Amp^R	MCPyV st-ag expression plasmid
pcDNA6-MCV.cLT206.V5	7550	Addgene	Amp^R	MCPyV LT-ag expression plasmid
pGL3-basic	4818	Promega	Amp^R	Cloning MCPyV promoters
pGL3-basic MCPyV LUC Early	5274	MIRG	Amp^R	MCPyV MCC350 early promoter
pGL3-basic MCPyV LUC Late	5274	MIRG	Amp^R	MCPyV MCC350 late promoter
pCMV-IL-17F		MIRG	Amp^R	IL-17F expression plasmid
Recombinant IL-17A/F		MIRG	Amp^R	Recombinant IL-17A/F expression plasmid
pGL3-Basic MCPyV-16b Early	5284	GenScript	Amp^R	MCPyV 16b early promoter
pGL3-Basic MCPyV-16b Late	5284	GenScript	Amp^R	MCPyV 16b late promoter
MKL-1	6271	This study	Amp^R	MCPyV MKL-1 tLT-ag expression plasmid
MKL-2	6436	This study	Amp^R	MCPyV MKL-2 tLT-ag expression plasmid
MS-1	6730	This study	Amp^R	MCPyV MS-1 tLT-ag expression plasmid
pcDNA3		invitrogen	Amp^R	control vector in luciferase assay and western blot
IL-17F-636- LUC		This study	Amp^R	IL-17F-636 promoter
IL-17F-166- LUC		This study	Amp^R	IL-17F-166 promoter
pEGFP-C1		Clonetech	Amp^R	Transfection efficiency

Table 2.7: Enzymes used in this study

Enzyme	Manufacturer	Purpose
AccuStart II	Quantabio	PCR
dNTP mix	Sigma-Aldrich	PCR
PFU turbo	Stratagene	Site directed mutagenesis
Dpn I	Bio Labs	Site directed mutagenesis

Table 2.8: Growth media used in this study

Growth media	Manufacturer / Contents	Purpose
LB (Luria-Bartani)	950 ml dH_2O, 10 g bactotryptone, 5 g yeast extract, 10 g NaCl, NaOH to pH 7.0 (~0.2 ml), appropriate antibiotics, dH_2O up to 1 L	Bacterial culture
SOC	950 ml dH_2O, 20 g bactotryptone, 5 g bacto-yeast extract, 0.5 g NaCl, 20 mM glucose, 10 ml 250 mM KCl, NaOH to pH 7.0 (~0.2 ml), dH2O up to 1 L	Transformation of bacterial cells
LB agar plate	LB medium, 15 g bacto-agar per L	Transformation and cloning of bacterial cells
DMEM	Sigma-Aldrich. Standard Dulbecco's Modified Eagle's medium, penicillin (100 U/ml), Streptomycin (100 µl/ml	Mammalian cell culture (HEK293 cells)
EMEM	Lonza. Eagle's Minimum Essential Medium, penicillin (100 U/ml), Streptomycin (100 µl/ml)	Mammalian cell culture (SK-N-BE(2) cells)
RPMI-1640	Sigma. Roswell Park Memorial Institute Medium-1640, + L-Glutamine and sodium bicarbonate, penicillin (100 U/ml), Streptomycin (100 µl/ml)	Mammalian cell culture (MCC13 cells)
FBS	Gibco®. Heat inactivated Fetal Bovine Serum	Mammalian cell culture

Table 2.9: Mammalian cell lines used in this study

Cell-line	Organism	Organ	Reference number	Purpose
MCC13	Human	skin	Baki Akgül (university of Cologne)	Transfection
HEK239	Human	Kidney	ATCC CRL-1573	Transfection
SK-N-BE(2)	Human	Brain	ATCC CRL-2271	Transfection
C33A	Human	Cervix	ATCC HTB-31	Transfection

Table 2.10: Transfection reagents used in this study

Transfection reagent	Manufacturer	Purpose
Jetprime	Polyplus transfection®	Transfection of mammalian cell cultures

Table 2.11: Antibodies used in this study

Antibody	Manufacturer	Catalogue	Cat.	Dilution	Purpose
CM2B4	Santa Cruz Biotechnology	Sc-136172	Ab97046	1:1000	Primary antibody for detection of MCPyV Large T antigens in Western blot
Anti-FLAG	Agilent	200471	Ab97046 Sc-2005	1:1000	Primary antibody for detection of FLAG-tagged MCPyV small t antigens in Western blot
ERK 2 (C-14) Rabbit polyclonal IgG	Santa Cruz Biotechnology	Sc- 154	Ab97080	1:1000	Primary antibody for detection of ERK2 protein in Western blot
Polyclonal Rabbit anti-Mouse Ig/AP	Santa Cruz Biotechnology	Sc-136172	Ab97046	1:5000	Secondary antibody for detection of MCPyV Large T antigens in Western blot

Goat Anti-Mouse Ig, AP	Santa Cruz Biotechnology	Sc-136172	Sc- 2005	1:2500	Secondary antibody for detection of MCPyV Large T antigens in Western blot

Table 2.12: Equipment used in this study

Equipment	Manufacturer	Purpose
Sub Cell System	Bio-Rad	Agarose gel electrophoresis
Gel Doc 2000	Bio-Rad	Agarose gels and Coomasie blue stained SDS-Page Photo documentation
Avanti® J-26 XP	Beckman Coulter™	Centrifugation of ≥ 15 ml tubes
Microfuge® 22R Refrigerated Centrifuge	Beckman Coulter™	Centrifugation of eppendorf tubes
Sonicating Machine	Heat systems ultrasonics	Sonification of cell lysates for Western blot
T-100 PCR machine	BioRad	PCR
KI 260 Basic	IKA®	Flat shaker
Leica Fluorescence microscope DM IRB	Leica	Fluorescent microscopy
AccuBlock™ Digital Dry Bath	Labnet	Heating block
Vortex	VWR	Mixing
Spectrophotometer ND-1000	Saveen Werner	Nucleic acid measurement
Clariostar Microplate reader	BMG-LABTECH	Protein measurement
Spectrafuge™ Mini Centrifuge	Labnet	Quick spin
XCell SureLock™ Mini-Cel	Invitrogen	SDS page/Western blotting
Scepter automatic cell counter	Millipore	Counting cells to be seeded for transient transfection
GeneAmp® PCR System 9700	Applied Biosystems	Thermal cycling

Rotator SB3	Stuart	Tube rotator
TW8	Julabo	Water bath
Immobilon®-P Transfer Membrane pore size 0.45 µm	Millipore®	Western blotting
Chromatography paper 3 mm	Whatman/ GE Healthcare	Western blotting
NuPAGE® 4-12 % Bis-Tris gel	Invitrogen	Western blotting
LumiAnalyst machine(LAS-4000)	Fujifilm	Western blotting Luminescent Image Analyzer
Cell culture CO2 incubator	Esco	Cell culture incubation
Luminometer	Labsystem	Measurement of luciferase activity

3. Methods

3.1 Purification of Nucleic acids

Presently, specifically engineered plasmids, usually referred to as vectors are utilized by scientist in studying and manipulating specific genes of interest as well as other genetic materials. Plasmids are therefore conceivably, amongst the molecular biologist tools, the most ubiquitous.

Different nucleic acid purification protocols were utilized in this thesis according to the required nucleic acid source, type and amount. The protocols are all column based and involve nucleic acids being released from their sources prior to loading. At high salt and pH conditions and after several washing steps, the nucleic acids bind to a silica-based membrane and are eluted respectively. (At high salt and pH conditions, the nucleic acids bind to a silica-based membrane and after several washing steps they are eluted.). Table 3.1 briefly describes the kits used for nucleic acid purification in this thesis.

Table 3.1: Purification Kits utilized in this thesis

Kit	Nucleic acid	Source of nucleic acid	Specifications
Nucleobond® Xtra Midi	Plasmid DNA	Medium sized bacterial cultures	Enlarged for high flow DNA binding capacity, removable filter for and loading of lysate
Nucleospin® Plasmid	Plasmid DNA	Small bacterial cultures	-

To test the effectiveness of the plasmids, and to confirm the sequence of the plasmids via transient transfection studies and PCR, plasmid DNA was isolated and purified.

3.1.1 Protocol for plasmid purification using Nucleobond®Xtra Midi Kit

In purifying high-copy plasmids from DH5 strain of *Escherichia coli* (*E. coli*), bacterial culture, Nucleobond®Xtra Midi Kit from Machery-Nagel (Table 2.1) [112]. This method involves an ionic interaction between the negatively charged phosphate backbone of the plasmid DNA and positively charged silica-based membrane, column binding by nucleic acid (DNA) and lastly,

pure nucleic acid (DNA) elution in an alkaline condition [112]. All the steps were performed at room temperature (RT).

Bacteria cells transformed with plasmid of interest were grown in 100ml LB medium containing the appropriate antibiotics (Table 2.8) overnight. This was done in an incubator shaker at 37ºC and 220 rpm. Harvesting of the bacterial cells was done by centrifuging the overnight culture at 6000rpm for 10mins at 4ºC to pellet the bacteria cells. The supernatant was discarded and pellets re-suspended in the tube with Resuspension buffer containing RNase (8ml). RNase eliminates any RNA present by catalyzing hydrolysis of all RNA molecules into nucleotides without the DNA being affected. Lysis buffer (8ml) was added, with gentle inversions of the tube and 5 minutes incubation to lyse the bacterial cells via NaOH/SDS alkaline lysis procedure. Sodium hydroxide (NaOH) disrupts the hydrogen bonding between the DNA bases converting the dsDNA into ssDNA as well as breaking the bacterial cell wall. Sodium dodecyl sulphate is an ionic detergent which disrupts and destabilizes cell membrane and hydrophobic interactions that keeps numerous macromolecules in their native conformation.

During incubation the column and filter were both prepared and equilibrated by applying equilibration buffer (12ml) to the column filter's rim and allow the column to empty via gravity flow. Neutralization buffer (8ml) was added to the lysate, followed by gentle inversion of the tube for about 15 times prior to loading onto the filter. This allows homogeneous mixing and complete neutralization of the lysate. Potassium acetate (CH_3CO_2K) is contained in the neutralization buffer. Its low pH neutralizes the alkalinity (or high pH) of NaOH, permitting renaturing of the plasmid DNA to dsDNA, while SDS, denatured cellular proteins and genomic DNA aggregate to form a white precipitate.

Subsequent to loading the lysate onto the filter and emptying of the filter by gravity flow, the column filter was washed by adding Equilibrium buffer (5ml) to clear out any remaining lysate. The filter was then discarded after the column had emptied and Wash buffer (8ml) was added to wash the column. The column-bound DNA plasmid was eluted by adding Elution buffer (5ml), which was then precipitated by adding and mixing with room temperature isopropanol (3.5ml). Centrifugation of the mix at 15,000 x g at 4ºC for 30 minutes was done to pellet the DNA, which was then washed with 96% room temperature ethanol (5ml) and centrifuged at 15,000 x g at 4ºC for 5 minutes. Subsequently, the ethanol was carefully discarded completely and the DNA pellets were left at room temperature for 5-8 minutes to dry. The pelleted plasmid DNA was then reconstituted by dissolving in TE buffer (200µl). EDTA is present in TE buffer, which chelates magnesium ions that acts as cofactor for several nucleases. TE buffer therefore

will inactivate nuclease contaminants if present in the isolated or purified DNA plasmid. The concentration and purity of the eluted plasmid DNA was evaluated using Nanodrop spectrophotometer, labelled and then stored at -20ºC.

3.1.2 Protocol for plasmid purification using Nucleospin®Plasmid Kit

In purifying plasmids from small bacterial culture, (DH5 strain of *Escherichia coli* (*E. coli*), the Nucleospin®Plasmid Kit from Machery-Nagel (Table 2.1) [113]. All steps and centrifugations were performed at room temperature and 11,000 x g respectively. Bacteria cells transformed with plasmid of interest were grown in 1-1.5 ml LB medium containing the appropriate antibiotics (Table 2.8) overnight in an incubator shaker at 37ºC and at 220 rpm. Harvesting of the bacterial cells was done by centrifuging the overnight culture for 30s to pellet the bacteria cells. The supernatant was discarded followed by resuspension of the pellets in buffer A1 (250µl) and then vortexed well to have a homogeneous mix with no visible cell clumps. Buffer A1 was to make the bacteria cells to swell and also contains RNase to get rid of any present RNA. Lysis buffer A2 (250µl) was then added with gentle inversion (approx. 8 times) of the tube to mix the contents and lyse the cells while avoiding shearing of genomic DNA. Buffer A2 contains a detergent that causes cells to explode and NaOH to facilitate DNA release into solution and avoid the DNA to be sticky to the membrane. Incubation of the lysate for 5mins until the lysate turned clear was done after which neutralizing buffer A3 (300µl) was added and then mixed by inverting (approx. 8 times). Buffer A3 which is acetic acid was to neutralize the NaOH and also take out all lipids, sugar and un-needed cell inclusions that may possibly interfere. Clarification of the lysate was done by centrifuging for 5mins. Into a collection tube, a Nucleospin® column was placed and onto the column a maximum of 750µl of the clarified supernatant was loaded. For 1 minute, the column was centrifuged and the flow through discarded. Washing of the column was done by adding buffer A4 (600µl) which has been supplemented with ethanol. Centrifugation of the column was done for 1minute and the flow through discarded. The column was then dried by centrifuging for 2min and the DNA was eluted into a 1.5ml Eppendorf tube by adding buffer AE (50µl). This was followed by 3 minutes incubation and 1 min centrifugation. The concentration and purity of the eluted plasmid DNA was then measured by Nanodrop spectrophotometer (Table 2.12), labelled and stored at -20ºC.

3.2 Nucleic acid evaluation

A number of methods are used for evaluating the purity and concentration of nucleic acids. In this thesis, UV-spectrophotometry was used in determining the purity and concentration of nucleic acids purified. Using the NanoDrop-1000 spectrophotometer, the UV-spectrophotometry method was performed.

In the Nucleic acid structure, the aromatic ring present absorbs Ultraviolet (UV) light of 230 - 320nm wavelength and possess a 260nm mean absorbance peak (possess a mean absorbance peak at 260nm). As illustrated by Beer-Lambert Law, the passage of light through a sample composed of light absorbing molecules such as nucleic acids (RNA, DNA and Oligo), a linear relationship between the concentration and light absorbance of nucleic acid occurs i.e. measured light absorbance correlates proportionally to concentration. An optical density unit (OD_{260}) i.e. 1 OD_{260} Unit equals 50µg/ml for dsDNA and 40µg/ml for ssRNA. Salts and proteins which are common contaminants also absorb light in this range and can therefore affect downstream analysis. The nucleic acids' (DNA or RNA) purity can be determined by evaluating the ratio of light absorbed amongst various wavelengths. The presence of substantial contaminants will render the quantification inaccurate [114].

Guanidium salts which enable the binding of DNA to silica membrane strongly absorb light at 230nm, while aromatic amino acids absorb light at 280nm. A 260/280nm absorbance ratio is used in estimating DNA contamination with protein. Generally, an A_{260}/A_{230} ratio of 1.8 and 2 while an A_{260}/A_{280} ratio of 1.8 and 2 exhibit a pure RNA and DNA respectively. A lower ratio indicates the possible presence of contaminants [115,116]. ND-1000 was used in this thesis to measure nucleic acid concentration.

Additionally, agarose gel electrophoresis could be used in evaluating the purity and integrity of the purified/isolated DNA plasmid.

3.3 PCR

Polymerase chain reaction (PCR) is a molecular biology technique used in amplifying, identifying and analyzing DNA sequence of interest. A fragment of a DNA template is amplified by PCR with a pair of oligonucleotide primers that are complementary to the flanking regions of the fragment template via base pairing, free nucleotides and DNA polymerase in solution.

The amplification process is achieved through thermal cycling with each cycle composed of three basic steps: denaturation, annealing and extension. At high temperatures over 90ºC, the denaturation of dsDNA into single strands of DNA (ssDNA) occurs. The annealing process takes place at a lower and optimal temperature (mostly 50-60ºC) which enables hybridization of specific oligonucleotide primers to each complementary ssDNA (DNA template). The length and base composition of the primers determines the annealing temperature. Addition of nucleotides to the 3' end of the oligonucleotide primer occurs in the extension step (72ºC) by proofreading and thermostable DNA polymerase enzymes, leading to the synthesis of a DNA strand. An exponential amplification of the target DNA during the reaction (2^n, with n being the number of cycles) ensues [117].

3.3.1 Standard PCR Protocol

In this study, a readily available PCR mix which includes a thermostable DNA polymerase enzyme (AccuStart II Taq-DNA polymerase), nucleotides and optimal PCR buffer solution was used. The reaction mix was prepared as presented in Table 3.2 and dispensed in the PCR tubes. The DNA volume used in the reaction varies and depends on their concentrations, with a total volume of 20µl in each PCR tube. Inside the PCR machine, the PCR tubes were placed for incubation at the conditions described in Table 3.3.

Table 3.2: Reaction mix for PCR

Reagents	**Amount per reaction (µl)**
Accustart II™ Taq ready Mix™	15
Forward primer (10µM) or (100ng/µl)	1 or 1.5
Reverse primer (10µM) or (100ng/µl)	1 or 1.5
Template DNA (500ng)	Up to 7
dH_2O	Up to total volume of 30

Table 3.3: Thermal cycling program used for PCR in this thesis

Number of cycles	**Temperature (ºC)**	**Time**
1	96	5 min
30	96	20 sec
	58	20 sec
	72	45 sec
1	72	6 min
1	4	∞

3.4 SDS-PAGE

Sodium dodecyl sulfate polyacrylamide gel electrophoresis (SDS-PAGE) is a separating technique used in characterizing and separating proteins based on their molecular weight. SDS-PAGE was used in this thesis to confirm the expression of the correct protein (MCPyV full-length LT-ag and st-ag, respectively) (Table 2.6). It was also used in determining the success of the site-directed mutagenesis performed in creating truncated versions of the MCPyV LT-ag i.e. MS-1, MKL-1 and MKL-2.

In the presence of bis-acrylamide, crosslinks of polymerized acrylamide chains are present as constituents of polyacrylamide gels. The gel's density can be graded or constant, and bring about migration of molecules of various sizes through the gel at different speeds. Treatment of proteins in the samples with SDS or LDS, heat and a reducing agent such as dithiothreitol (DTT) prior to their loading into wells of the gel, cause the dissociation of the protein into primary polypeptide chains. SDS is an anionic detergent that disrupts the protein's tertiary structure, heat at a temperature of 70^{o}C denatures the protein while DTT hydrogenates and reduces the disulphide bonds of the proteins to thiol groups (S-S to SH SH), thus inhibiting both inter and intramolecular sulfide bond formation between cysteine residues present in the protein. The denaturation of the protein enables separation to be entirely based on the protein's molecular weight and not its conformation. Thus, protein migration during electrophoresis in a gel is thus a function of its size. SDS binds the denatured polypeptides in amounts approximately proportional to the protein's molecular weight (a molecule of SDS to two amino acid residue). This binding adds a negatively charged sulphate group to the denatured protein thereby giving them an overall negative charge. Comparison and estimation of the protein's mass in kDa is achieved using markers of known molecular mass. After passage of electric current through the gel loaded with the markers and protein samples, the negatively charged molecules (protein samples) migrate through the gel from the negatively charged electrode (cathode) to the positively charged electrode (anode) at speeds based on their sizes and separating them on bands based on their sizes. The small sized protein samples migrated faster while the heavy ones migrated slowly. The proteins in the polyacrylamide gel can be visualized using specific antibodies after being transferred to a membrane during western blot or stained using Coomassie blue [114, 118].

3.4.1 Protocol for SDS PAGE

The precast NuPage® gels (4-12 % gradient) Bis-Tris Minigel from Invitrogen (Table 2.12) was used for the SDS-PAGE procedure. The SDS-denatured lysate was sonicated and heat-treated (10 min, 70^{o}C) prior to loading onto the wells of the gel. Lysate sonication was done using ultrasound (Table 2.12) to shear the DNA at the phosphoribose backbone but not the protein. Into the XCell SureLockTM Mini-Cell, submersed in running buffer (MES SDS), the gel was placed, and onto it 10µl of each sample and 1.5µl of molecular markers, SeeBlue® and MagicMarker® (Table 2.3) were loaded. The gels were then made to run at 200V for 45 minutes in the NuPage gel program.

3.5 DNA sequencing

Enzymatic method of sequencing was used which makes use of nucleotides: dNTP and fluorescent ddNTP. It makes use of a mixture of dNTP and ddNTP. The dNTP possesses the 3'-OH group which is essential for polymerase-regulated strand elongation in the PCR while the ddNTP lacks the essential 3'-OH group that is essential for polymerase-mediated strand elongation, therefore it serves as 3'-end terminator in sequencing (chain termination sequencing). The ddNTPs are fluorochrome labelled with each of the nucleotides labelled distinctly. They are referred to as chain-terminating inhibitors of DNA polymerase in Sanger method for DNA sequencing because after they have been added to a growing nucleotide chain by a DNA polymerase, the absence of the 3'-OH group prevents further addition of nucleotides as no phosphodiester bond can be created, thus the synthesis of a new strand ceases and becomes detectable by the laser light. This is because DNA chain synthesis occurs via condensation reaction between 5' phosphate of the incoming nucleotide with the 3'-OH group of the previous nucleotide and hence cause DNA sequence termination.

The polymerase picks either dNTP or fluorescent ddNTP at random. The concentration of dNTP is higher than that of ddNTP, so the chance that a dNTP is incorporated is higher. When DNA polymerase picks up the ddNTPs which have fluorescent labels, it stops DNA elongation and it gives a fluorescent color which is read by a laser. Nucleotide strands of varying or distinct lengths are created by the ddNTP inclusion. Through small capillaries which contain a liquid polymer, these synthesized strands pass and their distinct fluorochromes emit light of different wavelengths after being excited by a laser. Both the type of light emitted and travel time of the light are registered and interpreted by a computer, which produces a readable nucleotide

sequence [119, 120, 121]. Mutations and variations in sequences can be identified by sequencing.

3.5.1 Sequencing protocol

Table 3.4 shows the quantity and concentrations of the reagents and Table 3.5 describes the conditions used in performing the sequencing procedure. A ready mix of DNA-polymerase, fluoresecent- Analyzer from applied Biosystems/Hitachi were used.

Lastly, the BLAST program (http://blast.ncbi.nlm.nih.gov/Blast.cgi), from PubMed was used in analyzing the result by comparing the nucleotide and amino acid sequences with nucleotide sequence template.

Table 3.4: PCR program for sequencing

Reagents	**Amount per reaction (µl)**
5 x Sequencing buffer	3
Forward primer (10µM) or (100ng/µl)	1 or 1.5
Reverse primer (10µM) or (100ng/µl)	1 or 1.5
Template DNA (500ng)	1 or 2
Big Dye	0.5
dH_2O	Up to total volume of 20
Total	20

Table 3.5: Sequencing reaction mix

Number of cycles	**Temperature (ºC)**	**Time**
1	95	3 min
30	96	10 sec
	50	5 sec
	60	4 min
1	4	5 min
1	4	∞

3.6 Western Blotting

Western blotting which is also referred to as immunoblotting is an analytical method used for the detection of specific proteins in a sample. It involves the transfer and immobilization of proteins which have been separated on a gel via SDS-PAGE gel electrophoresis, onto a nitrocellulose membrane and stained using specific antibodies. Firstly, blotting which is the process of protein transfer from the gel onto the membrane is done by electrophoretic transfer and then followed by antibody staining of the protein. Sandwiched into a cassette are the gel and membrane together with filter papers, buffer and sponge pad. Current is then passed through which makes the proteins to permeate the gel and get trapped onto the membrane. On completion of the blotting process, blocking of the membrane is done. Blocking involves soaking the membrane in a protein solution of 5% non-fat dried milk to enable blockade of the remaining hydrophobic binding sites, thus, preventing non-specific anti-body binding to the membrane surface and non-specific signals. Primary antibodies (monoclonal or polyclonal) which are specific to an epitope of the protein and secondary antibodies which are specific to the constant heavy chain of the primary antibodies and conjugated to enzymes such as Horseradish peroxidase (HP) or alkaline phosphatase (AP). The chromogenic substrate is then added and becomes converted to a colored product by the enzyme and enhances detection of the antigen-primary antibody-secondary antibody complex. The secondary antibodies can also be fluorochrome labelled [114, 118].

3.6.1 Protocol for western blotting

The western blotting procedure was performed at room temperature unless stated otherwise. Washing of the Immobilin® transfer membrane (Table 2.12) was done in methanol for 3s, in dH_2O for 10s and in blotting buffer for 5 minutes. The Whatman filter papers and blotting pads were also soaked in blotting buffer. On completion of gel electrophoresis, the cassette was emptied and inside another cassette, the membrane and gel were sandwiched together with sponge pads, filter papers and blotting buffer. The order of assemblage is as follows: the cathode core is placed on the bottom, three blotting pads are placed on it, followed by two Whatman filter papers, the gel, the membrane, two Whatman filter papers, three blotting pads, and then the anode core placed on the top and sealed tightly. The sandwiched components were then placed inside the XCell SureLockTM Mini-Cell with the inner chamber and outer chamber of the mini cell filled with blotting buffer and cold water respectively. The blotting was performed

at 30V and 160mA for 1 hour. Based on charge and hydrophobic interactions between the proteins and membrane, protein transfer from the gel to membrane was achieved.

On completion of the blotting process, the membrane was washed in TBS (Table 2.2) for 10mins to remove traces of polyacrylamide gel, after which the membrane was incubated with blocking buffer containing non-fat dry milk in TBS with 0.1% Tween 20 detergent on the rocker plate for 1 hour at room temperature. Into a 50ml centrifuge tube, the membrane was transferred with the protein blotted side inwards, 3ml of blocking buffer and 3µl (1/1000) primary antibody (Table 2.11) were added and covered. The lid of the centrifuge tube was then sealed with parafilm and then incubated overnight at 4ºC on a rotating wheel. The blocking buffer with the primary antibody was discarded after incubation and the membrane was washed thrice with PBST for 5 minutes. The membrane was again incubated for 1 hour with 3ml blocking buffer and 1.5µl (1/2500) of the secondary antibody (Table 2.11) on the rotating wheel. The membrane was then washed twice with TBST and washing buffer for 5 minutes each and 4ml of CDP star buffer (Table 2.2) and CDP star substrate in a ratio of 1:1000 was added to the membrane with a 5 minutes incubation. The membrane was then carefully removed from the 50ml centrifuge tube, placed and sealed in a plastic bag and left in the dark for few minutes before analyzing the signal on the LumiAnalyst machine (LAS4000 machine) (Table 2.12).

3.6.2 Stripping the membrane

In order to allow new immunostaining to be performed with different antibodies on the same membrane, stripping is performed. Immunostaining is also required to ensure that the possible variation in protein levels are due to variations in expression and not the result of technical shortcomings (uneven cell harvesting, or unequal sample loading or unequal blotting). Stripped of primary: secondary antibody complex is achieved by treating the membrane with NaOH. Subsequently, the stripped membrane can be re-probed with antibodies that allow normalization of the first western blot. ERK2 protein is often used in performing a loading control because ERK2 is a protein that is constantly and ubiquitously expressed and whose expression is not altered by a large variety of stimuli tested [114]. This is advantageous in situations involving investigation of more than one protein, for example, the loading control and the protein of interest.

3.6.2.1 Protocol for membrane stripping

Incubation of the membrane after careful removal from the plastic was done in a tub with 0.2M sodium hydroxide (NaOH) for 5 minutes with shaking. Subsequently, the membrane was washed with PBST thrice with each washing step lasting for 5 minutes. The membrane was then transferred into a 50ml centrifuge tube and 3ml of blocking buffer was added, then followed by 1 hour incubation on the rotating wheel. Immediately after the 1 hour incubation, 3µl (1/1000 dilution) anti-ERK2 antibodies were added and the tube covered, sealed with parafilm and incubated overnight at 4ºC on the rotating wheel. The procedure from Western blotting protocol was continued from the PBST washing step.

3.7 Mammalian cell culture techniques

In Molecular Biology studies, mammalian cell cultures are extensively used experimental models for *in vivo* conditions. In this thesis, a number of cell lines were used and include: HEK 293, MCC 13, SK-N-BE(2) and C33A cells. Lysates from transfected cells were harvested and the protein were analyzed using Western blot, Luciferase assay and protein quantification (Figure 3.1). As a control, all these cells were transfected with EGFP to estimate the transfection efficiency in fluorescent microscope. All these cell lines have adherent growth mode, HEK 293 SK-N-BE(2) and C33A cells express an epithelial morphology while MCC13 are large and low contrast cells in morphology. Prior to use, all media, trypsin and PBS were preheated to 37ºC and the cells were kept in a humidified CO_2 incubator at 37ºC.

Derived from human embryonic cells are HEK 293 cells and transformed by adenovirus type 5. They were established at the University of Leiden, Holland in the early 1970s [122]. HEK 293 cells grow well, easy to handle and transfect with a transfection efficiency greater than 90%. MCC13 cells are MCPyV-negative Merkel cell carcinoma cell line derived from a metastatic cervical node biopsy from a female octogenarian patient of Merkel cell carcinoma in 1995 from the Queensland Institute of Medical research in Australia [123]. C33A cells are HPV-negative human cervical carcinoma cell lines derived from cervical cancer biopsies [124]. SK-N-BE(2) neuroblastoma cell lines are cells of the brain derived from a bone marrow (metastatic site) biopsy taken from a child with disseminated neuroblastoma in 1972 [125].

Figure 3.1: Flowchart of all analytic processes used in this thesis starting from transient transfection of mammalian cell lines.

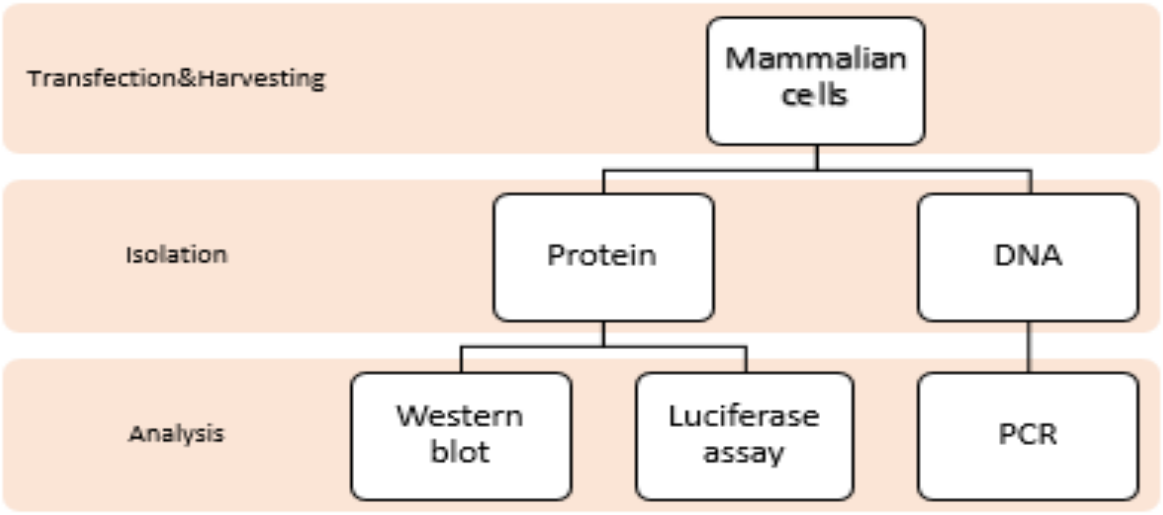

3.7.1 Sub-culturing of cells

It is vital to maintain and use cells in the log phase of growth in order to achieve optimal growth conditions of cell cultures. Adherent cells are observed to grow in vitro in culture flask until they either consume all nutrients from the medium or become confluent by covering the whole surface of the culture vessel. The cells should therefore be split or sub-cultured before they reach the stationary phase or become totally confluent in order to keep them healthy and viable. In this thesis, enzymatic treatment of the cells, was done to detach the cells and sub-culture them. Cells were rinsed with PBS and added prior to trypsin treatment to remove the serum present in FBS, which could inactivate the trypsin. They were then re-suspended and a portion the cell suspension was transferred into a new culture flask with fresh growth media [9].

3.7.1.1 Protocol for Sub-culturing of cells

The old medium was aspirated and the cells while still attached to the walls of the culture flask were washed with the appropriate volume of PBS (Table 2.2). The PBS was then aspirated and small volume of trypsin is then added and incubated for 30s - 2 minutes (depending on the cell line) in humidified CO_2 incubator at 37ºC to detach the cells from the walls of the culture flask. Addition of medium containing FBS inactivates trypsin. Resuspension of cells in the medium was done by gentle pipetting up and down. An appropriate dilution of the cell suspension was

transferred into a new flask with the addition of fresh medium depending on the size of the culture flask as described in Table 3.6.

Table 3.6: Regents used for sub-culturing of cells

Reagents	Medium culture flask	Large culture flask
Growth medium	Up to a total volume of 15 ml	Up to a total volume of 35 ml
FBS	10 %	10 %
PBS	5 ml	10 ml
Trypsin/EDTA	1 ml	2 ml
Growth medium for resuspension	4 ml	9 m

3.7.2 Protocol for seeding out cells

In this study, seeding of cells into plates was done at different ratios depending on the well size of the culture plates. Table 3.7 gives a detailed description.

Prior to seeding of the cells of interest, the cell suspension after trypsinizing, was centrifuged at 1,500-2,000 rpm for 5mins. This is to ensure dead cells are gotten rid of and single cells would be seeded. After centrifugation, the supernatant is aspirated and the clump of cells were re-suspended in 3ml of media and then 7ml of media is added diluted with PBS in a 1.5ml Eppendorf tube. Using the Scepter sensor of Scepter Cell Counter instrument (Table 2.12), the diluted cell suspension were aspirated and a histogram presenting the volume or size distribution of cell population, cell concentration per ml and average cell size is displayed on the screen of the instrument. The value obtained for the concentration of cells measured was multiplied with the dilution factor to obtain the number of cells per ml. The number of cells required in each well was multiplied by the total number of wells into which the cells would be seeded and then divided by the concentration of the cell suspension to calculate the total number of required cells. The volume of cell suspension containing the total amount of required cells was then diluted in growth medium, mixed properly to have an even distribution of cells and the appropriate amount of diluted cell suspension was dispensed into the wells. Subsequently, the plate was then gently and carefully rocked back and forth to ensure an even distribution of cells in the wells. In this study seeding out cells were basically for transient transfection studies.

Table 3.7: Cell number guidelines recommended for seeding a day prior to transfection

Culture Vessel	Number of adherent cells to seed	Surface area per well (cm^2)	Volume of medium per well to seed the cells (ml)
96-well	7500-10 000	0.3	0.1
24-well	50 000-80 000	1.9	0.5
12-well	80 000-150 000	3.8	1
6-well/3.5mm	150 000-250 000	9.4	2

3.7.3. Protocol for harvesting cells for protein analysis

Cells are harvested to analyze the results of the transfection study. Aspiration of media from the wells is the first step in harvesting cells. Warm PBS was gently added to each of wells while avoiding direct pipetting on cells to prevent the transfected cells from detaching. This washes off remaining media. The PBS was aspirated and 80µl of Lysis buffer for Western blot (preparation is described in Table 3.8) was then added to each of the wells. With the aid of cell scrapers, the cells were scraped and then transferred into Eppendorf tubes and placed on ice. The lysed samples were then sonicated, with each sample sonicated thrice for 2 seconds and then denatured at 70ºC for 10 minutes**.** Sonication of the lysed samples shears the DNA, makes it less viscous and easier to load on the polyacrylamide gel during SDS-PAGE**.**

Table 3.8: Lysis buffer constituents for western blot

Reagents	Amount for one well
4XLDS buffer	20
dH_20	52
1M DTT	8
Total volume	80

3.7.4 Protocol for harvesting the cells for Luciferase assay

To harvest cells for luciferase assay, aspiration of media from the wells was done and warm PBS was gently added to each of wells to wash off remaining media. Direct pipetting of PBS on the cells was avoided to prevent them from detaching. The PBS was aspirated and 100µl of Tropix Lysis buffer containing freshly added DTT to a final concentration of 0.5mM, was then

added to each of the wells. With the aid of cell scrapers, the cells were scraped and then transferred into eppendorf tubes while ensuring pipet tips were changes between each well and placed on ice. The lysates were centrifuged at 13,000 rpm at room temp for 3mins and 20µl of each lysate supernatant was used for luciferase assay.

3.8 Transfection of mammalian cells

Transient transfection involves the introduction of genetic materials into cells, their temporary expression and lastly their dilution via mitosis or degradation. It is a method used in achieving small scale protein synthesis and fast gene analysis.

The aims of this study were achieved via transient transfection studies in the mammalian cells used. A liposome-mediated transfection method was used in this study which involves foreign DNA uptake via endocytosis. The uptake is based on the ionic interaction between liposomes and the DNA as well as the interaction between the negatively charged cell membrane and cationic liposomes [118].

In transient transfection, pEGFP-C1 plasmid which encodes green fluorescence protein was used to estimate the number of mammalian cells that have internalized the plasmid DNA of interest i.e. transfection efficiency. Transfected cells will express EGFP and thus, emit green fluorescence when viewed under the fluorescent microscope.

3.8.1 JetPrime transfection protocol

Seeding of cells into the desired plates at optimal concentrations was done as described in cell seeding protocol for the experiment. The following day after incubating the seeded cells, and most importantly when the cells have reached 60-70% confluency, the cells are ready for transfection. All steps were performed at room temperature. The transfection mixes were prepared in labelled Eppendorf tubes as described in Table 3.9 [126]. The ratio of DNA to jetPrime transfection reagent was 1:2. The transfection mix in each of the labelled Eppendorf tubes were mixed by vortexing for 10sec and then spanned briefly. JetPrime reagent was then added to all the eppendorf tubes based on the ratio mentioned above and mixed by vortexing and brief spinning. The transfection mix was then incubated for 10min at room temperature and 75µl from each eppendorf tube was dispensed into the respective seeded wells of the plates. The plates were then covered, gently rocked back and forth from side to side to ensure even

spreading of the transfection mix and finally incubated in a humidified CO_2 incubator overnight at 37ºC.

Table 3.9: Guidelines for DNA transfection based on cell culture vessel per cell using jetPrime

Culture Vessel	Volume of jetPRIME Buffer(µl)	Amount of DNA(µg)	Volume of jetPRIME reagent(µl)	Volume of growth medium(ml)
96-well	5	0.1	0.2-0.3	0.1
24-well	50	0.5	1-1.5	0.5
12-well	75	0.8	1.6-2.4	1
6-well/35mm	200	2	4-6	2

Standard conditions require 1:2 DNA to jetPRIME® ratio. For 1 µg of DNA, 2 µl of jetPRIME® must be used [126].

3.9 Luciferase assay

This method makes use of luciferase as a reporter to test and compare promoter(s) activities. One of the commonly used reporter genes used in monitoring promoter strength of interest is the *luciferase* gene of the firefly *Photimus pyralis.* In this study, placed under the control of the promoter of interest is the *luciferase* reporter gene. Through transient transfection, the plasmid containing the promoter of interest and the *luciferase* gene are both introduced into the desired cells. Luciferase protein is then expressed by the transfected cells and the amount of luciferase produced is proportional to the strength of the promoter. The strengths of the various promoters can be determined by measuring the amount of luciferase produced. This indicates that a strong promoter produces more luciferase mRNA and therefore synthesizes more luciferase protein while weak promoter produces less luciferase mRNA and therefore expresses less luciferase protein.

Luciferase buffer used contains luciferin, a substrate of the produced luciferase protein (enzyme) which it oxidizes with the use of ATP to oxyluciferin with a concomitant emission of light, detectable in the blue range of the visible spectrum, 440-479nm (Figure 3.2) [127, 128]. The intensity of light emitted corresponds to the amount of oxidized luciferin and hence the

promoter's strength [127, 128]. A luminometer, which is a special instrument is used for a fast and effective measurement of the emitted light. This method is an excellent method because it is very sensitive, highly reproducible, fast, quantitative, and relatively cheap.

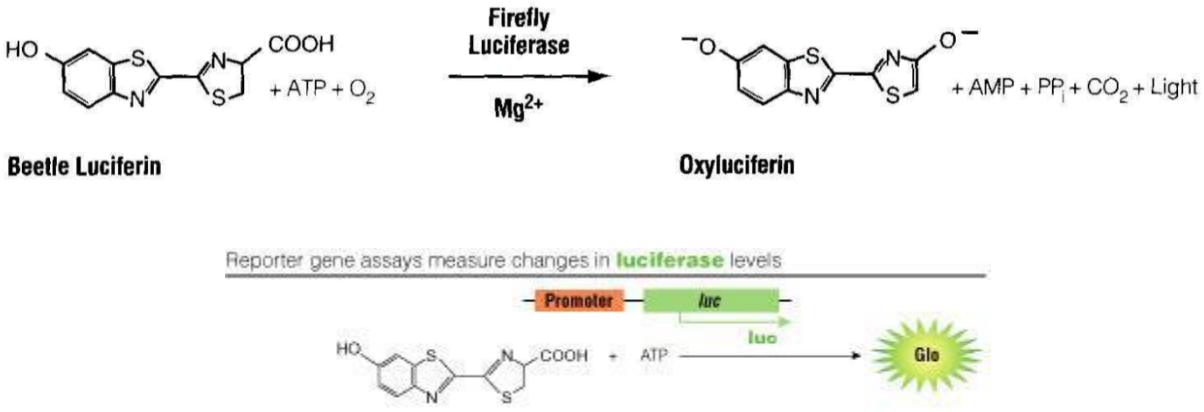

Figure 3.2: In the presence of ATP, luciferin is oxidized to oxyluciferin by luciferase enzyme. The released light accompanies this reaction. The reporter plasmid containing the *luciferase* gene encodes luciferase and is under the control of the promoter of interest [127,128].

3.9.1 Protocol for Luciferase assay

Starting from the left top well and continuing to the left bottom well of a luminometer microtiter plate, 20µl Tropix lysis buffer was dispensed into the first two wells (blank) and 20µl of each lysate supernatant were transferred into new wells of a 96-well white microtiter plate with flat bottom. While avoiding bubbles, 50µl of luciferase buffer (Table 2.2) was then added into each well to have a total volume of 70µl in each well. Immediately, the luminometer microtiter plate is placed inside a luminometer connected to a printer which measures luciferase activity and the values are printed.

3.10 PCR-based site-directed mutagenesis of MCPyV truncated LT-ag encoding plasmid

To generate expression plasmids encoding truncated variants of MCPyV LT-ag expressed in the virus-positive MKL1, MKL2, and MS-1 MCC cell lines, oligonucleotide-directed mutagenesis was performed. This is a method used for nucleotide addition, substitution or deletion in a DNA segment whose sequence is known. Oligonucleotide-mediated mutagenesis precisely generates mutations being designed by the experimenter as opposed to other methods of mutagenesis which commonly spawn mixed populations of variants. To achieve this, an oligonucleotide whose sequence contains the mutation of interest is firstly designed and synthesized. It is then hybridized to a template consisting of the wild-type sequence and the primer extended with a DNA polymerase that expresses proof-reading capabilities in a Polymerase Chain reaction (PCR) [114]. The premix was made in PCR Eppendorf tubes and a graded PCR was done as described in Table 3.10 and Table 3.11 respectively

Table 3.10: Premix for site-directed mutagenesis

Reagent	Amount (µl)
dH_2O	39
10 x Pfu buffer	5
template (MCPyV plasmid 25ng/µl	2
Forward Primer (10µM)	1
Reverse Primer (10µM)	1
12.5 mM dNTP	1
Pfu Turbo enzyme	1
TOTAL:	50

In this thesis, a graded PCR was employed to achieve a good investigation of the optimal annealing temperature of the primers.

Table 3.11: Thermal cycling program used for site-directed mutagenesis

Number of cycles	Temperature (°C)	Time
1	94	5 min
18	94	30 sec
	55	1 min
	68	18 min
1	4	∞

On completion of the PCR reaction, 1µl of *Dpn*I enzyme was added to each of the samples and incubated for 1 hour at 37ºC. The addition of the enzyme was to digest the methylated parent/template DNA as it cleaves only at the methylated site. The generated DNA will contain the desired mutation but un-methylated.

3.11 Protein measurement (of samples used in luciferase assay)

To ensure that the variations in luciferase values are due to differences in promoter strength and not as a result of technical shortcomings, the protein concentration of all cell lysates for luciferase assay were measured. This was done to enable the correction for possible variation in the number of cells per well (protein content) which may possibly affect luciferase measurement. It also helps to verify the success of the lysis step, protein yield and to normalize numerous samples to be compared side-by-side. In this thesis, the Protein Quantification Assay Kit from Machery-Nagel (Table 2.1) was used.

This method is principally designed for proteins solved in protein solving buffer (PSB). It involves the preparation of bovine serum albumin (BSA, reference protein) dilution series, at the start of the procedure in labelled Eppendorf tubes. A mixture of PSB with the samples are prepared in the wells of a microplate (96-well Falcon plate), followed by a 30 minutes incubation of the PSB-Sample mixture with Quantification reagent (QR) (Table 2.2). A photometrical measurement of light extinction at a wavelength of 570nm, is then done after the incubation. The turbid appearance of the mixture after QR addition evokes the light extinction. Determination of protein quantification is done in reference to a Bovine Serum Albumin (BSA) calibration curve [129].

3.11.1 Protein measurement protocol

The microplate assay procedure from Machery-Nagel (Table 2.2) was used. Seven reaction tubes are prepared and labelled as described in the Table 3.12 [129]. Into the first tube (#1), a stock solution of BSA was dispensed. 50µl of PSB was then added into the second to seventh tube (#2 - #7) i.e. column B. Into tubes #2- #6, BSA solution is added according to column C. Columns D and E shows the resulting amount and concentration of proteins. While dispensing PBS and BSA solution into the tubes, the formation of bubbles and foam were avoided. 20µl of the dilution series were then dispensed into the wells of the microplate and taking note that the contents of the numbered tube is as follows: #1: BSA stock solution, #2- #6: BSA dilution.

#7: BSA-free PSB. 20µl of the protein samples were then added into empty wells and then both the dispensed dilution series and protein samples were filled up with 40µl of PSB. Finally, 40µl of QR was the added to all wells making all the used wells to have a content of 100µl. Shaking of the microplate was done until a complete color change from blue to yellow occurred. This was followed with 30 minutes incubation of the microplate at room temperature. During the incubation, bubbles which had been created were removed using a clean needle and cleaned between wells. Using the Clariostar microplate reader (Table 2.12) light extinction was measured photometrically at 570nm. Within a wavelength range of 530-570nm, typical correlation coefficients (concentration of BSA against extinction value) of 0.97- 1.00 was obtained. In relation to the BSA dilution series, the protein concentration was then calculated.

Table 3.12: Preparation of BSA (reference protein) dilution series

A	B	C	D	E
Tube	**Add PSB to tube**	**Add BSA solution to tube**	**Resulting BSA concentration**	**Resulting BSA in 20 µl**
#1	BSA stock solution		1 µg/µL	20 µg
#2	50 µL	50 µL from tube #1	0.5 µg/µL	10 µg
#3	50 µL	50 µL from tube #2	0.25 µg/µL	5 µg
#4	50 µL	50 µL from tube #3	0.125 µg/µL	2.5 µg
#5	50 µL	50 µL from tube #4	0.063 µg/µL	1.25 µg
#6	50 µL	50 µL from tube #5	0.031 µg/µL	0.625 µg
#7	50 µL	-	0 µg/µL	0 µg

3.12 Statistical Analysis

Graph pad prism 6.01 was used in plotting graph pads used in representing luciferase results and determining the statistical differences in luciferase values.

4. Results

4.1 Detection of MCPyV Large T antigens

A hallmark of MCPyV-positive Merkel cell carcinoma (MCCs) is the expression of truncated LT-ag [10, 16]. Full-length LT-ag consists of 817 amino acids (~100 kDa), while the virus positive MCC cell lines MKL-1, MKL-2, and MS1 express truncated LT-ag of respectively 330 (~50 kDa), 275 (~37 kDa), and 428 (~60 kDa) amino acids (Figure 4.1). To study the effect of LT-ag on the MCPyV promoter, expression plasmids for the three truncated versions of Merkel cell polyomavirus Large T antigen (MCPyV LT-ag) were constructed by site-directed mutagenesis.

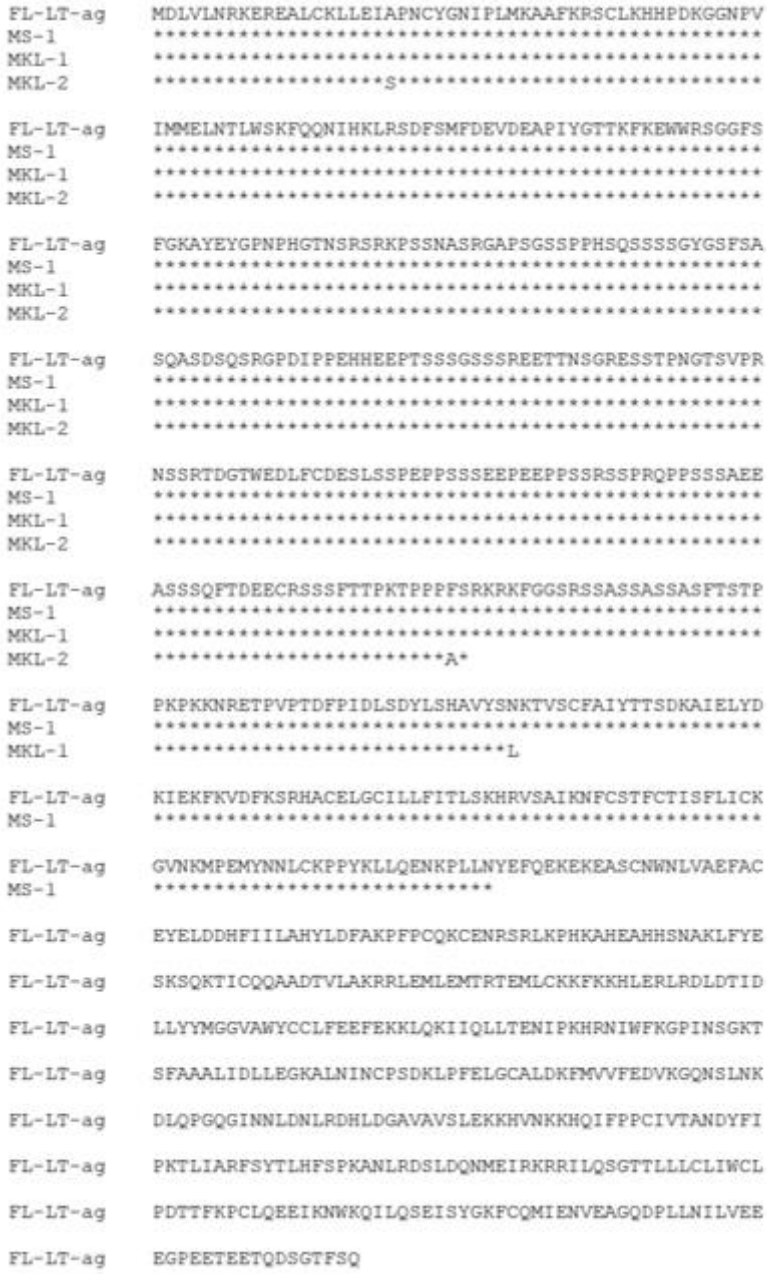

Figure 4.1: Sequence alignment of full-length LT-ag (FL-LT-ag; accession number ACI25296), and the truncated variants expressed in MKL-1 (FJI73815), MKL-2 (JX045708), and MS-1 (JX045709) MCCs. Identical amino acid residues are indicated by asterisks**.**

The expression vector pcDNA6-MCPyV-LT-ag, encoding full-length MCPyV LT-ag, present in MIRG Laboratory was used as the DNA template, for the construction of truncated LT-ag found in MCC cell lines MKL1, MKL2 and MS-1, whose sequences are known [130]. To confirm the successful construction of expression plasmids for these truncated versions of MCPyV LT-ag that are found in MCC, the plasmids were sequenced (data not shown) and their protein expressions were analyzed by western blotting in HEK 293 cells. HEK293 cells were

transfected with expression plasmids encoding versions of MCPyV LT-ag (FLT-ag, MKL-1, MKL-2 and MS-1), and the MCPyV LT-ag specific antibody CM2B4, that recognizes both full-length and truncated LT-ag, was tested on the lysates from the respective transfected cells. Used as a positive and negative control were expression plasmids for FLT-ag and empty vector (pcDNA3) respectively.

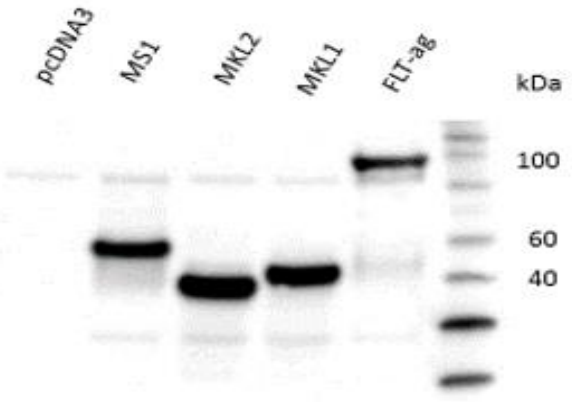

Figure 4.2: Western blot detection of MCPyV LT-ag protein expression in HEK 293 cells. HEK293 cells were transfected with empty vector pcDNA3 or expression plasmids for full-length LT-ag (pcDNA6-MCPyV-LT-ag) or truncated versions (MKL-1, MKL-2, MS-1) found in their respective MCC cell lines. Cellular proteins were subjected to SDS PAGE and western blot analysis with the MCPyV LT-ag antibody CM2B4 to detect the presence or expression of the different forms of MCPyV LT-ags. Lanes are designated with their respective LT-ag forms while the pcDNA3-designated lane contained lysates from cells transfected with empty vector and gave no visible band as a negative control. Lysates from the FLT-ag transfected cells showed a strong band at approximately 100kDa as a positive control and lysates from MKL-1, MKL-2 and MS-I transfected cells gave different bands or protein expressions at approximately 50kDa, 37kDa, and 60kDa respectively.

Figure 4.2 shows western blot analysis of expressed protein by the constructed expression plasmids for the truncated versions of MCPyV LT-ag. Truncated LT-ag proteins with the expected molecular mass of 37 kDa (MKL-2), 50 kDa (MKL-1) and 60 kDa (MS-1) were obtained, demonstrating that the site-directed mutagenesis was successful. Lysates from cells transfected with the plasmid encoding FLT-ag gave a band corresponding to ~100 kDa.

4.2 Detection of MCPyV small t antigen expression in MCC13 cells

At the inception of this study, prior to the transient transfection studies with small t antigen (st-ag) expression plasmid (pcDNA5-flag MCPyV st-ag), the integrity (efficiency) of this expression plasmid was verified by western blot. The st-ag expression plasmid was FLAG-tagged which enabled its identification by using an anti-flag antibody in the absence of an anti-st-ag antibody [63].

In order to confirm the integrity of this expression plasmid for MCPyV st-ag protein (pcDNA5-flag MCPyV st-ag), MCC13 cells were transfected with this plasmid and the cells were harvested. Anti-flag antibody that recognizes the flag-tag of small t antigen expression plasmid (pcDNA5-flag MCPyV st-ag) was tested on the lysates from the respective transfected cells. Two controls were used for this western blotting analysis to detect MCPyV st-ag expression, where wells of cells were not transfected and labeled negative and another population of cells were transfected with empty vector (pcDNA3).

This western blot analysis (Figure 4.3) confirmed the expression and integrity/effectiveness of the st-ag expression plasmid. A signal of approximately 20 kDa was visible corresponding to the 186 aa long MCPyV st-ag.

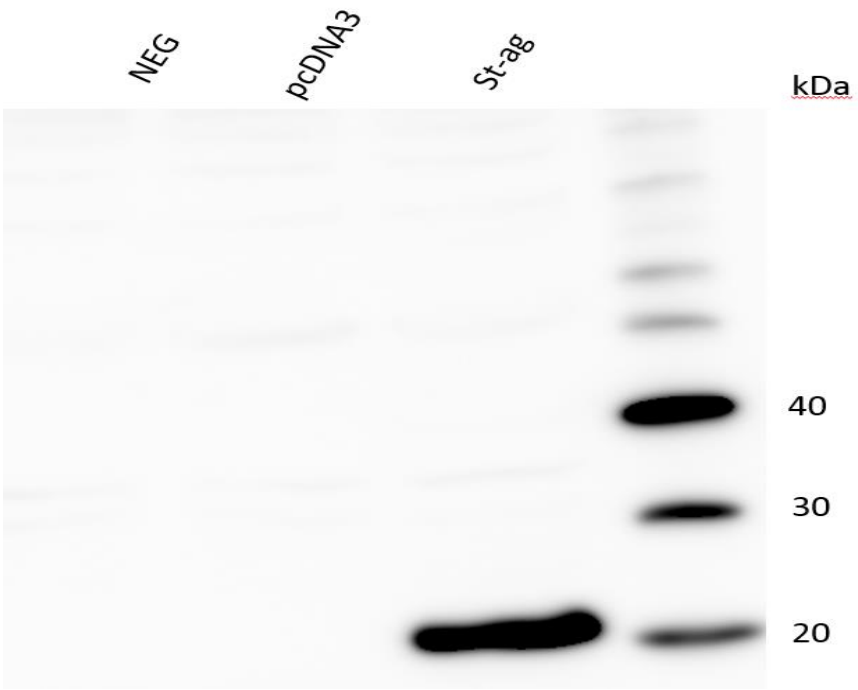

Figure 4.3: Western blot with anti-flag antibody of cell lysates prepared from MCC13 cell lines showing a predominant signal for MCPyV st-ag. MCC13 cells were transfected with empty vector (pcDNA3) or expression plasmids for small t-antigen (pCDNA5-Flag MCPyV st-ag). Cellular proteins were subjected to SDS PAGE and western blot analysis with anti-FLAG antibody to detect presence/expression of st-ag which has been flag-tagged. Lanes were labelled with their respective protein expression. The pcDNA3 and NEG designated lanes contained lysates from empty vector transfected cells and un-transfected cells respectively. Lysates from both un-transfected and pcDNA3 transfected cells gave no visible band as negative controls, while the lysates from the st-ag transfected cells showed a strong band at approximately 20kDa, detecting the expression of MCPyV small t-antigen.

4.3 NCCR nucleotide alignment for MCPyV strains (MCC350 and 16b)

On comparison of the genomes of the several different Human Polyomaviruses, conservation of the coding regions was revealed but a variation in NCCR region was seen. Studies have shown that the strength of the viral promoter is influenced by these mutations and may be linked to an alteration in virulence of the virus [131,132].

So far, the NCCR of 50 different MCPyV isolates have been sequences (GenBank; May 2016). Their NCCRs are highly conserved with only few point mutations (see Supplementary Table 1). However, one variant, MCPyV 16b isolated from healthy skin [20], displays larger insertions compared to the NCCRs of other MCPyV isolates (Figure 4.4).

The alignment and comparison between the NCCR of the two MCPyV strains shows that there is a high percentage of conserved regions and homology with a number of deletions in that of

MCC350 relative to that of 16b NCCR. The NCCR of MCC350 and 16b MCPyV strains have a size of 464bp and 496bp respectively. The NCCR of the 16b strain is approximately 20bp longer than that of the MCC350 NCCR showing some differences in their NCCR nucleotide sequence. These changes in the NCCR could give an inference on promoter activities and the pathogenic properties of the virus.

```
MCC350      CCTGAAAAATAAATAAGGATACTTACTCTTTTAATGTC-------------------------CTCCT
16b         CCTGAAAAATAAATAGGGATACTTACTCTTTTAATGTCCTCCTCCCTTTGTAAGAGAAATGTCCTCCT
            *************** ***********************                           *****

MCC350      CCCTTTGTAAGAGAAAAAAAAGCCTCCGGGCCTCCCTTGTTGAA-------AAAAAGTTAAGAGTTTT
16b         CCCTTTGTAAGAGAAAAAAAAGCCTCCGGGCCTCCCTTTTGTTGAAAAAAAGTTGAGTTAAGAGTTTT
            ************************************* *           *****************

MCC350      CCGTCTCCCTCCCAAACAGAAAGAAAAAAAGTTTTGTTTATCAGTCAAACTCCGCCTCTCCAGGAAAT
16b         CCGTCTCCCTCCCAAACAGAAAGAAAAAAAGTTTTGTTTATCAGTCAAACTCCGCCTCTCCAGGAAAT
            ************************************************************************

MCC350      GAGTCAATGCCAGAAACCCTGCAGCAATAAAAGTTCAATCATGTAACCACAACTTGGCTGCCTAGGTG
16b         GAGTCAATGCCAGAAACCCTGCAGCAATAAAAGTTCAATCATGTAACCACAACTTGGCAGCCTAGGTG
            ************************************************************ **********

MCC350      ACTTTTTTTTTTCAAGTTGGCAGAGGCTTGGGGCTCCTAGCCTCCGAGGCCTCTGGAAAAAAAAGAGA
16b         ACTTTTTTTTTTCAAGTTGGCAGAGGCTTGGGGCTCCTAGCCTCCGAGGCCTCTGGAAAAAAAAGAGA
            ************************************************************************

MCC350      GAGGACTCTGAGGCTTAAGAGGCTTAATTAGCAAAAAAGGCAGTATCTAAGGGCAGATCCCAAGGGCG
16b         GAGGCCTCTGAGGCTTAAGAGGCTTAATTAGCAAAAAAGGCAGTATCTAAGGGCAGATCCCAAGGGCG
            **** ********************************************************************

MCC350      GGCGGGAAACTGCAGTATAAAAACCACTCCTTAGTGAGGTAGCTCATTTGCTCCTCTGCTGTTTCTGC
16b         GGCGGGAAACTGCAGTATAAAAACCACTCCTTAGTGAGGTAGCTCATTTGCTCCTCTGCTCTTTCTGC
            ************************************************************ *******

MCC350      AAACTCCTTCTGCATATAGACAAG
16b         AAACTCCTTCTGCATATAGACAAG
            ************************
```

Figure 4.4: Sequence alignment of the MCC350 and 16b NCCR. The nucleotide sequence of the NCCR of MCC350 (GenBank accession number EU375803) and 16b strains (GenBank accession number HM011548) of MCPyV were aligned using BLAST program from PUBMED. Identical, deleted and mismatched/substituted sequences are indicated by asterisks, dashes, and spaces respectively.

4.4 Estimation of relative transfection efficiency of cell lines

Transfection studies in this study were done in three different cell lines: HEK 293, MCC13 and C33A.The rationale behind choosing these three cell lines is mentioned in 4.6. In evaluating the transfection efficiency in the cell lines used, the respective cells were seeded as described in 3.7.2 and transfected with expression plasmid for green fluorescence protein (pEGFP-C1) as

described in 3.8. The number of green cells viewed with fluorescent microscope (i.e. cells expressing green fluorescent protein) compared to the total number of un-transfected cells as seen in visible light (bright field) gave an estimate of the transfection efficiency expressed by respective cells.

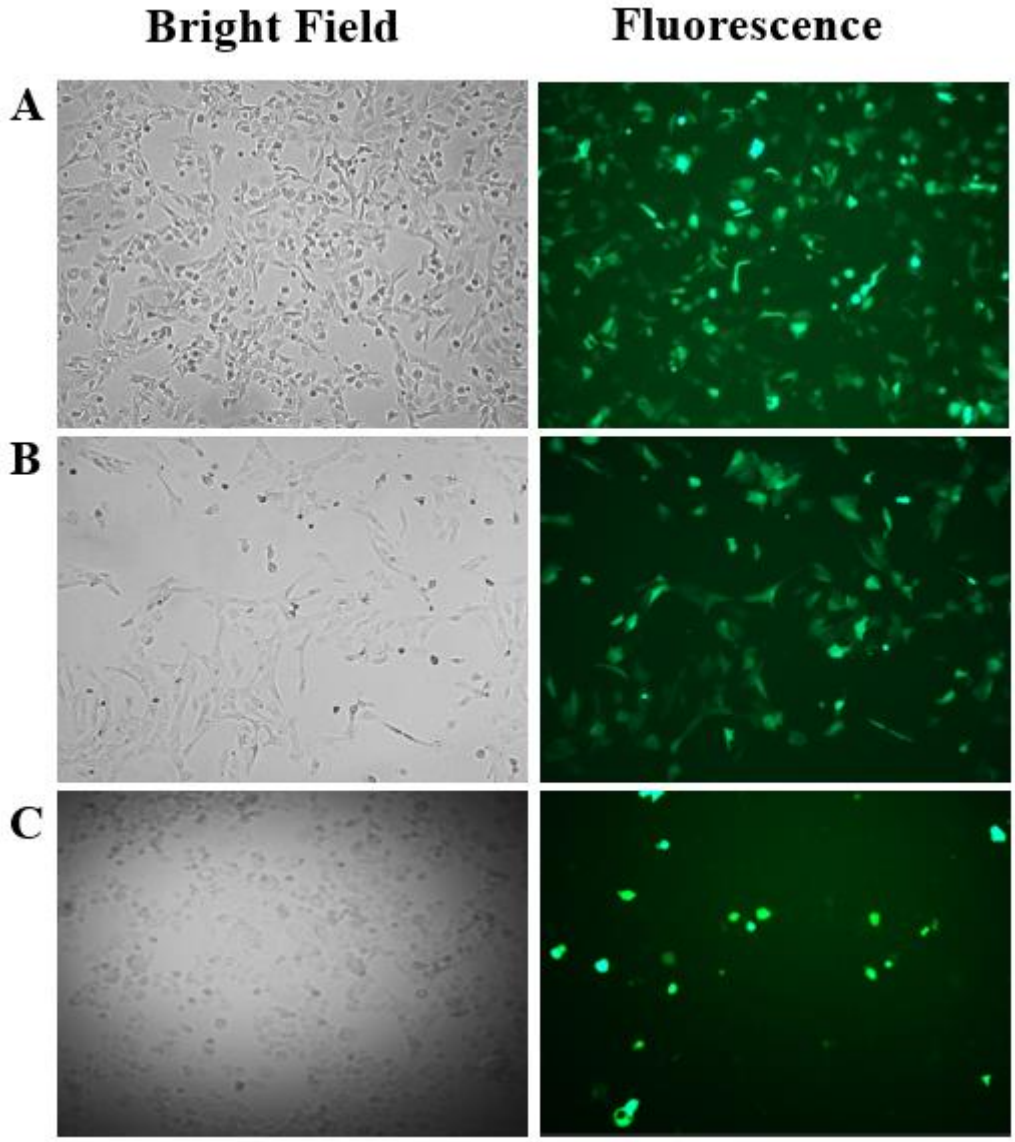

Figure 4.5: Comparable transfection efficacy among cells of HEK 293 (**A**), MCC13 (**B**) and C33A (**C**). HEK 293 or MCC13 or C33A cells were seeded and transfected the next day with expression plasmid for green fluorescence protein (pEGFP-C1). Twenty-four hours after the cells were transfected., the cells were examined by a fluorescent microscopy with visible light (left panel) or fluorescent light (right panel).

Figure 4.1 displays the respective transfection efficiencies in cells of HEK 293, MCC13 and C33A as approximately 90%, 75% and ~30% respectively. Relative transfection efficiency is highest in HEK293 and lowest in C33A cells.

4.5 Comparison of the early promoter activities of MCPyV MCC350 and 16b strains

The early and late promoters of MCPyV are vital in regulating entry into viral cycle and infectivity [10]. The observation of differences between the NCCR nucleotide sequences of MCC350 and 16b MCPyV instigated an investigation to compare the activities of their early and late promoters.

To compare the promoter activities between MCC350 and 16b MCPyV strains, transient transfection studies in HEK293, MCC13 and C33A cells with a luciferase reporter plasmid containing either the MCPyV early or late promoter were done**.** So far, a cell line that supports MCPyV replication is lacking. HEK293 cells were chosen because they are easy to transfect and previous study by our group in 10 different cell lines had shown that the MCPyV early and late promoter activity is among the strongest in this cell line [133]. Merkel cell lines are not available, so therefore MCC13 as a MCPyV-negative Merkel cell carcinoma cell line was selected [44]. Twenty-four hours after transfection, the cells were harvested for early and late promoter strength analyzes by monitoring activity of the *luciferase* reporter gene. The amount of luciferase protein produced is directly proportional to the promoter strength of the MCPyV promoter. The protein concentration of each lysate, excluding lysates from C33A cells, were measured and used to normalize the relative luciferase value of the corresponding sample.

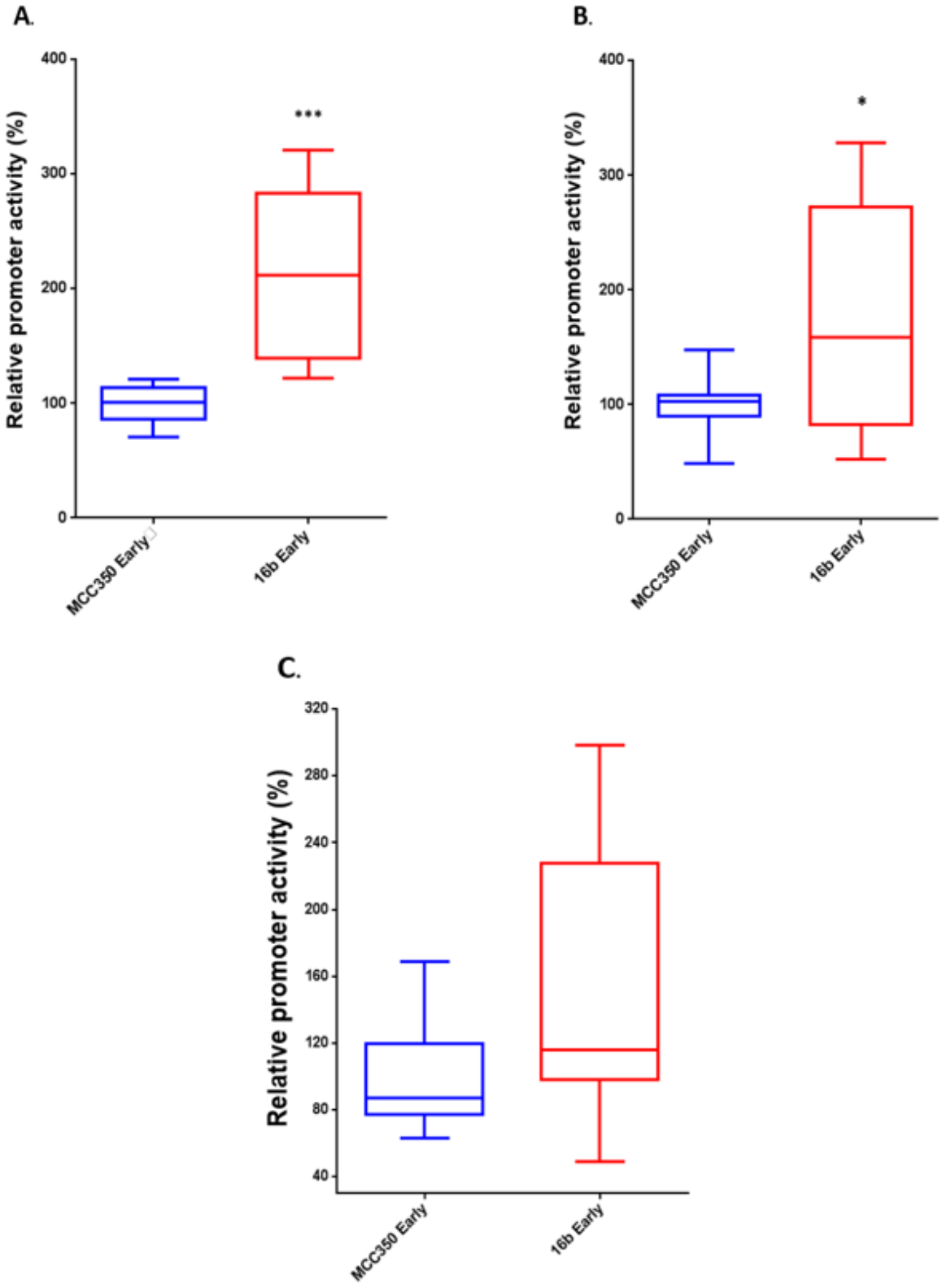

Figure 4.6: MCPyV 16b early promoter activity is higher relative to that of MCC350 MCPyV strain in HEK293 and MCC13 cells**. (A)** Comparison of early promoter activities between MCC350 and 16b MCPyV strains in HEK 293 cells. HEK 293 cells were transfected with luciferase reporter plasmids containing either the MCC350 early promoter (pGL3-basic MCPyV LUC Early) or 16b early promoter (Forward-MCPyV-16b pGL3-Basic). Relative luciferase units (RLU) of luciferase activity driven by either the MCC350 early promoter or 16b early promoter in transiently transfected cells was measured and

normalized to the protein contents in each sample. Represented with box plots are the median, first and third quartile of three independent parallels 24 hours after transfection. The whiskers represent the minimum and maximum value. The data are representative of three independent experiments with each experiment performed with three independent parallels. The luciferase activity of the MCC350 early promoter was arbitrarily set as 100% and the 16b early promoter was related to the relative activity of MCC350. An unpaired t-test represented with asterisks (***) showed that the difference between the data sets was significant (p = 0.0003). **(B).** as in **(A)** but MCC13 cells were used. An unpaired t-test represented with an asterisk (*) shows that the difference between the data sets was significant (p = 0.03). **(C).** as in **(A)** but C33A cells were used. An unpaired t-test shows that the difference between the data sets was insignificant.

Figures 4.6A and 4.6B both indicate that the MCPyV 16b strain has a stronger early promoter activity relative to that of MCPyV MCC350 strain in HEK 293 and MCC13 cells respectively, while in C33A cells, the relative early promoter strength were similar (Figure 4.6C) In HEK 293 cells (Figure 4.6A), 16b strain exhibited a significant upregulation by about 2 times its early promoter activity relative to the normalized MCC350 control, while in MCC13 cells (Figure 4.6B) 16b strain exhibited a significant upregulation by 1.8 times its promoter activity relative to the MCC350 promoter. Thus in both cell lines, the difference between the early promoter strength of MCPyV MCC350 and 16b was significant. The relative stronger activity of the MCPyV 16b early promoter compared to MCC350 was similar (about 2-fold) in both cell lines.

4.6 Comparison of the late promoter activities of MCPyV MCC350 and 16b strains

The activities of the late promoters of the MCPyV MCC350 and 16b strains were monitored in HEK293, MCC13 and C33A cells. The result shows that in HEK293 cells, the MCC350 late promoter activity was 1.5-fold stronger ($p=0.0003$) than the late 16b promoter (Figure 4.7A). Conversely, in both MCC13 and C33A cells, the late promoter activity of 16b MCPyV strain was about 2-fold stronger ($p<0.0001$) and ($p=0.0109$) respectively than the late MCC350 promoter (Figures 4.7B and 4.7C). The significant differences (fold increase or decrease) is seen to be higher, in the luciferase activity measured in MCC13 cells (Figure 4.7B) when compared to that seen in HEK 293 and C33A cells (Figures 4.7A and 4.7C). The relative late promoter activities between MCPyV MCC350 and 16b strains appear to differ in only HEK293 cells.

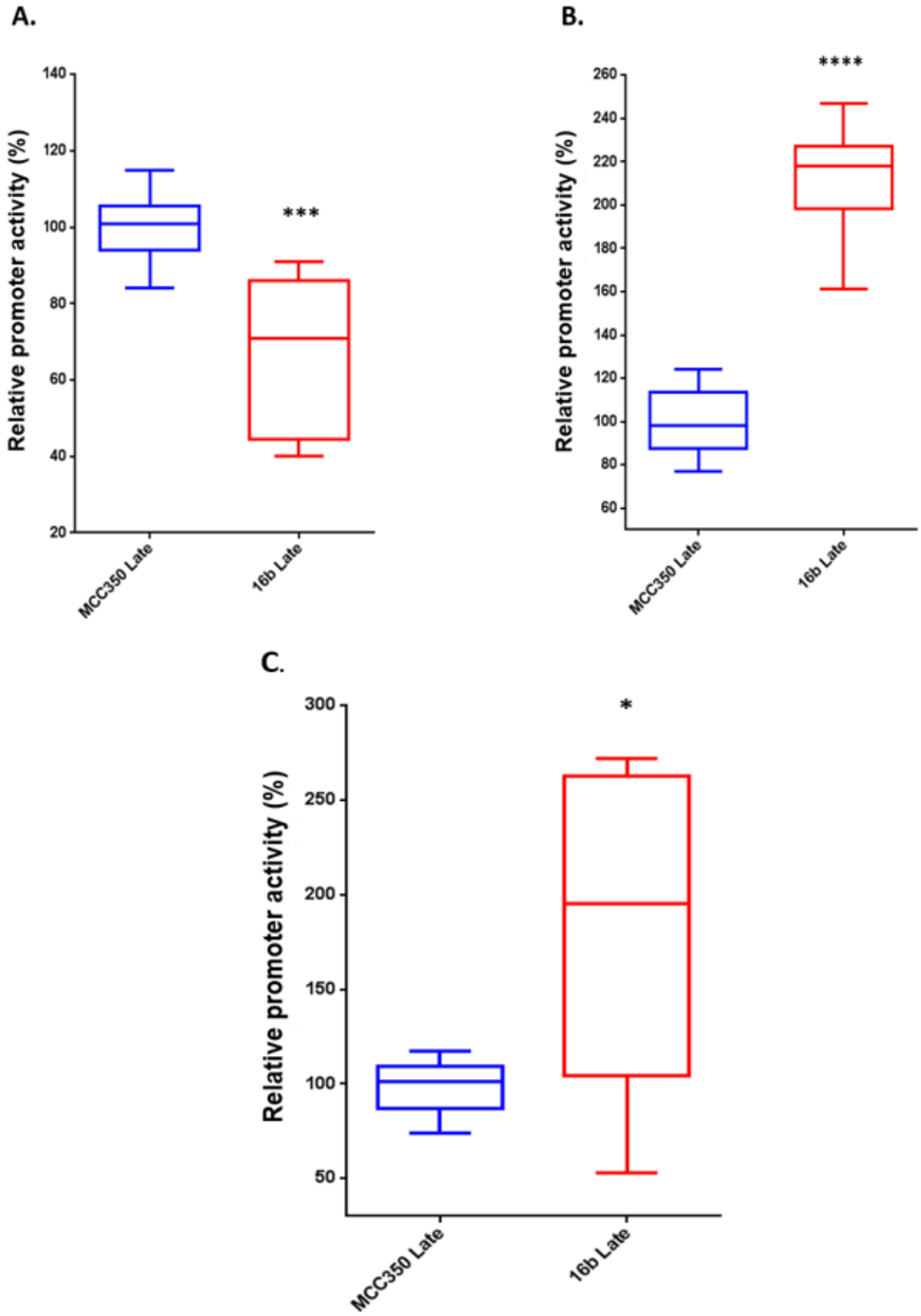

Figure 4.7: MCPyV MCC350 late promoter activity is higher in HEK293 cells but lower in MCC13 and C33A cells relative to MCPyV 16b late promoter activity**.** (**A**) Comparison of late promoter activities between MCC350 and 16b MCPyV strains in HEK 293 cells. HEK 293 cells were transfected with luciferase reporter plasmids containing MCC350 late promoter (pGL3-basic MCPyV LUC Late) or 16b

late promoter (Reverse-MCPyV-16b pGL3-Basic). Luciferase activity driven by either the MCC350 late promoter or 16b late promoter in transiently transfected cells was measured and corrected for the protein concentration of each sample. The normalized luciferase activity of the MCC350 late promoter was arbitrarily set as 100% and the 16b late promoter was related to the relative activity of MCC350. Each box plot represents the average of 3 independent experiments performed with three independent parallels. The blue box plot displays the MCC350 late promoter activity, while the red plots 16b late promoter activity. An unpaired t-test represented with asterisks (***) showed that the difference between the data sets was significant (p = 0.0003). **(B).** As in **(A),** but the late promoter activities of the MCC350 and 16b MCPyV strains were compared in MCC13 cells. An unpaired t-test represented with asterisks (****) showed that the difference between the data sets was significant (p < 0.0001). **(C).** as in **(A)** but C33A cells were used. An unpaired t-test represented with asterisks (*) showed that the difference between the data sets was significant (p = 0.0109).

4.7 Regulatory effect of MCPyV small t antigen expression on the activities of MCPyV MCC350 and 16b early and late promoters

The st-ag promotes the expression of LT-ag and possesses oncogenic potentials in cell culture and animal models [44, 50, 53]. Therefore, it is assumed to play a significant role in tumor cell maintenance and MCC tumorigenesis [134]. Whether st-ag can influence the MCPyV promoter is unknown, but exploring its putative regulatory role on the expression of early and late MCPyV proteins (i.e. early and late MCPyV promoter activities) would give an insight into its function in tumor cell maintenance and MCC tumorigenesis.

Transient transfection studies in both MCC13 and HEK293 were done to investigate the effect of MCPyV st-ag expression on early and late promoter activities of MCPyV MCC350 and 16b strains. Co-transfection of HEK293 and MCC13 cells with expression vectors encoding MCPyV st-ag (pcDNA5 flag MCPyV st-ag) together with luciferase reporter plasmids containing either the MCPyV (MCC350 or 16b strain) early or late promoter showed that MCPyV st-ag significantly upregulates the activity of MCC350 early and late promoters. The rate or magnitude at which the st-ag enhances the activity of the late promoter (Figure 4.8B) is higher when compared to that of the early promoter (Figure 4.8A). A 3-fold and 2-fold increase was observed in the late and early promoters of MCC350 respectively in the presence of MCPyV st-ag.

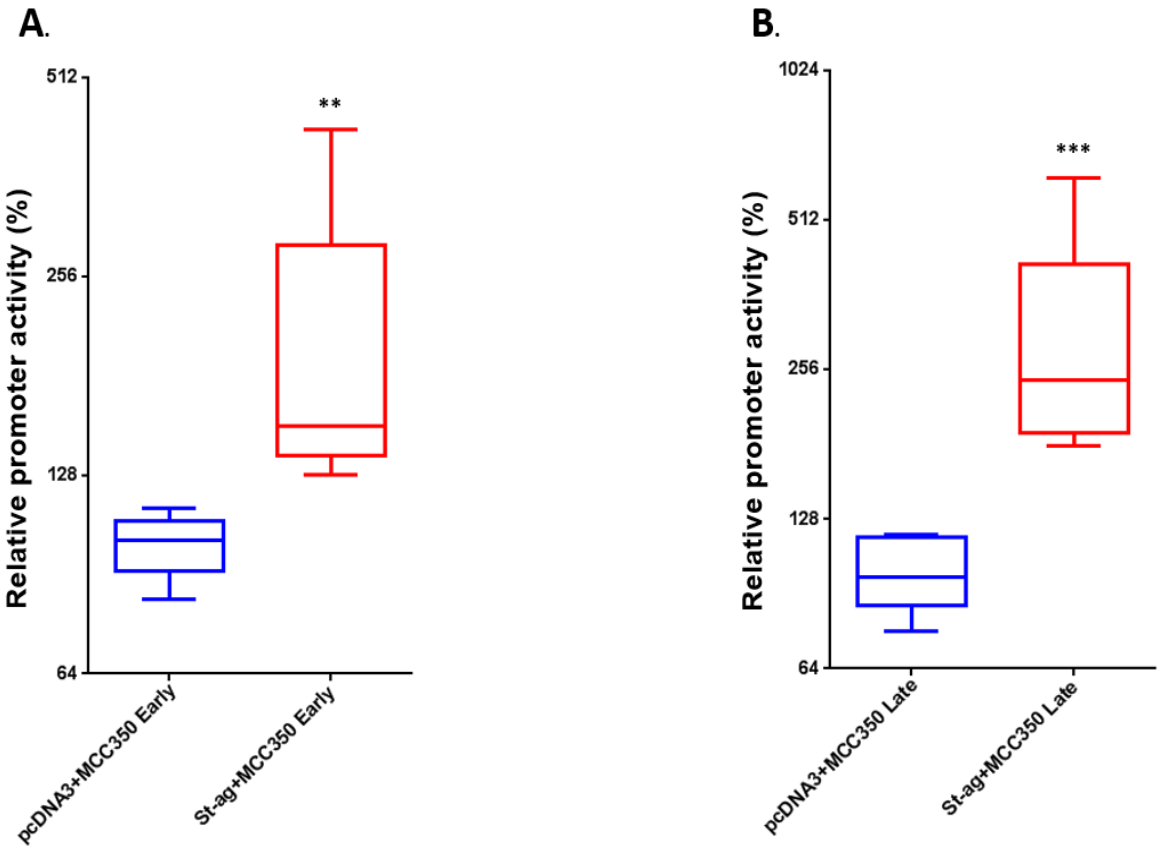

Figure 4.8: MCPyV st-ag expression enhances early and late MCC350 promoter activity in HEK293 cells. **(A)** MCC350 early promoter activity in the presence of empty vector pcDNA3 or MCPyV st-ag expression plasmid in HEK 293 cells. The luciferase values were corrected for the protein concentration in the corresponding sample and the activity of the MCC350 early (respectively late) promoter in the presence of pcDNA3 was arbitrarily set as 100%. The activity of the promoter in the presence of st-ag was related to the activity in the absence of st-ag. The values for three independent parallels are depicted. All experiments were done in triplicates and the median, first and third quartile represented herein. The whiskers represent the minimum and maximum value. An unpaired t-test represented with asterisks (**) showed that the effect of MCPyV st-ag expression on MCC350 Early promoter is significant (P = 0.0054). **(B)** As in **(A)** but MCC350 late promoter activity was monitored in the presence or absence of MCPyV st-ag. An unpaired t-test represented with asterisks (***) showed that the difference between the data sets was significant (P =0.0008).

These results (Figure 4.8 A and 4.8B) signify that in the presence of MCPyV st-ag, the early and late promoter activities of MCPyV MCC350 were stimulated by about 2folds (Figure 4.8A) and 3folds (Figure 4.8B) respectively.

Similarly, results shown in Figures 4.9A and 4.9B indicate that the activity of 16b MCPyV early promoter (Figure 4.9A) and late promoter (Figure 4.9B) were enhanced about 2-fold in the presence of MCPyV st-ag in HEK293 cells.

.

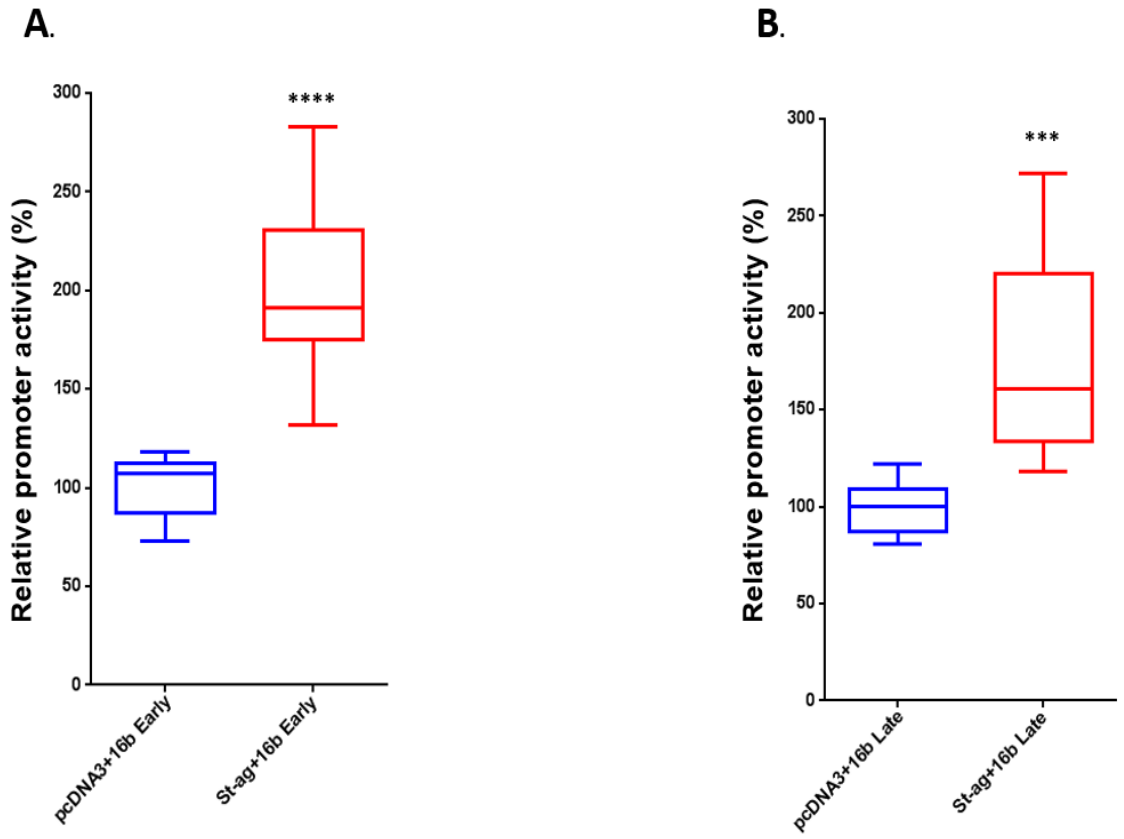

Figure 4.9: MCPyV st-ag expression enhances early and late 16b MCPyV promoter activities in HEK293 cells. **(A)** Effect of MCPyV st-ag on the MCPyV 16b early promoter activity in HEK 293 cells. The activity of the promoter in absence of st-ag was arbitrarily set as 100% and the activity in the presence of st-ag was correlated to this. An unpaired t-test represented with asterisks (****) showed that the effect of st-ag expression on MCC350 Early promoter is significant ($P < 0.0001$). **(B)** As in (A), but MCPyV 16b late promoter activity was monitored in the presence or absence of MCPyV st-ag. An unpaired t-test represented with asterisks (***) showed that the difference between the data sets was significant ($P = 0.0005$).

4.8 Comparison of the effect of MCPyV small t antigen on the activities of MCPyV MCC350 and 16b early and late promoters in HEK293 cells

A comparison of the regulatory effect of MCPyV st-ag on early and late MCC350 and 16b promoters was done to determine the relative stimulatory magnitude between the early and late promoters of the two MCPyV strains in HEK 293 cells. The activity of the early MCPyV 16b promoter in the presence of st-ag was significantly higher than that of the early MCC350 promoter (Figure 4.10A). However, no significant differences in MCC350 and 16b late promoter was observed when st-ag was expressed (Figure 4.10B).

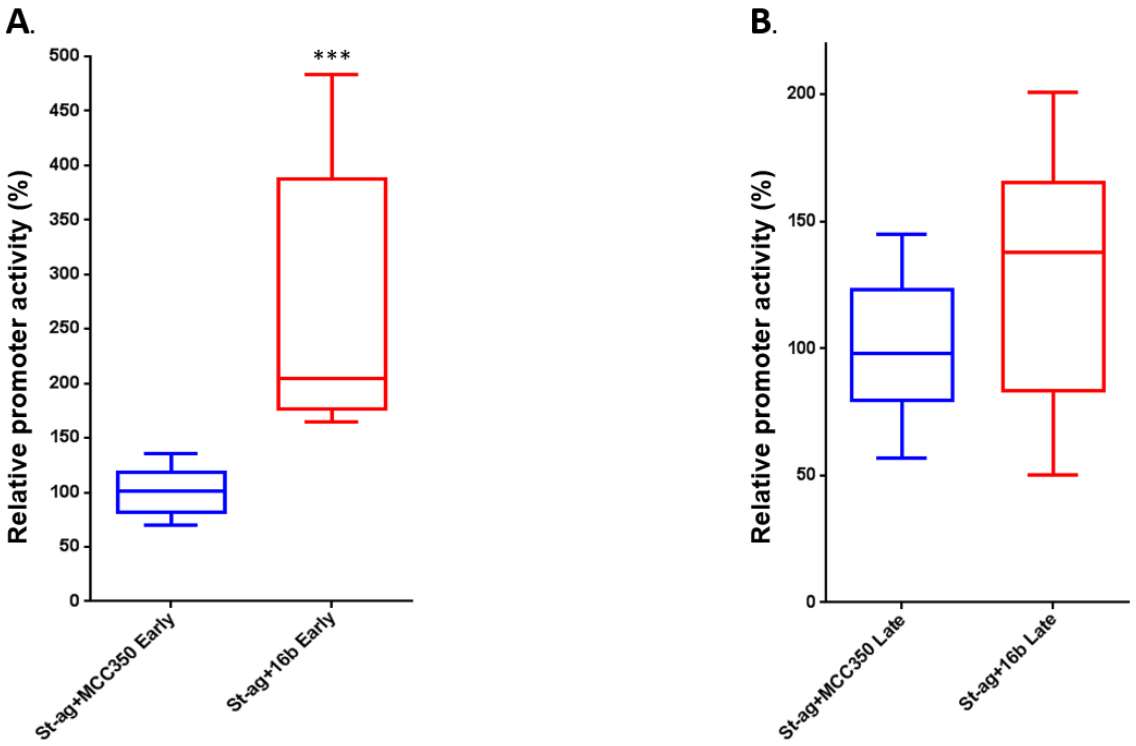

Figure 4.10: Comparison of the stimulatory effect of MCPyV st-ag on 16b early and late and MCC350 early and late promoters in HEK 293 cells. **(A).** Relative stimulation of MCC350 and 16b early promoter activities on MCPyV st-ag expression in HEK 293 cells. The activity of the MCC350 early promoter in the presence of st-ag was arbitrarily set as 100%. The results represent the average of 3 experiments performed with three separate parallels. An unpaired t-test represented with asterisks (***) showed that the difference between the data sets was significant (p =0.0008). **(B)** As in **(A)**, but the late promoter activity of MCC350 and 16b in the presence of st-ag were examined. An unpaired t-test indicated that no significant difference was observed.

4.9 Regulatory effects of MCPyV full length Large T antigen expression on the activities of MCPyV MCC350 and 16b early and late promoters in HEK293 cells.

LT-ag of human polyomaviruses is able to regulate its own expression by activating the early promoter, but it can also effect viral late gene expression. Hence, LT-ag-regulated expression of viral genes is important because it will affect the activity of the virus [63, 135]. To examine whether MCPyV LT-ag interferes with early and late expression, transfection studies were performed in HEK293 and MCC13 cells with a luciferase reporter plasmid containing the MCPyV early or late promoter. Both the MCC350 and 16b promoter variants were tested. Full length LT-ag (FLT-ag) inhibited the MCC350 early and late promoter in HEK293 cells, however FL T-ag has a stronger inhibitory effect on the early promoter (83-fold versus 11-fold; Figure 4.11). Similarly, FLT-ag repressed the 16b early and late promoter in these cells. The

inhibitory effect of FLT-ag was higher on early promoter (27-fold) than on the late 16b promoter (8-fold; Figure 4.12).

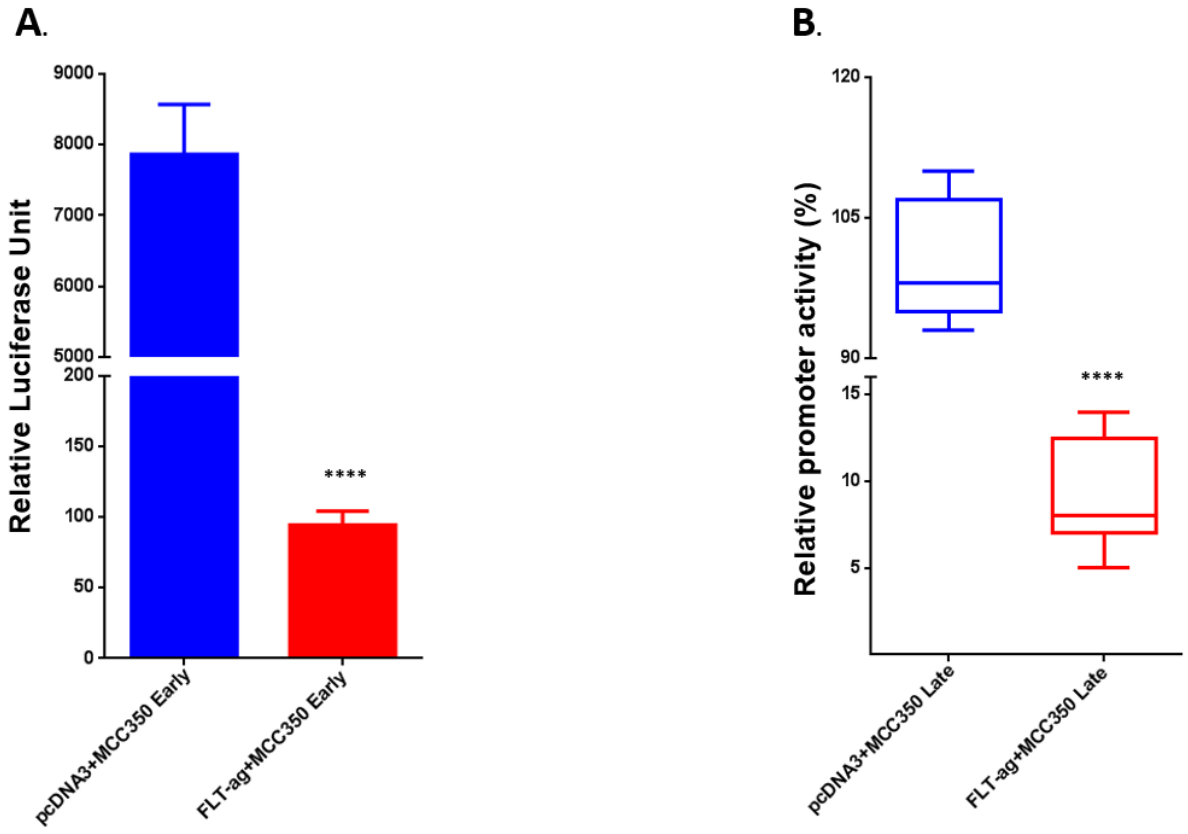

Figure 4.11: MCPyV FLT-ag expression inhibits MCC350 early and late promoter activities in HEK293 cells. The data were represented differently using bars (**A**) and box plot (**B**) because the magnitude of FLT-ag inhibition in (**A**) was extreme and a box plot would not sufficiently represent the data. **(A)** MCC350 early promoter activity in the presence of empty vector or MCPyV FLT-ag expression plasmid in HEK 293 cells. The relative promoter activities were calculated as described in the legend of **Figure 4.8A.** Data represented with bars are the means ± SD of relative promoter activity from three determinations and are a representative of three separate experiments. The gaps and direction on the Y axis is presented in two segments in order to give a visible representation of the FLT-ag inhibition which was at a high magnitude. An unpaired t-test represented with asterisks (****) showed that the difference between the data sets was very significant ($p < 0.0001$). **(B).** As in (Figure 4.8A), but MCPyV MCC350 late promoter activity was monitored in the presence or absence of MCPyV FLTag-ag. The results represent the average of 3 experiments performed with three independent parallels. The gaps and direction on the Y axis are as in **(A)**. An unpaired t-test represented with asterisks (****) showed that the difference between the late promoter activities in the presence of pcDNA3 and FLT-ag expression was very significant ($p < 0.0001$).

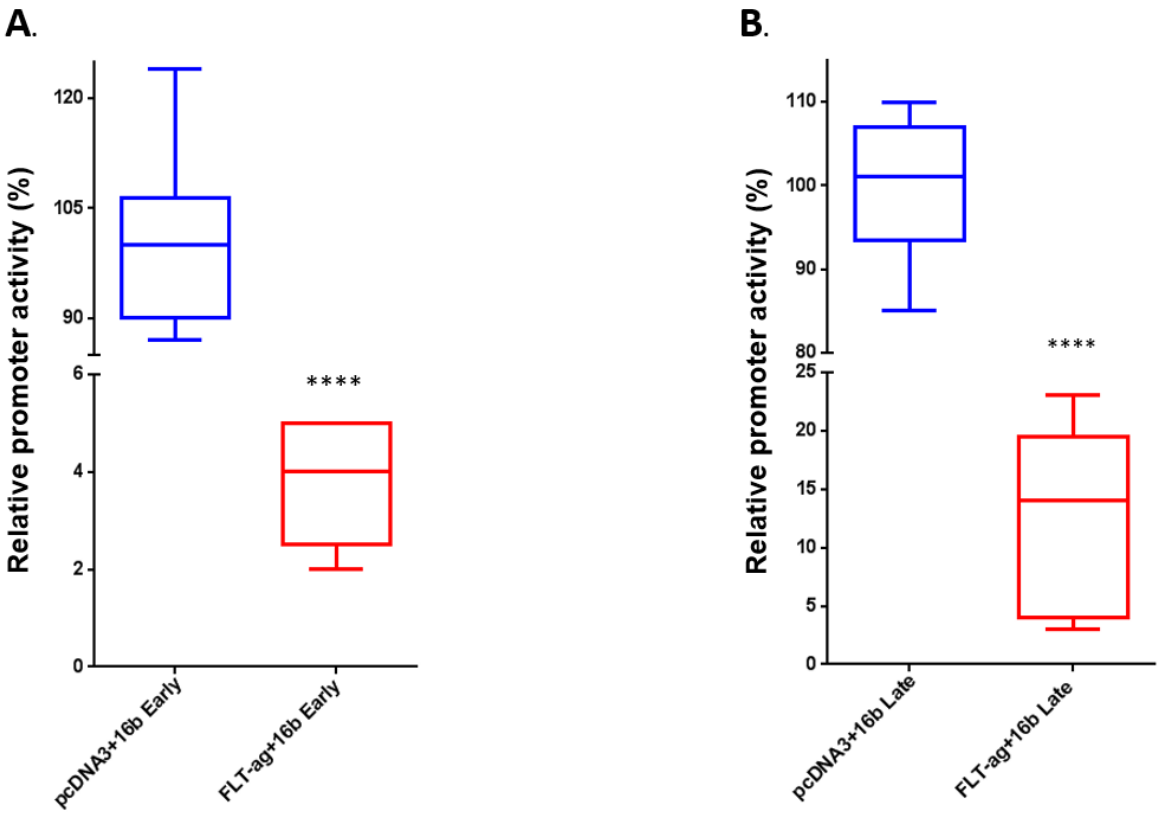

Figure 4.12: FLT-ag expression inhibits MCPyV 16b early and late promoter in HEK293. **(A)** Effect of MCPyV FLT-ag on the MCPyV 16b early promoter activity in HEK 293 cells. The activity of the promoter in the presence of pcDNA3 was arbitrarily set as 100% and the activity in the presence of FLT-ag was correlated to this. An unpaired t-test represented with asterisks (****) showed that the effect of FLT-ag expression on MCC350 Early promoter is significant ($P < 0.0001$). **(B)** As in **(A)**, but MCPyV 16b late promoter activity was monitored in the presence or absence of MCPyV FLT-ag. An unpaired t-test represented with asterisks (***) showed that the difference between the data sets was significant ($P < 0.0001$).

4.10 Regulatory effect of MCPyV st-ag and FLT-ag co-expression on the activities of MCPyV MCC350 and 16b early and late promoters in HEK 293 and MCC13 cells.

Human polyomavirus st-ag exerts an auxiliary role for LT-ag [42, 43]. Since MCPyV st-ag and LT-ag have been observed to enhance and repress activities of early and late MCPyV promoters (Results 4.8 and 4.11) respectively, an investigation into the regulatory effect of their co-expression on MCPyV early and late promoter activities became necessary.

Co-expression of MCPyV st-ag and FLT-ag evoked a repression of MCC350 early and late promoter activities in HEK293 cells (Figure 4.13A and 4.13B). MCPyV st-ag and FLT-ag co-expression inhibited activity of MCC350 early promoter about 11-fold, while a 2-fold inhibition was measured on the MCC350 late promoter.

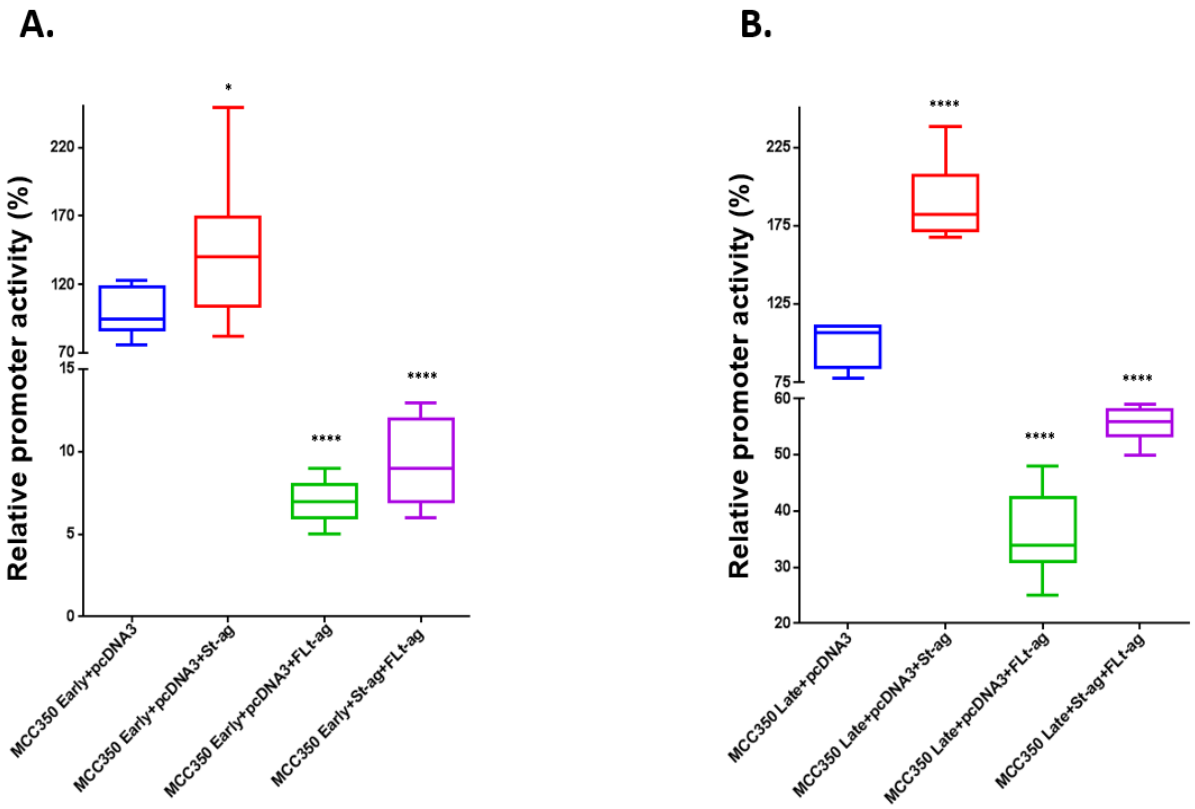

Figure 4.13: MCPyV st-ag and FLT-ag co-expression repress activities of MCC350 early and late promoters in HEK293 cells. **(A).** Effect of MCPyV st-ag and FLT-ag co-expression on the MCPyV 350 early promoter activity. HEK 293 cells were co-transfected using 400ng luciferase reporter plasmids containing the MCC350 early promoter (pGL3-basic MCPyV LUC Early) with pcDNA3 (400ng) or pcDNA3 (200ng) + st-ag (200ng) or st-ag (200ng) + FLT-ag. The promoter activity in the presence of pcDNA3 was arbitrarily set as 100% and the activity in the presence of st-ag, or FLT-ag or st-ag+FLT-ag was corrected to this. Represented with box plots are the median, first and third quartile of three independent parallels and are representative of three independent experiments. The whiskers indicate the minimum and maximum values. The blue, red, green and purple box plots display promoter activities in the presence of pcDNA3, st-ag, FLT-ag or st-ag+FLT-ag respectively. An unpaired t-test represented with asterisks showed that the differences between the data sets were significant, with MCC350 early promoter activity on st-ag and FLT-ag co-expression specifically having a P value < 0.0001. **(B).** As in **(A)** but MCPyV MCC350 late promoter activity was monitored in the presence of MCPyV st-ag, or FLT-ag or St-ag+FLT-ag. An unpaired t-test represented with asterisks showed that the differences between the data sets were significant, with MCC350 late promoter activity on st-ag and FLT-ag co-expression specifically having a P value < 0.0001.

A confirmation of the impeding effect of MCPyV st-ag plus FLT-ag on the MCC350 early and late promoter was also observed in MCC13 cells (Figure 4.14A and 4.14B). In MCC13 cells, co-expression of early MCPyV proteins inhibited the activities of MCC350 early promoter about 1.3-fold (Figure 4.14A) and MCC350 late promoter about 2-fold (Figure 4.14B). Thus a

higher extent of promoter activity repression by the early MCPyV proteins was measured on MCC350 late promoter than on its early promoter.

On comparison of both studies, the magnitude of inhibition elicited by co-expression of early MCPyV proteins on the activities of MCC350 early and late promoter was more pronounced in HEK293 cells relative to MCC13 cells.

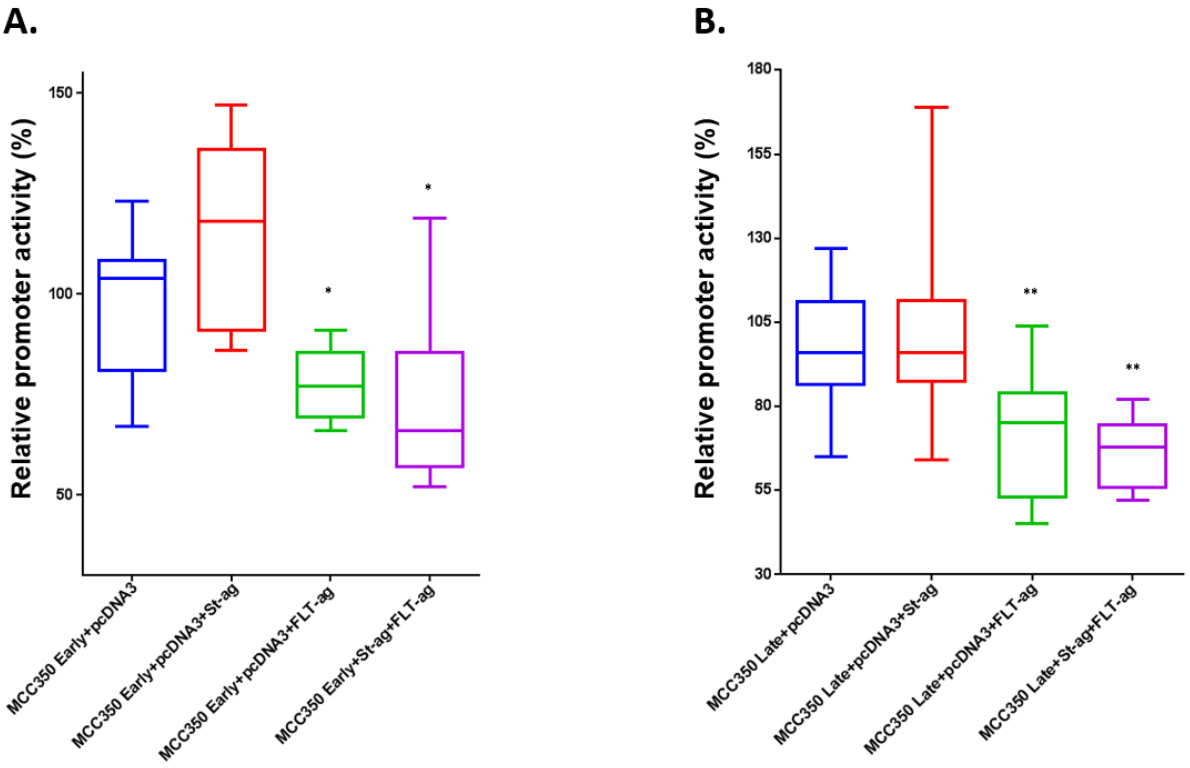

Figure 4.14: MCPyV st-ag and FLT-ag co-expression repress activities of MCC350 early and late promoters in MCC13 cells. **(A).** As in **Figure 4.13A** but MCC13 cells were used. An unpaired t-test represented with asterisks showed that the differences between the data sets were significant, with MCC350 early promoter activity on st-ag and FLT-ag co-expression specifically having a P value = 0.026. **(B)** As in **Figure 4.13A** but MCPyV MCC350 late promoter activity was monitored in the presence of MCPyV st-ag, or FLT-ag or st-ag+FLT-ag in MCC13 cells. An unpaired t-test represented with asterisks showed that the differences between the data sets were significant, with MCC350 late promoter activity on st-ag and FLT-ag co-expression specifically having a P value = 0.004.

Next, we explored the effect of the MCPyV early proteins on the 16b promoter variant. Similarly, the activities of MCPyV 16b early and late promoters were down-regulated on co-expression of early MCPyV proteins (Figure 4.15A and 4.15B). The activities of the MCPyV 16b early and late promoters were reduced: 2- fold and 18-fold, respectively.

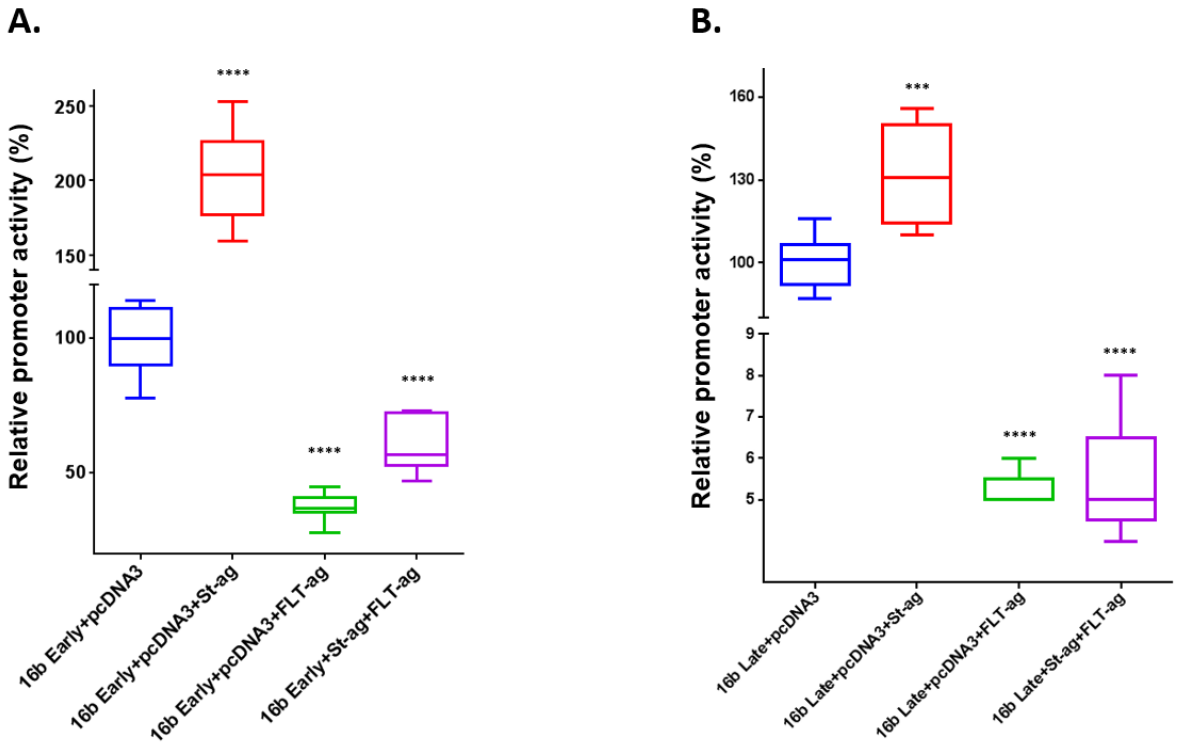

Figure 4.15: MCPyV st-ag and FLT-ag co-expression repress activities of 16b early and late promoters in HEK293 cells. **(A).** As in **Figure 4.13A** but MCPyV 16b early promoter activity was monitored in the presence of MCPyV st-ag, or FLT-ag or St-ag+FLT-ag. An unpaired t-test represented with asterisks showed that the differences between the data sets were significant, with 16b early promoter activity on expression of st-ag+FLT-ag specifically having a P value < 0.0001. **(B)** As in **Figure 4.13A** but MCPyV 16b late promoter activity was monitored in the presence of MCPyV st-ag, or FLT-ag or st-ag+FLT-ag. An unpaired t-test represented with asterisks showed that the differences between the data sets were significant, with 16b late promoter activity on expression of st-ag+FLT-ag specifically having a P value < 0.0001.

To further confirm the inhibitory effect of MCPyV st-ag plus FLT-ag co-expression on the activities of MCPyV 16b early and late promoters, the study was performed in MCC13 cells. The inhibition of MCPyV 16b early promoter activity was shown to be insignificant (Figure 4.16A), while approximately 2-fold significant repression of MCPyV 16b late promoter was observed (Figure 4.16B). This indicates that the repressive effect of MCPyV st-ag and FLT-ag co-expression on MCPyV 16b late promoter was more pronounced than on MCPyV 16b early promoter and that the effect of the early proteins may be cell-dependent.

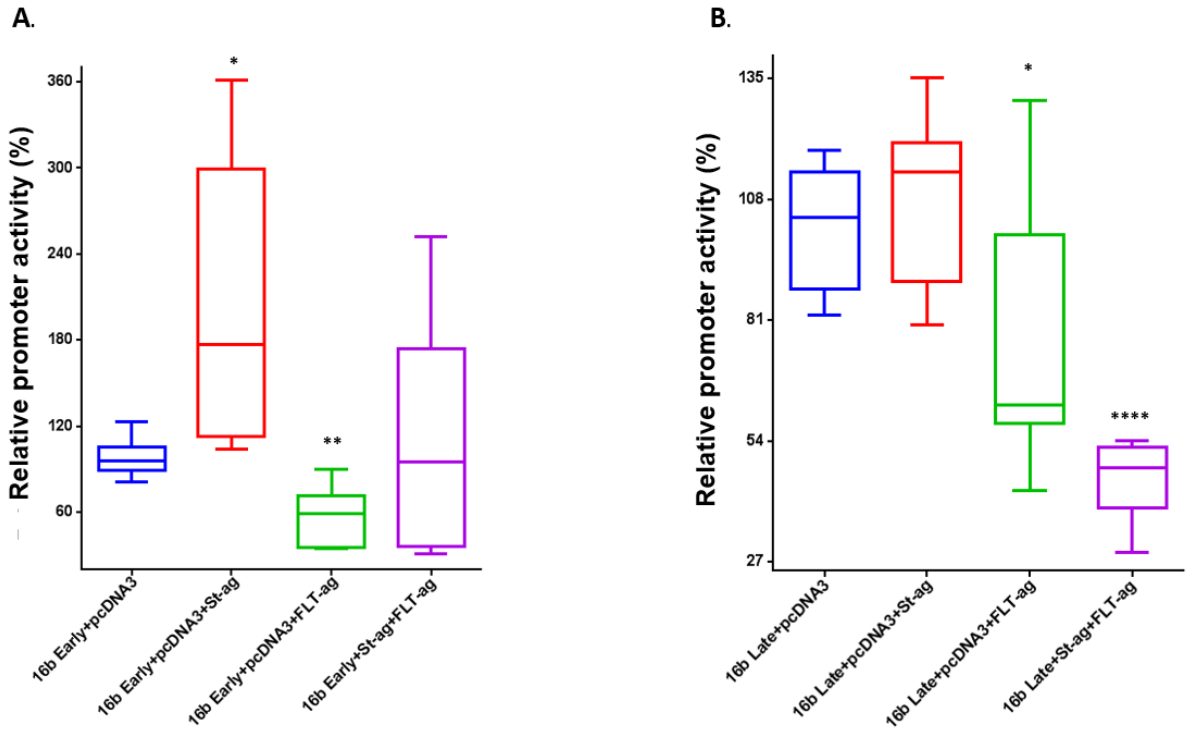

Figure 4.16: Effect of MCPyV st-ag and FLT-ag co-expression on 16b early and late promoter activities in MCC13 cells. **(A).** As in **Figure 4.13A** but MCPyV 16b early promoter activity was monitored in the presence of MCPyV st-ag, or FLT-ag or St-ag+FLT-ag in MCC13 cells. An unpaired t-test represented with asterisks showed that the differences between the data sets were significant, except 16b early promoter activity on expression of St-ag+FLT-ag which was not significant. **(B)** As in **Figure 4.13B**, but MCPyV 16b late promoter activity was monitored in the presence of MCPyV st-ag, or FLT-ag or St-ag+FLT-ag in MCC13 cells. An unpaired t-test represented with asterisks showed that the differences between the data sets were significant, with 16b late promoter activity on expression of St-ag+FLT-ag specifically having a P value < 0.0001.

4.11. Regulatory effect of truncated MKL1 LT-ag on the activities of MCPyV MCC350 early and late promoters in HEK 293 cells

The hallmarks for MCC include viral DNA integration and truncation of viral LT-ag [10, 16]. The MCC-derived truncated LT-ag (tLT-ag) promote cell proliferation and induce tumors in transgenic animals. In contrast, the FLT-ag shows a decreased potential to support cellular proliferation, focus formation, and anchorage-independent growth of osteosarcoma U2-OS cells, and it cannot induce oncogenesis until it undergoes mutations that truncates it. However, FLT-ag can transform primary baby rat kidney cells [10, 52, 48, 136]. Whether tLT-ag influences the activities of early and late promoters of MCPyV remains unknown.

To investigate the regulatory effect of tLT-ag on activities of MCPyV early and late promoters, tLT-ag derived from the MKL-1 MCC was used. Transient transfection studies were performed in HEK293 cells.

MKL-1 tLT-ag evoked a regression of early MCC350 promoter activity in a dose-dependent manner (Figure 4.17A). At low concentrations of MKL-1, there was no significant inhibition of early MCC350 promoter activity. At higher concentrations of MKL-1 tLT-ag expression, a significant activity inhibition was observed on early MCC350 promoter activity. The magnitude of activity regression was ~2-fold at the highest MKL1 tLT-ag concentration tested. Conversely, MKL-1 tLT-ag, stimulated the MCC350 late promoter activity (Figure 4.17B). The stimulatory effect elicited on MCC350 late promoter activity by MKL-1 tLT-ag expression was significant at MKL-1 tLT-ag expression plasmid concentrations of 300ng and 600ng, with the magnitude of stimulation being more conspicuous at the former than the latter concentration. Thus the effect of MKL-1 tLT-ag expression on the activities of MCC350 early and late promoters differ, with an inhibitory and stimulatory effect on the activity of the early and late promoters respectively.

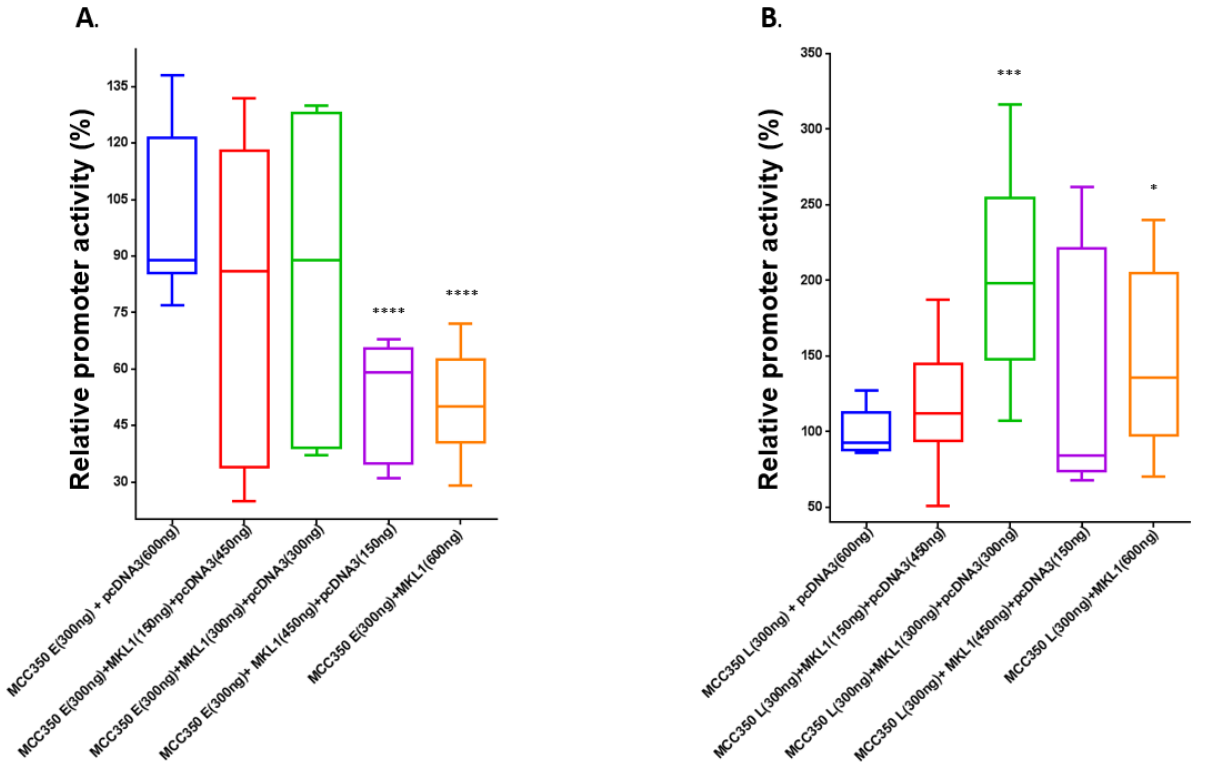

Figure 4.17: MKL1 tLT-ag expression inhibits and enhances activities of early and late MCC350 promoters respectively in HEK293 cells**. (A).** Effect of MKL1 tLT-ag on the MCPyV MCC350 early promoter activity in HEK 293 cells. Cells were co-transfected using 300ng luciferase reporter plasmids containing the MCC350 early promoter (pGL3-basic MCPyV LUC Early) with pcDNA3 (600ng) or MKL-1

(150ng) + pcDNA3 (450ng) or MKL-1 (300ng) + pcDNA3 (300ng) or MKL-1 (450ng) + pcDNA3 (150ng) or MKL-1 (600ng). The promoter activity in the presence of pcDNA3 was arbitrarily set as 100% and the activity in the presence of the varied concentration of MKL-1 tLT-ag was corrected to this. Represented with box plots are the median, minimum and maximum values of three independent parallels and are representative of three independent experiments. The blue, red, green, purple and orange box plots display promoter activities in the presence of pcDNA3 (600ng), MKL1 (150ng) + pcDNA3 (450ng), MKL1 (300ng) + pcDNA3 (300ng), MKL1 (450ng) + pcDNA3 (150ng) and MKL1 (600ng) respectively. An unpaired t-test represented with asterisks showed that the effect of MKL-1 expression on MCC350 early promoter is significant at 450ng and 600ng concentration of MKL-1 with P value < 0.0001 for both. **(B).** As in **(A)** but MCPyV MCC350 late promoter activity was monitored in the presence of the varied MKL-1 concentrations. An unpaired t-test represented with asterisks showed that the effect of MKL-1 expression on MCC350 early promoter was significant at 300ng and 600ng concentration of MKL-1 with P values < 0.0001 and = 0.048 respectively.

The results of all transfection studies with the early and late MCC350 and 16b promoters in the absence and presence of LT-ag or/and st-ag are summarized in Table 1.

Table 1: Relative early (E) and late (L) MCC350 and 16b promoter activities in the absence or presence of LT-ag or/and st-ag in HEK293, MCC13 and C33A cells.

Co-transfected expression plasmid	HEK293	MCC13	C33A
	MCC350-E<16b-E	MCC350-E<16b-E	MCC350-E=16b-E
	MCC350-L>16b-L	MCC350-L<16b-L	MCC350-L<16b-L
MCC350-E+st-ag	stimulation	stimulation	NT
MCC350-L+st-ag	stimulation	stimulation	NT
16b-E+st-ag	stimulation	stimulation	NT
16b-L+st-ag	stimulation	stimulation	NT
MCC350-E+FLT-ag	repression	NT	NT
MCC350-L+FLT-ag	repression	NT	NT

16b-E+FLT-ag	repression	no significant effect	NT
16b-L+FLT-ag	repression	repression	NT
MCC350-E+FLT-ag+st-ag	repression	repression	NT
MCC350-L+FLT-ag+st-ag	repression	repression	NT
MCC350-E+MKL1 tLT-ag	repression	NT	NT
MCC350-L +MKL1 tLT-ag	stimulation	NT	NT

[#]Not tested.

4.12 MCPyV Large T antigen increases IL-17F promoter activity

IL-17F secretion is upregulated in MCPyV-positive MCC compared to virus-negative MCC, and transient expression of MCPyV LT-ag in virus-negative MCC also resulted in elevated IL-17F mRNA levels compared to control cells [Unpublished result from MIRG]. Because, IL-17 has been convincingly shown to play vital roles in cancer progression [94], LT-ag-induced expression of IL-17F may play a contributing role in MCC oncogenesis. To test the role of LT-ag in IL-17F production, transient co-transfection studies in HEK293 cells were done with a luciferase reporter plasmid containing IL-17F promoter sequences and expression plasmids for FLT-ag or tLT-ag.

IL-17F promoter sequences -166/+1 (IL-17F (166)-LUC) and -636/+1 (IL-17F (636)-LUC) were tested. The IL-17F promoter activity was enhanced on expression of FLT-ag expression in a dose-dependent manner (Figure 4.18A and 4.18B). A more pronounced effect was seen on the shorter IL-17F promoter fragment. (Figure 4.18A).

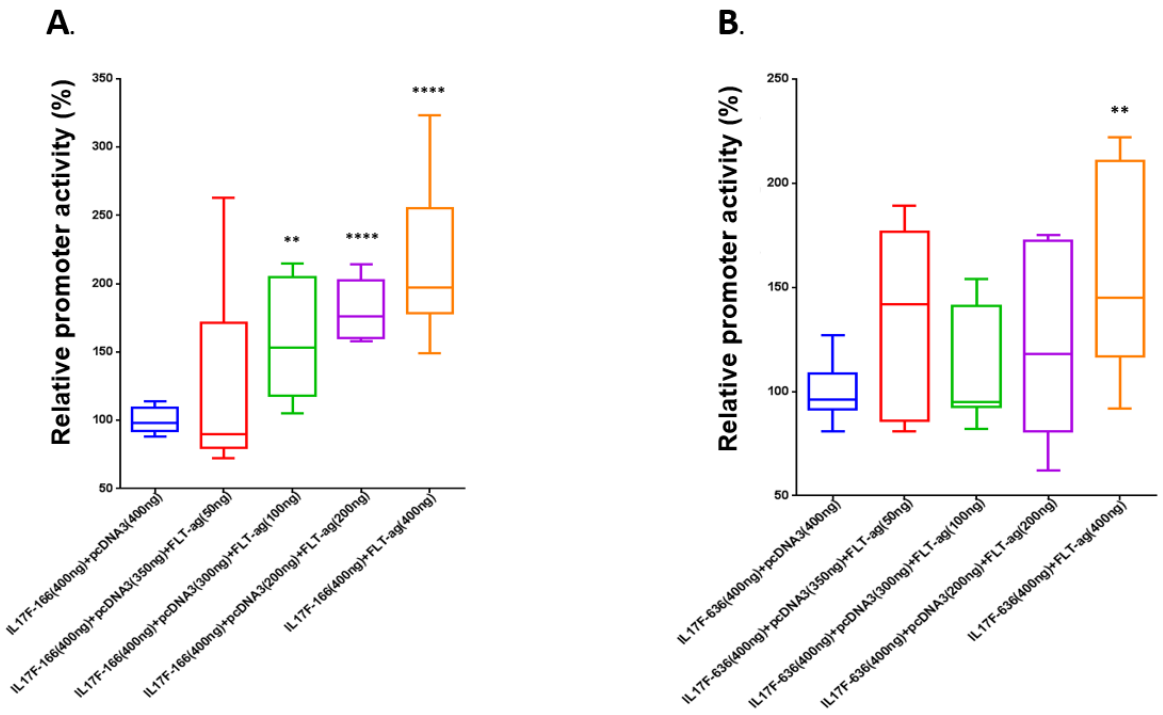

Figure 4.18: FLT-ag expression enhances activities of IL-17F promoters in HEK293 cells**. (A).** Effect of MCPyV FLT-ag on IL-17F (166) promoter activity in HEK 293 cells. Cells were co-transfected using 300ng luciferase reporter plasmids containing IL-17F promoter (IL-17F-166- LUC) with pcDNA3 (400ng) or pcDNA3 (350ng) +FLT-ag (50ng) or pcDNA3 (300ng) +FLT-ag (100ng) or pcDNA3 (200ng) +FLT-ag (200ng) or FLT-ag (400ng). The promoter activity in the presence of pcDNA3 only was arbitrarily set as 100% and the activity in the presence of the increasing concentrations of FLT-ag was corrected to this. Represented with box plots are the median, minimum and maximum values of three independent parallels and are representative of three independent experiments. The whiskers indicate the minimum and maximum value. The blue, red, green, purple and orange box plots display promoter activities in the presence of pcDNA3 (400ng), pcDNA3 (350ng) +FLT-ag (50ng), pcDNA3 (300ng) +FLT-ag (100ng), pcDNA3 (200ng) +FLT-ag (200ng), FLT-ag (400ng) respectively. An unpaired t-test represented with asterisks showed that the effect of FLT-ag expression on IL-17F-166 promoter is significant at 100ng, 200ng and 400ng concentration of FLT-ag with P values = 0.011, < 0.0001 and < 0.0001 respectively. **(B).** As in **(A)** but IL-17F (636) promoter activity was monitored in the presence of the varied MCPyV FLT-ag concentrations. An unpaired t-test represented with asterisks showed that the effect of FLT-ag expression on IL-17F-636 promoter is significant only at 400ng concentration of FLT-ag with P values = 0.002.

A similar stimulatory effect of IL-17F-166 promoter was also observed with MKL-2 tLT-ag expression (Figure 4.19A). Again, the effect was dose-dependent. However, MKL-2 tLT-ag expression elicited an inhibitory effect on IL-17F-636 promoter activity (Figure 4.19B). Hence, the regulatory effect of MKL-2 tLT-ag on IL-17F-166 and IL-17F-636 promoter activity differs.

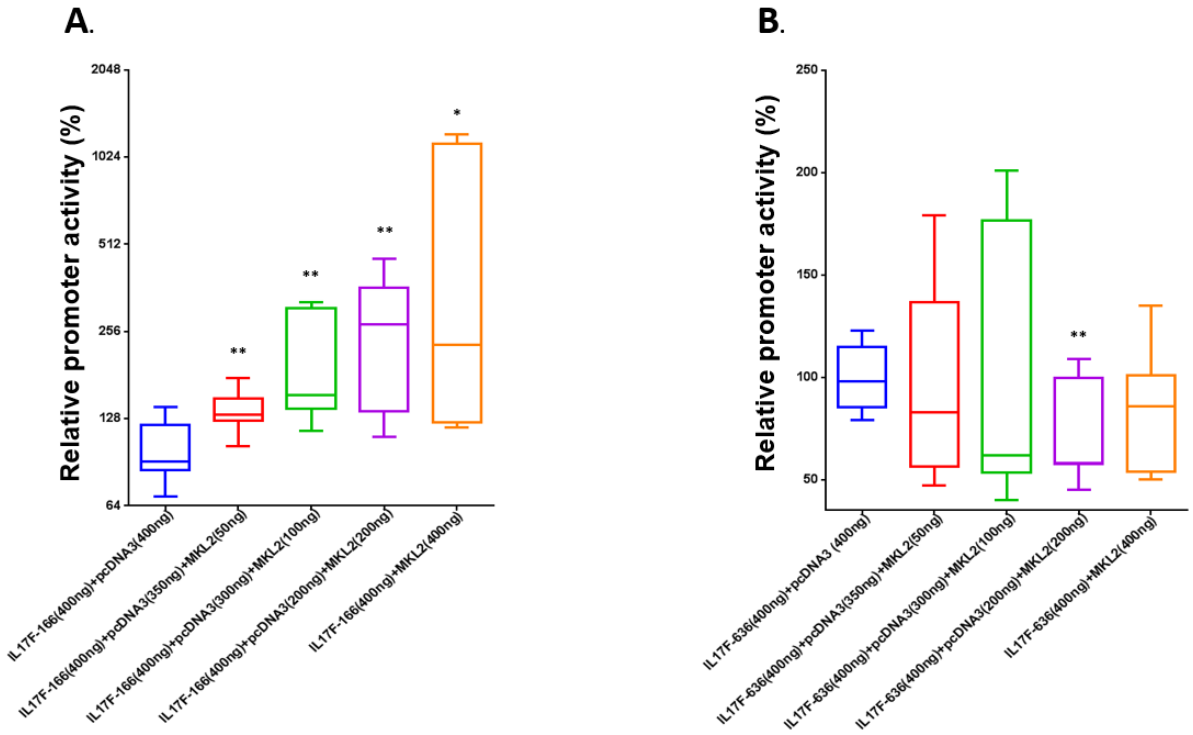

Figure 4.19. MKL2 tLT-ag expression stimulates and inhibits activities of IL-17F-166 and IL-17F636 promoters respectively in HEK293 cells**. (A).** As in **Figure 4.17A,** but IL-17F (166) promoter activity was monitored in the presence of pcDNA3 (400ng) or pcDNA3 (350ng) +MKL2 tLT-ag (50ng) or pcDNA3 (300ng) +MKL2 tLT-ag (100ng) or pcDNA3 (200ng) +MKL2 tLT-ag (200ng) or MKL2 tLT-ag (400ng). An unpaired t-test represented with asterisks showed that the effect of MKL2 tLT-ag expression on IL-17F-166 promoter is significant at 50ng, 100ng, 200ng and 400ng concentration of MKL2 tLT-ag with P values = 0.0028, 0.0023, 0.0014 and 0.024 respectively. **(B)** As in **Figure 4.17A,** but IL-17F (636) promoter activity was monitored in the presence of pcDNA3 (400ng) or pcDNA3 (350ng) +MKL2 tLT-ag (50ng) or pcDNA3 (300ng) +MKL2 tLT-ag (100ng) or pcDNA3 (200ng) +MKL2 tLT-ag (200ng) or MKL2 tLT-ag (400ng). An unpaired t-test represented with asterisks showed that the effect of MKL-2 tLT-ag expression on IL-17F-636 promoter is significant only at 200ng concentration of tLT-ag with P value = 0.009.

4.13 Regulatory effect of IL-17F and IL-17A/F secretion on activities of MCPyV MCC350 early and late promoters in SK-N-BE(2) cells.

Cytokines such as TNFα and IL-1β have been shown to stimulate the promoter activity of human polyomaviruses [137 - 140]. This prompted us to investigate whether IL-17F had an effect on the MCPyV promoter. Neuroblastoma SK-N-BE(2) cells were used because they have been characterized to express the IL-17F receptors IL-17RA and IL-17RC [unpublished results MIRG]. Expression of IL-17F significantly stimulated the activities of both the MCC350 early and late promoter in SK-N-BE(2) cells (Figure 4.20). IL-17F expression stimulated the activity

of late MCC350 promoter about 2- fold (Figure 4.20A), while the early MCC350 promoter was stimulated ~1.5-fold (Figure 4.20B).

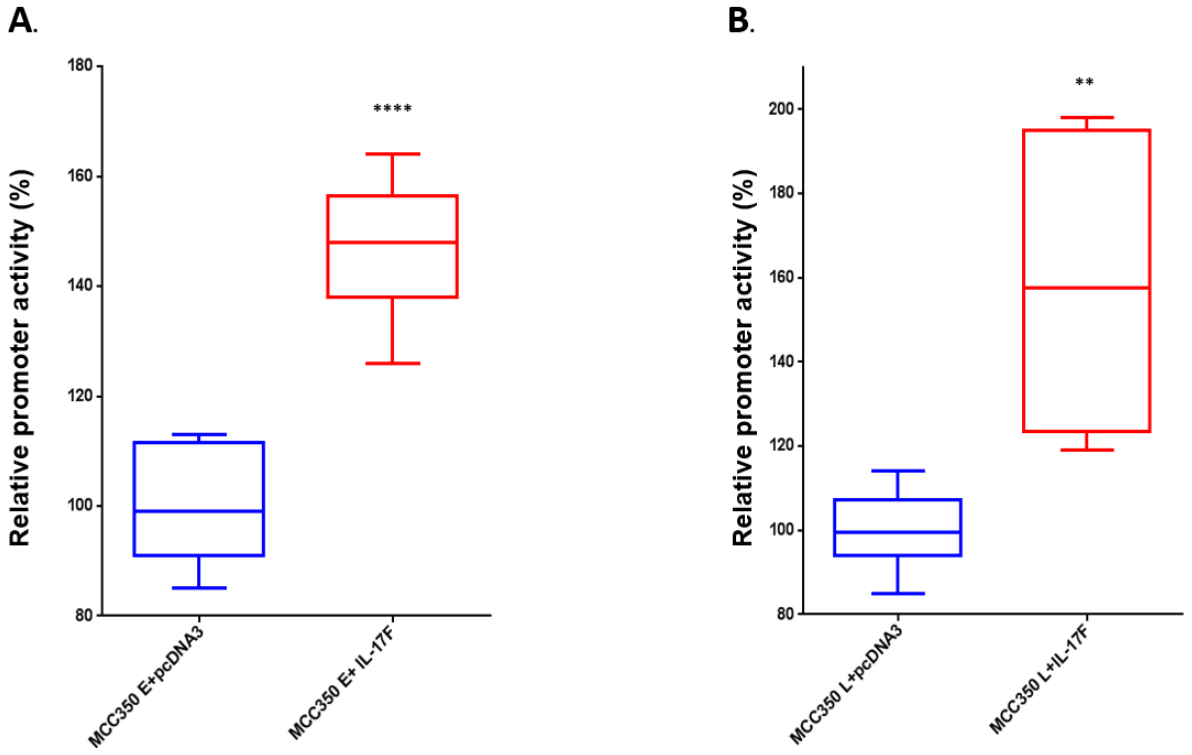

Figure 4.20. IL-17F expression enhances MCC350 MCPyV early and late promoter activities in SK-N-BE(2) cells**. (A)** MCC350 early promoter activity in the presence of empty vector pcDNA3 or IL-17F expression plasmid in SK-N-BE(2) cells. SK-N-BE(2) cells were co-transfected using luciferase reporter plasmids containing the MCC350 early promoter with pcDNA3 or an expression plasmid for IL-17F. The luciferase values were corrected for the protein concentration in the corresponding sample and the activity of the MCC350 early (respectively late) promoter in the presence of pcDNA3 was arbitrarily set as 100%. The activity of the promoter in the presence of IL-17F was related to the activity in the absence of IL-17F. Represented with box plots are the median, minimum and maximum values of three independent parallels and are representative of two independent experiments. The whiskers represent the minimum and maximum value. The blue and red box plot display the early promoter activities in the presence of pcDNA3 and IL-17F respectively. An unpaired t-test represented with asterisks showed that the differences between the data sets were significant ($P < 0.0001$). **(B)** As in **(A)** but MCC350 late promoter activity was monitored in the presence or absence of MCV IL-17F. An unpaired t-test represented with asterisks showed that the differences between the data sets were significant ($P = 0.0043$).

The magnitude with which the late MCC350 promoter activity was enhanced on expression of IL-17F (Figure 4.20B) was observed to be greater than that of MCC350 early promoter (Figure 4.20A).

To further investigate the regulatory effect of IL-17F on MCPyV early and late promoter, recombinant IL-17A/F were used in treating SK-N-BE(2) cells. Administering recombinant IL-17A/F significantly stimulated the late (1.4-fold) MCC350 promoter activity (Figure 4.21B), while no significant effect was observed for the MCC350 early promoter (Figure 4.20A).

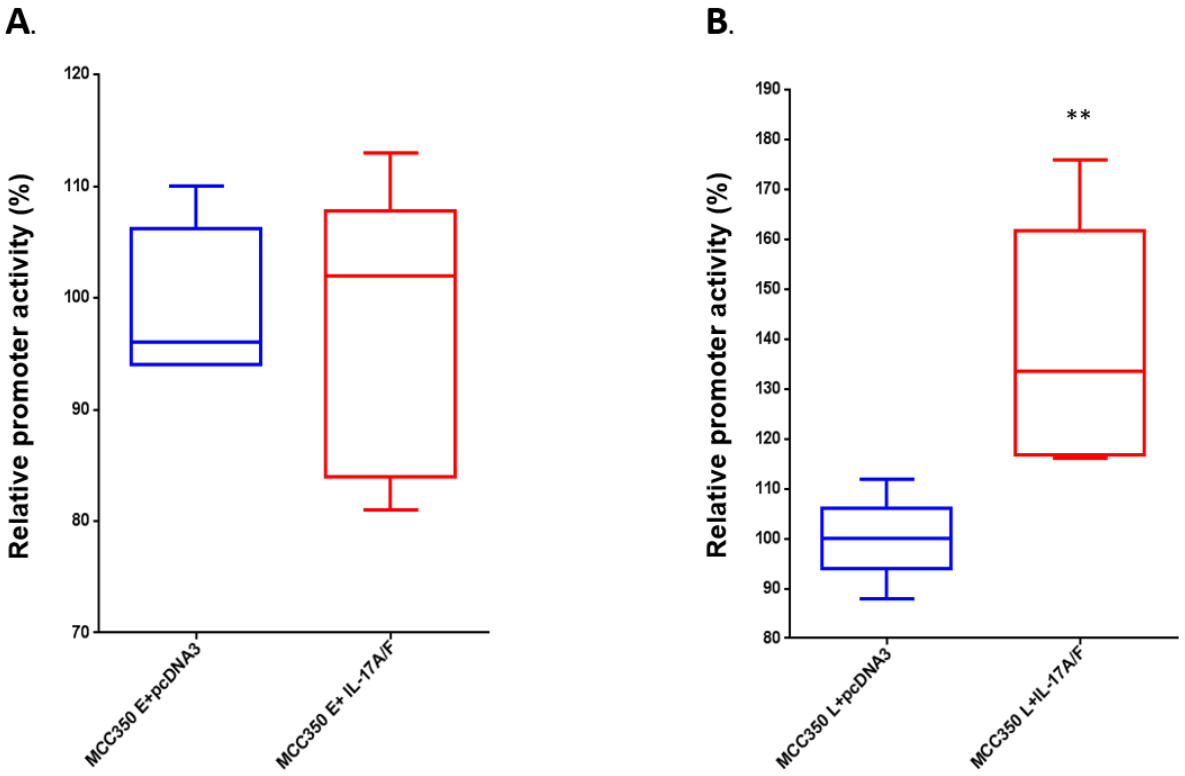

Figure 4.21 Treatment with Recombinant IL-17A/F enhances MCC350 MCPyV early and late promoter activities in SK-N-BE(2) cells. **(A)** As in **Figure 4.20A** but MCPyV MCC350 early promoter activity was monitored in the presence of recombinant IL-17A/F protein. The cells were serum-starved for 18hrs, and then treated with 50ng/ml IL7A/F for 3hours. An unpaired t-test showed that the differences between the data sets were insignificant. **(B)** As in **Figure 4.20A** but MCPyV MCC350 early promoter activity was monitored in the presence of recombinant IL-17A/F protein. The cells were serum-starved for 18hrs, and then treated with 50ng/ml IL7A/F for 3hours. An unpaired t-test represented with asterisks (**) showed that the differences between the data sets were significant (P = 0.0045).

5. DISCUSSION

A substantial comprehension of the tumorigenesis of the highly belligerent and lethal Merkel cell carcinoma malignancy has been enhanced by MCPyV discovery as well as the detection of tumor-antigens and viral DNA in MCC [16, 141,142]. A number of disparate methods have been employed in the detection of viral DNA, such as PCR amplification [143], RT-PCR and viral tumor antigens identification via immunohistochemistry [141]. These investigations have revealed that the viral genome is integrated and that a truncated version of LT-ag is expressed in the tumors [10,95]. This study achieved a successful construction of expression plasmids for the truncated versions of MCPyV LT antigens expressed by three different MCC cell lines via site-directed mutagenesis as confirmed with their respective sizes on western blot analysis using CM2B4 antibody (Figure 4.2) which has been observed to express about 80% sensitivity in MCPyV LT-ag detection [141]. The FLAG-tagged MCPyV st-ag was also successfully detected via western blot using antibody against FLAG (as explained in 4.3).

In spite of MCPyV's isolation by Feng et al, 8 years ago [16], a definite cell tropism as well as a cell culture system to maintain a complete replication or life cycle of the virus are yet to be established. Highly transducible cell types have been confirmed via transfection studies using complete MCPyV genomes, yet none of them permitted production of virulent viral particles [144]. Subsequently, a separate group used medium from complete MCPyV DNA-transfected cells and still could not identify viral transmission into recipient cells [40]. Hence, so far a permissive cell line that allows studying the complete replication cycle of MCPyV is not available. This study was done by transfecting MCPyV genome and not by virus infection.

The NCCR structure of polyomaviruses has been observed by disparate studies to influence the replication of polyomaviruses in cell culture [110, 111, 145]. In 10 different cell lines, our group tested the relative promoter strength of the MCPyV MCC350 strain [133]. Cell lines in which highest promoter activities were observed, may be appropriate for virus propagation. This study tested two additional cell lines and also compared the promoter activity of the MCC350 strain with the naturally occurring variant MCPyV 16b. The latter has a 25 bp insertion and several single point mutations compared to the MCC350 NCCR (Figure 4.4). MCPyV with a 16b NCCR architecture has also been detected in strains isolated from Kaposi's sarcoma tissue from a Japanese patient [30] and in feces of Chinese children [GenBank accession number KC571692].

In this study, the promoters of MCPyV strains: MCC350 and 16b were examined in three cell lines and are as follows: human embryonal kidney cells (HEK293), a MCPyV-negative Merkel cell carcinoma cell line (MCC13), and the human papillomavirus-negative cervical cancer cell line C33A. The rationale behind our selection of these cell lines include: (i) MCPyV MCC350 promoter exhibited the strongest activity in HEK293 cells in our earlier study with 10 different cell lines [133], (ii) A virus-negative MCC cell line was used because of the unavailability of established Merkel cell cultures, (iii) during the course of this study, MCPyV DNA was discovered in cervical tissue (33-55%, n =112 and n=190, respectively; [24, 146]). Using transient transfection studies with a plasmid containing the MCPyV promoter controlling the expression of the *luciferase* reporter gene, we found that both the MCC350 and 16b early and late promoters were strongest in HEK293 cells (1800 folds and 6000 folds stronger than in MCC13 and C33A cells respectively). In HEK 293, MCC13 and C33A the relative luciferase values are ~ 800- 1000, ~ 8 -12 and ~ 1-3 respectively. These variations aren't the only result of differences in transfection efficiency because all cells express comparable transfection efficiencies (HEK293: 90%; MCC13: 75%; C33A: ~30%) (Figure 4.5). The variations could be due to cell-specific expression of transcription factors that regulate the activity of the MCPyV early and late promoters.

The compared NCCR regions of both MCPyV MCC350 and 16b strains are sufficiently distinct (Figure 4.4) and could be a consequence of their functional and regulatory differences. This observation is consistent to that seen in the pathological strains of JCPyV, a human polyomavirus, where rearrangements such as point mutations, deletions and duplications occur in a specific region (transcriptional region) of their control region (NCCR) [147]. Cell-type specific transcription factors involved in the transcriptional modulation of JCPyV promoters (NCCR) could be a consequence of their transforming capabilities being limited to neural cells [147]. The nature of the viral NCCR was also observed to elicit an impact on the tumor type formed by JCPyV [148, 149]. The NCCR diversity is probably able to confer on the virus a selective advantage in its host, enhancing high efficiency of transcription and replication of the viral genome [150]. In furtherance, a rearranged NCCR has been made evident by current studies to promote upregulated DNA replication and expression of early viral genes abilities in glial cells [111].

Available in the GenBank are sequences of 46 complete MCPyV genomes, and these isolates were discovered in MCC and non-MCC tissues. In addition, four NCCR sequences have been submitted to GenBank. Excluding the 16b strain, all other isolates have a NCCR almost

completely identical to MCC350 with exception of one or a few point mutations. The fact that MCPyV strains with 16b-like NCCRs were found in non-MCC tissues (16b: skin, HB039: feces; YKS: Kaposi' sarcoma), [20] while MCPyV 350 was found in MCC patient from North American MCC (Gen Bank accession no. EU375803) [16, 151] and Europe [111], may indicate that the MCC350 promoter is correlated with a more oncogenic variant of MCPyV. However, MCC is majorly discovered in Caucasians but unfrequently in Asians and Afro-Americans. [16, supplementary table 1]. Moreover, MCPyV isolates with quasi-identical MCC350 NCCR anatomy have been detected in non-MCC samples [Supplementary Table 1].

This study investigates for the first time the effect of NCCR polymorphism in a naturally occurring MCPyV variant on transcriptional activity. We found that the early promoter activities of MCC350 and 16b were similar (Figure 4.6C), while the 16b late promoter activity was higher than that of MCC350 in C33A cells (Figure 4.7C). In MCC13 cells, both the early and late 16b promoter was stronger than that of MCC350 promoter (Figures 4.6B and 4.7B). In HEK293 cells, however, the early 16b promoter was stronger than the early MCC350 promoter (Figure 4.6A), but the opposite was true for the late promoters (Figure 4.7A). The magnitude of differential early promoter activity between the two MCPyV strains was more pronounced in HEK293 cells when compared to that seen in MCC13. The major difference between the 16b and MCC350 promoters is the 25bp CTCCTCCCTTTGTAAGAGAAATGTC insert (Figure 4.4). The 25 bp insertion contains putative binding sites for the ubiquitously expressed transcription factors p300, Elk-1, and Foxo3A [152]. Whether any of these transcription factors play a role in regulating the transcriptional activity of the MCPyV promoter remains to be investigated.

Previous studies with other polyomaviruses had shown that the LT-ag and st-ag affect the viral promoter activity [42,41]. This prompted us to investigate the role of the MCPyV early proteins on the MCPyV promoter. St-ag elicits an up-regulatory effect on MCPyV MCC350 and 16b early and late promoter activities in HEK 293 cells (Figures 4.8 and 4.9). A similar effect was observed in MCC13 cells. This stimulation of MCPyV promoter activity can be buttressed by the fact that the st-ag of MCPyV has been observed to enhance the ability of the LT-ag in inducing cellular transformation [153,154]. The MCPyV st-ag independently expresses oncogenic properties via a mechanism that alters the phosphorylation state of 4E-BP1 (4E binding protein 1 regulator) and by functioning downstream in the mammalian target of rapamycin (mTOR) pathway, thereby demonstrating its transformation capability in rat-1 cells [44]. Furthermore, the st-ag enhances the expression of LT-ag via cellular ubiquitin ligase SCF

(Fbw7) blockade, consequently causing a repression in LT-ag's proteasomal degradation [65]. The up-regulatory effect of MCPyV st-ag was seen to be more pronounced on MCPyV 16b promoters relative to that of MCC350, (Figure 4.10A). This stronger effect of MCPyV st-ag on 16b may indicate that the effect is mediated through the 25bp insertion.

In the presence of FLT-ag, a substantial inhibition of MCPyV MCC50 and 16b early and late promoter activities were observed (Figures 4.11 and 4.12). This inhibitory effect of LT-ag is in agreement with its ability to auto-regulate its own transcription via a negative feedback mechanism [155]. Additionally, Cheng *et al.* showed that MCPyV LT-ag represses cell growth by expression of its C- terminal 100 residues and Exon 3 region [46].

The magnitude of inhibition exerted by FLT-ag on the early promoter was higher than that of the late promoter in both MCPyV NCCR variants. The MCPyV 16b promoter activity can further be seen to be higher than that of MCC350 since the FLT-ag repression was more pronounced on MCC350 promoter activity relative to that of MCPyV 16b in HEK 293 cells.

Since the st-ag and LT-ag of the MCPyV have been strongly suggested to both be oncogenic and be directly involved in the tumorigenesis of MCC based on MCPyV's homology to other members of the polyomavirus family [142], we tested the effect of st-ag and FLT-ag co-expression on MCPyV promoter activities to see if they both have a synergistic modulatory effect. Our investigation into the regulatory effect elicited by co-expression of both T-antigens (early proteins) on MCPyV MCC350 and 16b promoter activities revealed a down-regulatory effect in HEK293 as well as in MCC13 cells (Figures 4.13 and 4.14, 4.15 and 4.16). Independently, both early proteins express contrasting regulatory effects on the activities of MCPyV promoters, but the inhibitory effect elicited on their co-expression indicates that the LT-ag's down-regulatory effect is more pronounced than st-ag's up-regulatory effect on MCPyV promoter activities in both cell lines. Thus, FLT-ag is a more potent regulator of the activities of MCPyV promoters and no synergistic effect occurred on their co-expression.

We also tested the effect of truncated LT-ag on MCPyV promoter activities using MKL-1 tLT-ag. We observed a repressive effect evoked by MKL-1 tLT-ag on regulating the activity of MCC350 early promoter (Figure 4.17A). The repressive effect of MKL-1 tLT-ag on the activity of MCC350 early promoter was seen to occur in a concentration-dependent fashion. Contrary to this, MKL-1 tLT-ag enhanced MCC350 late promoter activity in a dose-dependent manner but in an inversely proportional fashion (Figure 4.17B). The inhibitory effect of MKL-1 tLT-ag on early promoter activity was only substantiated at high concentrations of tLT-ag, while its

stimulatory effect on late promoter activity was apparent at low concentrations, but decreased at high concentrations. (Figure 4.17B). Due to time restrictions, the effect of the truncated LT-ag variants MKL-1, MKL-2 and MS-1 on the MCPyV early and late promoter in MCC13 cells was not tested.

In exploring the possible role of IL-17F in MCC oncogenesis, since increased mRNA levels of IL-17F were observed in MCPyV-positive MCC or LT-ag expressing virus-negative MCC compared with virus-negative cells [unpublished result from MIRG] and IL-17 has been sufficiently shown to promote carcinogenesis [94], our results evidently show that FLT-ag upregulated IL-17F promoter activities in a dose-dependent fashion (Figures 4.18A and 4.18B). The shorter IL-17F promoter fragment (IL-17F (166)-LUC) was observed to be more responsive to FLT-ag regulatory effect (Figure 4.18A) relative to the longer IL-17F promoter fragment (IL-17F (636)-LUC) (Figure 4.18B). At low concentrations of FLT-ag, the stimulatory effect on the shorter IL-17F promoter fragment became obvious, but that of the longer IL-17F promoter fragment was only observed at the highest concentration.

Similarly, truncated LT-ag (MKL-2), was seen to enhance the IL-17F-166 promoter activity in a dose-dependent fashion but repressed IL-17F-636 promoter activity (Figures 4.19A and 4.19B respectively). The presence of MKL-2 tLT-ag at the lowest concentration was able to evoke an up-regulatory effect on the activity of IL-17F-166 promoter (Figure 4.19A) while an increased concentration of MKL-2 tLT-ag was required to elicit an inhibitory effect on the activity of IL-17F-636 promoter (Figure 4.19B). These results suggest that the shorter IL-17F promoter fragment (IL-17F (166)-LUC) was more sensitive to MKL-2 tLT-ag-mediated regulation relative to the longer IL-17F promoter fragment (IL-17F (636)-LUC) in HEK 293 cells, indicating that the sequences that mediate the effect of LT-ag are encompassed in the proximal part of the IL-17F promoter.

Lastly, we examined the possible regulatory roles of IL-17F on the activities of MCPyV promoters in IL-17 receptor-expressing SK-N-BE(2) cells, and results revealed an up-regulatory function by IL-17F and IL-17A/F release on the activities of MCPyV promoters. Co-transfection of an IL-17F expression plasmid robustly enhanced both MCPyV promoters (Figures 4.20A and 4.20B), while recombinant IL-17A/F significantly enhanced MCPyV late promoter only (Figure 4.21B). This observation is in accordance with the stimulatory effect of IL-17 on pro-inflammatory cytokines locally (through CCL2) and systemically (through the NF-κB pathway) in enhancing tumor growth [94,104]. Additionally, IL-17 has been seen to

upregulate the production of VEGF and expression of MMP-2 and MMP-9, which promotes angiogenesis [94,104]. These results imply that IL-17 may be involved in the angiogenetic process in the highly aggressive and metastatic MCPyV-positive MCC.

SK-N-BE(2) cells were particularly used for this study because they have been shown to express IL-17R A/C receptor [unpublished results from MIRG] to which IL-17A and IL-17F homodimers as well as IL-17A/F heterodimer bind to during signaling to elicit their pro-inflammatory functions [91, 92]. As a negative control, we tested the effect of recombinant IL-17F on MCC350 in HEK293 cells but no significant effect was observed. This would probably be due to the fact that HEK 293 cells do not express the receptor for IL-17F.

6. Conclusion & future perspectives

HEK 293 cells appear to be the most suitable cell line for transfection studies using MCPyV genome based on their high transfection efficiency and relative luciferase values. The strength of the early promoter of MCPyV 16b variant is higher than that of MCC350 in HEK293, MCC13 and C33A cells while the late promoter strength of MCPyV16b variant is as well higher than that of MCC350 in HEK293 and MCC13, but similar in C33A cells. The differences in MCPyV promoter architecture influences the transcriptional activity in a cell-dependent manner.

We demonstrated that the MCPyV LT-ag and st-ag regulate the expression of the viral promoter, whereby st-ag positively regulated viral promoters while FLT-ag negatively regulated them. Co-expression of MCPyV early proteins elicited no synergism on regulating viral promoters. Truncated LT-ag (MKL1 and MKL2) respective regulation of MCPyV promoter and IL-17F occurred in a concentration-dependent fashion.

Moreover, we have shown a reciprocal interaction between MCPyV and IL-17F. MCPyV LT-ag stimulates the expression of IL-17F and vice versa, IL-17F enhanced the MCPyV promoter. IL-17F is hypothesized to be associated with the angiogenetic and metastatic processes in MCC pathobiology, and may therefore contribute to MCPyV-induced tumorigenesis of Merkel cells.

The effect of truncated LT-ag variants expressed in MCCs on the MCPyV promoter has not been tested. It would be interesting to examine if truncated LT-ag modulates the MCPyV promoter to the same extent as full-length LT-ag or if a truncated form is a stronger activator resulting in higher concentrations of the oncoproteins: LT-ag and st-ag, in Merkel cells than in other cell types.

Investigating the effect of the truncated LT-ag variants MKL-1, MKL-2 and MS-1 on the MCPyV early and late promoters in MCC13 and C33A, role of the early proteins on MCPyV promoter in C33A, as well as a comparison of the results amongst the three cell lines (HEK 293, MCC13 and C33A) would be interesting and give more insight into cell-specific MCPyV promoter regulation by early MCPyV proteins and truncated LT-ag variants.

The IL-17F may be a contributing factor in MCPyV-induced MCC tumorigenesis. Inhibiting IL-17F activity by neutralizing antibody, may thus be a potential therapeutic target in MCC treatment.

The co-existence of MCPyV and high-risk human papillomavirus (HR-HPV) in cervical tissue [26, 27] suggests that MCPyV can act as a co-factor in HPV-induced cervical cancer. The effect of MCPyV LT-ag and st-ag on expression of HR-HPV oncoproteins such as E6 and E7 can be tested and the impact of these on the expression levels of LT-ag and st-ag can be examined. The E6, E7 and LT-ag proteins target the tumor suppressor proteins p53 and pRb and may thus collaborate to inactivate p53 and pRb [156].

The ganglioside GT1b has been identified as a putative receptor for MCPyV [157]. This receptor is expressed on human kidney proximal tubuline epithelial cells [158], T cells [159] and neural cells [160], but so far MCPyV has not been detected in any of these cells. GT1b is also found on the surface of keratinocytes [161], which is in agreement with the dermatotropism of this virus [20]. Virus propagation, however, does not only depend on successful binding to the receptor and entering the target cell, the host cell must also sustain expression and replication of the viral genome, and new virions have to be assembled and released from the infected cell. It was previously shown that the MCPyV early and late promoters are very weak in the human keratinocyte cell line HaCaT [133]. It is possible that complete virus life cycle requires differentiation of the host cell in analogy with HPV [162]. The quest for a permissive cell line for MCPyV continues.

On the overall, a good comprehension of the reciprocal interaction between the inflammation process and MCPyV may allow the design of therapeutic drugs.

References

1. World Health Organization (WHO), Media Centre, Cancer Fact Sheet. 2015 [15.03.2016]; Available from: http://who.int/mediacentre/factsheets/fs297/en.
2. Morales-Sánchez A, Fuentes-Pananá EM. Human viruses and cancer. Viruses. 2014 Oct 23;6(10):4047-79.
3. Moore PS, Chang Y. Why do viruses cause cancer? Highlights of the first century of human tumour virology. Nature Reviews Cancer. 2010 Dec 1;10(12):878-89.
4. Chen CJ, Hsu WL, Yang HI, Lee MH, Chen HC, Chien YC, You SL. Epidemiology of virus infection and human cancer. InViruses and Human Cancer 2014 (pp. 11-32). Springer Berlin Heidelberg.
5. Schiller JT, Lowy DR. Virus infection and human cancer: an overview. InViruses and Human Cancer 2014 (pp. 1-10). Springer Berlin Heidelberg.
6. Moore PS, Chang Y. The conundrum of causality in tumor virology: the cases of KSHV and MCV. InSeminars in cancer biology 2014 Jun 30 (Vol. 26, pp. 4-12). Academic Press.
7. Szeder V, Grim M, Halata Z, Sieber-Blum M. Neural crest origin of mammalian Merkel cells. Developmental biology. 2003 Jan 15;253(2):258-63.
8. Morrison KM, Miesegaes GR, Lumpkin EA, Maricich SM. Mammalian Merkel cells are descended from the epidermal lineage. Developmental biology. 2009 Dec 1;336(1):76-83.
9. Van Keymeulen A, Mascre G, Youseff KK, Harel I, Michaux C, De Geest N, Szpalski C, Achouri Y, Bloch W, Hassan BA, Blanpain C. Epidermal progenitors give rise to Merkel cells during embryonic development and adult homeostasis. The Journal of cell biology. 2009 Oct 5;187(1):91-100.
10. Stakaitytė G, Wood JJ, Knight LM, Abdul-Sada H, Adzahar NS, Nwogu N, Macdonald A, Whitehouse A. Merkel cell polyomavirus: molecular insights into the most recently discovered human tumour virus. Cancers. 2014 Jun 27;6(3):1267-97.
11. Mahrle G, Orfanos CE. Merkel cells as human cutaneous neuroreceptor cells. Archiv für dermatologische Forschung. 1974 Mar 1;251(1):19-26.
12. Maricich SM, Wellnitz SA, Nelson AM, Lesniak DR, Gerling GJ, Lumpkin EA, Zoghbi HY. Merkel cells are essential for light-touch responses. Science. 2009 Jun 19;324(5934):1580-2.

13. Toker C. Trabecular carcinoma of the skin. Archives of dermatology. 1972 Jan 1;105(1):107-10.
14. Sibley RK, Rosai J, Foucar E, Dehner LP, Bosl G. Neuroendocrine (Merkel cell) carcinoma of the skin: A histologic and ultrastructural study of two cases. The American journal of surgical pathology. 1980 Jun 1;4(3):211-22.
15. Heath M, Jaimes N, Lemos B, Mostaghimi A, Wang LC, Peñas PF, Nghiem P. Clinical characteristics of Merkel cell carcinoma at diagnosis in 195 patients: the AEIOU features. Journal of the American Academy of Dermatology. 2008 Mar 31;58(3):375-81.
16. Feng H, Shuda M, Chang Y, Moore PS. Clonal integration of a polyomavirus in human Merkel cell carcinoma. Science. 2008 Feb 22;319(5866):1096-100.
17. Coursaget P, Samimi M, Nicol JT, Gardair C, Touzé A. Human Merkel cell polyomavirus: virological background and clinical implications. Apmis. 2013 Aug 1;121(8):755-69.
18. Šroller V, Hamšíková E, Ludvíková V, Vochozkova P, Kojzarová M, Fraiberk M, Saláková M, Morávková A, Forstová J, Němečková Š. Seroprevalence rates of BKV, JCV, and MCPyV polyomaviruses in the general Czech Republic population. Journal of medical virology. 2014 Sep 1;86(9):1560-8.
19. Martel-Jantin C, Pedergnana V, Nicol JT, Leblond V, Trégouët DA, Tortevoye P, Plancoulaine S, Coursaget P, Touzé A, Abel L, Gessain A. Merkel cell polyomavirus infection occurs during early childhood and is transmitted between siblings. Journal of Clinical Virology. 2013 Sep 30;58(1):288-91.
20. Schowalter RM, Pastrana DV, Pumphrey KA, Moyer AL, Buck CB. Merkel cell polyomavirus and two previously unknown polyomaviruses are chronically shed from human skin. Cell host & microbe. 2010 Jun 17;7(6):509-15.
21. Kean JM, Rao S, Wang M, Garcea RL. Seroepidemiology of human polyomaviruses. PLoS Pathog. 2009 Mar 27;5(3): e1000363.
22. Van Ghelue M, Moens U. Merkel Cell Polyomavirus: A Causal Factor in Merkel Cell Carcinoma. INTECH Open Access Publisher; 2011.
23. Imajoh M, Hashida Y, Nemoto Y, Oguri H, Maeda N, Furihata M, Fukaya T, Daibata M. Detection of Merkel cell polyomavirus in cervical squamous cell carcinomas and adenocarcinomas from Japanese patients. Virology journal. 2012 Aug 9;9(1):1.
24. Kolia-Diafouka P, Foulongne V, Boulle N, Ngou J, Kelly H, Sawadogo B, Delany-Moretlwe S, Mayaud P, Segondy M, Chikandiwa A, Omar T. Detection of four human

polyomaviruses (MCPyV, HPyV6, HPyV7 and TSPyV) in cervical specimens from HIV-infected and HIV-uninfected women. Sexually Transmitted Infections. 2016 Mar 24: sextrans-2015.

25. Saláková M, Košlabová E, Vojtěchová Z, Tachezy R, Šroller V. Detection of human polyomaviruses MCPyV, HPyV6, and HPyV7 in malignant and non-malignant tonsillar tissues. Journal of medical virology. 2015 Nov 1.
26. Urso C, Pierucci F, Sollai M, Arvia R, Massi D, Zakrzewska K. Detection of Merkel cell polyomavirus and human papillomavirus DNA in porocarcinoma. Journal of Clinical Virology. 2016 May 31; 78:71-3.
27. Yahyapour Y, Sadeghi F, Alizadeh A, Rajabnia R, Siadati S. Detection of Merkel Cell Polyomavirus and Human Papillomavirus in Esophageal Squamous Cell Carcinomas and Non-Cancerous Esophageal Samples in Northern Iran. Pathology & Oncology Research. 2016 Feb 15:1-6.
28. Tanio S, Matsushita M, Kuwamoto S, Horie Y, Kodani I, Murakami I, Ryoke K, Hayashi K. Low prevalence of Merkel cell polyomavirus with low viral loads in oral and maxillofacial tumours or tumour-like lesions from immunocompetent patients: Absence of Merkel cell polyomavirus-associated neoplasms. Molecular and Clinical Oncology. 2015 Nov 1;3(6):1301-6.
29. Fisher CA, Harms PW, McHugh JB, Edwards PC, Siddiqui J, Palanisamy N, Bichakjian CK, Benavides E, Danciu TE. Small cell carcinoma in the parotid harboring Merkel cell polyomavirus. Oral surgery, oral medicine, oral pathology and oral radiology. 2014 Dec 31;118(6):703-12.
30. Katano H, Ito H, Suzuki Y, Nakamura T, Sato Y, Tsuji T, Matsuo K, Nakagawa H, Sata T. Detection of Merkel cell polyomavirus in Merkel cell carcinoma and Kaposi's sarcoma. Journal of medical virology. 2009 Nov 1;81(11):1951-8.
31. Du-Thanh A, Guillot B, Dereure O, Foulongne V. Detection of Merkel cell and other human polyomavirus DNA in lesional and nonlesional skin from patients with Kaposi sarcoma. British Journal of Dermatology. 2015 Oct 1;173(4):1063-5.
32. Sadeghi F, Salehi-Vaziri M, Alizadeh A, Ghodsi SM, Bokharaei-Salim F, Fateh A, Monavari SH, Keyvani H. Detection of Merkel cell polyomavirus large T-antigen sequences in human central nervous system tumors. Journal of medical virology. 2015 Jul 1;87(7):1241-7.

33. Hashida Y, Imajoh M, Daibata M. Integrated and mutated forms of Merkel cell polyomavirus in non-small cell lung cancer. British journal of cancer. 2013 Jun 25;108(12):2624-.
34. Comar M, Cuneo A, Maestri I, Melloni E, Pozzato G, Soffritti O, Secchiero P, Zauli G. Merkel-cell polyomavirus (MCPyV) is rarely associated to B-chronic lymphocytic leukemia (1 out of 50) samples and occurs late in the natural history of the disease. Journal of Clinical Virology. 2012 Dec 31;55(4):367-9.
35. Toptan T, Yousem SA, Ho J, Matsushima Y, Stabile LP, Fernández-Figueras MT, Bhargava R, Ryo A, Moore PS, Chang Y. Survey for human polyomaviruses in cancer. JCI insight. 2016 Feb;1(2).
36. Li TC, Iwasaki K, Katano H, Kataoka M, Nagata N, Kobayashi K, Mizutani T, Takeda N, Wakita T, Suzuki T. Characterization of self-assembled virus-like particles of Merkel cell polyomavirus. PloS one. 2015 Feb 11;10(2): e0115646.
37. Carter JJ, Daugherty MD, Qi X, Bheda-Malge A, Wipf GC, Robinson K, Roman A, Malik HS, Galloway DA. Identification of an overprinting gene in Merkel cell polyomavirus provides evolutionary insight into the birth of viral genes. Proceedings of the National Academy of Sciences. 2013 Jul 30;110(31):12744-9.
38. Wendzicki JA, Moore PS, Chang Y. Large T and small T antigens of Merkel cell polyomavirus. Current opinion in virology. 2015 Apr 30; 11:38-43.
39. Kwun HJ, Guastafierro A, Shuda M, Meinke G, Bohm A, Moore PS, Chang Y. The minimum replication origin of merkel cell polyomavirus has a unique large T-antigen loading architecture and requires small T-antigen expression for optimal replication. Journal of virology. 2009 Dec 1;83(23):12118-28.
40. Feng H, Kwun HJ, Liu X, Gjoerup O, Stolz DB, Chang Y, Moore PS. Cellular and viral factors regulating Merkel cell polyomavirus replication. PLoS One. 2011 Jul 22;6(7): e22468.
41. An P, Sáenz Robles MT, Pipas JM. Large T antigens of polyomaviruses: amazing molecular machines. Annual review of microbiology. 2012 Oct 13; 66:213-36.
42. Topalis D, Andrei G, Snoeck R. The large tumor antigen: A “Swiss Army knife” protein possessing the functions required for the polyomavirus life cycle. Antiviral research. 2013 Feb 28;97(2):122-36.
43. DeCaprio JA, Garcea RL. A cornucopia of human polyomaviruses. Nature reviews Microbiology. 2013 Apr 1;11(4):264-76.

44. Shuda M, Kwun HJ, Feng H, Chang Y, Moore PS. Human Merkel cell polyomavirus small T antigen is an oncoprotein targeting the 4E-BP1 translation regulator. The Journal of clinical investigation. 2011 Aug 15;121(9):0-.
45. Demetriou SK, Ona-Vu K, Sullivan EM, Dong TK, Hsu SW, Oh DH. Defective DNA repair and cell cycle arrest in cells expressing Merkel cell polyomavirus T antigen. International Journal of Cancer. 2012 Oct 15;131(8):1818-27.
46. Cheng J, Rozenblatt-Rosen O, Paulson KG, Nghiem P, DeCaprio JA. Merkel cell polyomavirus large T antigen has growth-promoting and inhibitory activities. Journal of virology. 2013 Jun 1;87(11):6118-26.
47. Gomez B, He L, Tsai YC, Wu TC, Viscidi RP, Hung CF. Creation of a Merkel cell polyomavirus small T antigen-expressing murine tumor model and a DNA vaccine targeting small T antigen. Cell & bioscience. 2013 Jul 15;3(1):1.
48. Shuda M, Chang Y, Moore PS. Merkel Cell Polyomavirus–Positive Merkel Cell Carcinoma Requires Viral Small T-Antigen for Cell Proliferation. Journal of Investigative Dermatology. 2014 May 1;134(5):1479-81.
49. Borchert S, Czech-Sioli M, Neumann F, Schmidt C, Wimmer P, Dobner T, Grundhoff A, Fischer N. High-affinity Rb binding, p53 inhibition, subcellular localization, and transformation by wild-type or tumor-derived shortened Merkel cell polyomavirus large T antigens. Journal of virology. 2014 Mar 15;88(6):3144-60.
50. Verhaegen ME, Mangelberger D, Harms PW, Vozheiko TD, Weick JW, Wilbert DM, Saunders TL, Ermilov AN, Bichakjian CK, Johnson TM, Imperiale MJ. Merkel cell polyomavirus small T antigen is oncogenic in transgenic mice. Journal of Investigative Dermatology. 2015 May 1;135(5):1415-24.
51. Knight LM, Stakaityte G, Jennifer JW, Abdul-Sada H, Griffiths DA, Howell GJ, Wheat R, Blair GE, Steven NM, Macdonald A, Blackbourn DJ. Merkel cell polyomavirus small T antigen mediates microtubule destabilization to promote cell motility and migration. Journal of virology. 2015 Jan 1;89(1):35-47.
52. Spurgeon ME, Cheng J, Bronson RT, Lambert PF, DeCaprio JA. Tumorigenic activity of Merkel cell polyomavirus T antigens expressed in the stratified epithelium of mice. Cancer research. 2015 Mar 15;75(6):1068-79.
53. Shuda M, Guastafierro A, Geng X, Shuda Y, Ostrowski SM, Lukianov S, Jenkins FJ, Honda K, Maricich SM, Moore PS, Chang Y. Merkel Cell Polyomavirus Small T Antigen Induces Cancer and Embryonic Merkel Cell Proliferation in a Transgenic Mouse Model. PloS one. 2015 Nov 6;10(11): e0142329.

54. Richards KF, Guastafierro A, Shuda M, Toptan T, Moore PS, Chang Y. Merkel cell polyomavirus T antigens promote cell proliferation and inflammatory cytokine gene expression. Journal of General Virology. 2015 Dec 1;96(12):3532-44.
55. Li J, Diaz J, Wang X, Tsang SH, You J. Phosphorylation of merkel cell polyomavirus large tumor antigen at serine 816 by atm kinase induces apoptosis in host cells. Journal of Biological Chemistry. 2015 Jan 16;290(3):1874-84.
56. Adam C, Baeurle A, Brodsky JL, Wipf P, Schrama D, Becker JC, Houben R. The HSP70 modulator MAL3-101 inhibits Merkel cell carcinoma. PloS one. 2014 Apr 2;9(4):e92041.
57. Shuda M, Feng H, Kwun HJ, Rosen ST, Gjoerup O, Moore PS, Chang Y. T antigen mutations are a human tumor-specific signature for Merkel cell polyomavirus. Proceedings of the National Academy of Sciences. 2008 Oct 21;105(42):16272-7.
58. en R, Adam C, Baeurle A, Hesbacher S, Grimm J, Angermeyer S, Henzel K, Hauser S, Elling R, Bröcker EB, Gaubatz S. An intact retinoblastoma protein-binding site in Merkel cell polyomavirus large T antigen is required for promoting growth of Merkel cell carcinoma cells. International journal of cancer. 2012 Feb 15;130(4):847-56.
59. Liu X, Hein J, Richardson SC, Basse PH, Toptan T, Moore PS, Gjoerup OV, Chang Y. Merkel cell polyomavirus large T antigen disrupts lysosome clustering by translocating human Vam6p from the cytoplasm to the nucleus. Journal of Biological Chemistry. 2011 May 13;286(19):17079-90.
60. Wang X, Li J, Schowalter RM, Jiao J, Buck CB, You J. Bromodomain protein Brd4 plays a key role in Merkel cell polyomavirus DNA replication. PLoS Pathog. 2012 Nov 8;8(11): e1003021.
61. Shuda M, Velásquez C, Cheng E, Cordek DG, Kwun HJ, Chang Y, Moore PS. CDK1 substitutes for mTOR kinase to activate mitotic cap-dependent protein translation. Proceedings of the National Academy of Sciences. 2015 May 12;112(19):5875-82.
62. Wu JH, Simonette RA, Hsiao T, Doan HQ, Rady PL, Tyring SK. Cutaneous Human Polyomavirus Small T Antigens and 4E-BP1 Targeting. Intervirology. 2016 Apr 8;58(6):382-5.
63. Griffiths DA, Abdul-Sada H, Knight LM, Jackson BR, Richards K, Prescott EL, Peach AH, Blair GE, Macdonald A, Whitehouse A. Merkel cell polyomavirus small T antigen targets the NEMO adaptor protein to disrupt inflammatory signaling. Journal of virology. 2013 Dec 15;87(24):13853-67.

64. Kwun HJ, Shuda M, Camacho CJ, Gamper AM, Thant M, Chang Y, Moore PS. Restricted protein phosphatase 2A targeting by Merkel cell polyomavirus small T antigen. Journal of virology. 2015 Apr 15;89(8):4191-200.
65. Kwun HJ, Shuda M, Feng H, Camacho CJ, Moore PS, Chang Y. Merkel Cell Polyomavirus Small T Antigen Controls Viral Replication and Oncoprotein Expression by Targeting the Cellular Ubiquitin Ligase SCF Fbw7. Cell host & microbe. 2013 Aug 14;14(2):125-35.
66. M. Czech-Sioli, S. Siebels, T. Dobner, A. Grundhoff, N. Fischer. Usp7, an ubiquitin specific protease interacts with Merkel cell polyomavirus Large T-Antigen and modulates viral DNA replication. Presented at the 26th Annual Meeting of the Society of Virology; Munster, Germany; 6-9 April, 2016
67. S. Siebels, M. Czech-Sioli, C. Schmidt, F. Neumann, A. Grundhoff, N. Fischer. Merkel cell polyomavirus (MCPyV) replication is negatively regulated by the host restriction factor Kap1/TRIM28. Presented at the 26th Annual Meeting of the Society of Virology; Munster, Germany; 6-9 April, 2016
68. Schowalter RM, Buck CB. The Merkel cell polyomavirus minor capsid protein. PLoS Pathog. 2013 Aug 22;9(8):e1003558.
69. Seo GJ, Chen CJ, Sullivan CS. Merkel cell polyomavirus encodes a microRNA with the ability to autoregulate viral gene expression. Virology. 2009 Jan 20;383(2):183-7.
70. Lee S, Paulson KG, Murchison EP, Afanasiev OK, Alkan C, Leonard JH, Byrd DR, Hannon GJ, Nghiem P. Identification and validation of a novel mature microRNA encoded by the Merkel cell polyomavirus in human Merkel cell carcinomas. Journal of Clinical Virology. 2011 Nov 30;52(3):272-5.
71. Renwick N, Cekan P, Masry PA, McGeary SE, Miller JB, Hafner M, Li Z, Mihailovic A, Morozov P, Brown M, Gogakos T. Multicolor microRNA FISH effectively differentiates tumor types. The Journal of clinical investigation. 2013 Jun 3;123(6):2694-702.
72. B Vendramini-Costa D, E Carvalho J. Molecular link mechanisms between inflammation and cancer. Current pharmaceutical design. 2012 Sep 1;18(26):3831-52.
73. Medzhitov R. Origin and physiological roles of inflammation. Nature. 2008 Jul 24;454(7203):428-35.
74. Medzhitov R. Inflammation 2010: new adventures of an old flame. Cell. 2010 Mar 19;140(6):771-6.

75. Joris I, Majno G. Cells, tissues, and disease: principles of general pathology. Oxford University Press, USA; 2004.
76. Kumar V, Cotran RS, Stanley L. Robbins, Robbins basic pathology.
77. Barton GM. A calculated response: control of inflammation by the innate immune system. The Journal of clinical investigation. 2008 Feb 1;118(2):413-20.
78. Hanahan D, Weinberg RA. Hallmarks of cancer: the next generation. cell. 2011 Mar 4;144(5):646-74.
79. Mesri EA, Feitelson MA, Munger K. Human viral oncogenesis: a cancer hallmarks analysis. Cell host & microbe. 2014 Mar 12;15(3):266-82.
80. Mantovani A, Allavena P, Sica A, Balkwill F. Cancer-related inflammation. Nature. 2008 Jul 24;454(7203):436-44.
81. Mogensen TH, Paludan SR. Molecular pathways in virus-induced cytokine production. Microbiology and Molecular Biology Reviews. 2001 Mar 1;65(1):131-50.
82. Smyth MJ, Cretney E, Kershaw MH, Hayakawa Y. Cytokines in cancer immunity and immunotherapy. Immunological reviews. 2004 Dec 1;202(1):275-93.
83. Mukaida N, Sasakki SI, Popivanova BK. Tumor necrosis factor (TNF) and chemokines in colitis-associated cancer. Cancers. 2011 Jun 27;3(3):2811-26.
84. Fernandes JV, Fernandes TA, de Azevedo JC, Cobucci RN, de Carvalho MG, Andrade VS, De Araujo JM. Link between chronic inflammation and human papillomavirus-induced carcinogenesis (Review). Oncology letters. 2015 Mar 1;9(3):1015-26.
85. Yang P, Markowitz GJ, Wang XF. The hepatitis B virus-associated tumor microenvironment in hepatocellular carcinoma. National science review. 2014 Sep 1;1(3):396-412.
86. Ouaguia L, Mrizak D, Renaud S, Moralès O, Delhem N. Control of the inflammatory response mechanisms mediated by natural and induced regulatory T-cells in HCV-, HTLV-1-, and EBV-associated cancers. Mediators of inflammation. 2014 Nov 30;2014.
87. Beringer A, Noack M, Miossec P. IL-17 in Chronic Inflammation: From Discovery to Targeting. Trends in molecular medicine. 2016 Mar 31;22(3):230-41.
88. Fossiez F, Djossou O, Chomarat P, Flores-Romo L, Ait-Yahia S, Maat C, Pin JJ, Garrone P, Garcia E, Saeland S, Blanchard D. T cell interleukin-17 induces stromal cells to produce proinflammatory and hematopoietic cytokines. The Journal of experimental medicine. 1996 Jun 1;183(6):2593-603.

89. Harrington LE, Hatton RD, Mangan PR, Turner H, Murphy TL, Murphy KM, Weaver CT. Interleukin 17–producing CD4+ effector T cells develop via a lineage distinct from the T helper type 1 and 2 lineages. Nature immunology. 2005 Nov 1;6(11):1123-32.
90. Jin W, Dong C. IL-17 cytokines in immunity and inflammation. Emerging microbes & infections. 2013 Sep 1;2(9): e60.
91. Gaffen SL. Recent advances in the IL-17 cytokine family. Current opinion in immunology. 2011 Oct 31;23(5):613-9.
92. Liu S, Song X, Chrunyk BA, Shanker S, Hoth LR, Marr ES, Griffor MC. Crystal structures of interleukin 17A and its complex with IL-17 receptor A. Nature communications. 2013 May 21; 4:1888.
93. Miossec P, Kolls JK. Targeting IL-17 and TH17 cells in chronic inflammation. Nature reviews Drug discovery. 2012 Oct 1;11(10):763-76.
94. Yang B, Kang H, Fung A, Zhao H, Wang T, Ma D. The role of interleukin 17 in tumour proliferation, angiogenesis, and metastasis. Mediators of inflammation. 2014 Jul 7;2014.
95. Moens U, Rasheed K, Abdulsalam I, Sveinbjørnsson B. The role of Merkel cell polyomavirus and other human polyomaviruses in emerging hallmarks of cancer. Viruses. 2015 Apr 10;7(4):1871-901.
96. Mishra R, Polic B, Welsh RM, Szomolanyi-Tsuda E. Inflammatory Cytokine–Mediated Evasion of Virus-Induced Tumors from NK Cell Control. The Journal of Immunology. 2013 Jul 15;191(2):961-70.
97. Lipson EJ, Vincent JG, Loyo M, Kagohara LT, Luber BS, Wang H, Xu H, Nayar SK, Wang TS, Sidransky D, Anders RA. PD-L1 expression in the merkel cell carcinoma microenvironment: association with inflammation, merkel cell polyomavirus, and overall survival. Cancer immunology research. 2013 Jul 1;1(1):54-63.
98. Afanasiev OK, Yelistratova L, Miller N, Nagase K, Paulson K, Iyer JG, Ibrani D, Koelle DM, Nghiem P. Merkel polyomavirus-specific T cells fluctuate with merkel cell carcinoma burden and express therapeutically targetable PD-1 and Tim-3 exhaustion markers. Clinical Cancer Research. 2013 Oct 1;19(19):5351-60.
99. Sakuishi K, Apetoh L, Sullivan JM, Blazar BR, Kuchroo VK, Anderson AC. Targeting Tim-3 and PD-1 pathways to reverse T cell exhaustion and restore anti-tumor immunity. The Journal of experimental medicine. 2011 Jun 6;208(6):1331.
100. Fourcade J, Sun Z, Benallaoua M, Guillaume P, Luescher IF, Sander C, Kirkwood JM, Kuchroo V, Zarour HM. Upregulation of Tim-3 and PD-1 expression is associated with

tumor antigen–specific CD8+ T cell dysfunction in melanoma patients. The Journal of experimental medicine. 2010 Sep 27;207(10):2175-86.

101. Weber N. Immune Evasion by Merkel Cell Cancer Could Involve Inhibitory Markers. Science Spotlight. 2014 Dec 16;3(12).

102. Bhatia S, Afanasiev O, Nghiem P. Immunobiology of Merkel cell carcinoma: implications for immunotherapy of a polyomavirus-associated cancer. Current oncology reports. 2011 Dec 1;13(6):488-97.

103. Afanasiev OK, Nagase K, Simonson W, Vandeven N, Blom A, Koelle DM, Clark R, Nghiem P. Vascular E-selectin expression correlates with CD8 lymphocyte infiltration and improved outcome in Merkel cell carcinoma. Journal of Investigative Dermatology. 2013 Aug 1;133(8):2065-73.

104. Chen XW, Zhou SF. Inflammation, cytokines, the IL-17/IL-6/STAT3/NF-κB axis, and tumorigenesis. Drug design, development and therapy. 2015; 9:2941.

105. Zou W, Restifo NP. TH17 cells in tumour immunity and immunotherapy. Nature Reviews Immunology. 2010 Apr 1;10(4):248-56.

106. Shinohara T, Matsuda M, Yasui K, Yoshiike K. Host range bias of the JC virus mutant enhancer with DNA rearrangement. Virology. 1989 May 31;170(1):261-3.

107. Arasaradnam RP, McFarlane MJ, Ryan-Fisher C, Westenbrink E, Hodges P, Thomas MG, Chambers S, O'Connell N, Bailey C, Harmston C, Nwokolo CU. Detection of colorectal cancer (CRC) by urinary volatile organic compound analysis. PloS one. 2014 Sep 30;9(9):e108750.

108. Daniel AM, Swenson JJ, Mayreddy RP, Khalili K, Frisque RJ. Sequences within the early and late promoters of archetype JC virus restrict viral DNA replication and infectivity. Virology. 1996 Feb 1;216(1):90-101.

109. Ault GS. Activity of JC virus archetype and PML-type regulatory regions in glial cells. Journal of general virology. 1997 Jan 1;78(1):163-9.

110. Johnsen JI, Seternes OM, Johansen T, Moens U, Mäntyjärvi R, Traavik T. Subpopulations of non-coding control region variants within a cell culture-passaged stock of BK virus: sequence comparisons and biological characteristics. Journal of general virology. 1995 Jul 1;76(7):1571-81.

111. Gosert R, Rinaldo CH, Funk GA, Egli A, Ramos E, Drachenberg CB, Hirsch HH. Polyomavirus BK with rearranged noncoding control region emerge in vivo in renal transplant patients and increase viral replication and cytopathology. The Journal of experimental medicine. 2008 Apr 14;205(4):841-52.

112. Macherey-Nagel. User Manual: Nucleobond®Xtra Midi kit. March 2014/Rev. 12 [05.04.2016]; Available from: http://2015.igem.org/wiki/images/4/47/Midiprep.pdf
113. Macherey-Nagel. User Manual: NucleoSpin®Plasmid kit December 2015/Rev. 09 [05.04.2016]; Available from: http://www.mn-net.com/Portals/8/attachments/Redakteure_Bio/Protocols/Plasmid%20DNA%20Purification/UM_pDNA_NS.pdf
114. Sambrook J. Russell. DW: Molecular Cloning: A Laboratory Manual, Third eds. ISBN 0-87969-577-3
115. Bitesizebio. Quick reference: Determining DNA Concentration & Purity. 2007 [05.04.15]; Available from: http://bitesizebio.com/articles/dna-concentration-purity/.
116. Thermo FisherScientificInc. User Manual: NanoDrop 1000 Spectrophotometer V3.7. 2008 [05.04.16]; Available from: http://nanodrop.com/Library/nd-1000-v3.7-users-manual-8.5x11.pdf
117. MoBio, Polymerase chain reaction (PCR). [05.04.2016]; Available from: http://www.web-books.com/MoBio/Free/Ch9E.htm
118. Primrose SB, Twyman R. Principles of gene manipulation and genomics. John Wiley & Sons; 2013 May 28.
119. Reece RJ. Analysis of genes and genomes. Hoboken, NJ: John Wiley & Sons; 2004 Jan.
120. Wilson K, Walker J, editors. Principles and techniques of biochemistry and molecular biology. Cambridge university press; 2010 Mar 4.
121. Yao Fei, DNA sequencing, Sanger and Next -generation sequencing, omics group ebook, 2014 [05.04.2016]; Available from http:www.esciencecentral.org/ebooks, 2014
122. Graham FL, Smiley J, Russell WC, Nairn R. Characteristics of a human cell line transformed by DNA from human adenovirus type 5. Journal of General Virology. 1977 Jul 1;36(1):59-72.
123. Leonard JH, Bell JR, Kearsley JH. Characterization of cell lines established from merkel-cell ("small-cell") carcinoma of the skin. International journal of cancer. 1993 Nov 11;55(5):803-10.
124. Scheffner M, Münger K, Byrne JC, Howley PM. The state of the p53 and retinoblastoma genes in human cervical carcinoma cell lines. Proceedings of the National Academy of Sciences. 1991 Jul 1;88(13):5523-7.
125. Biedler JL, Spengler BA. A novel chromosome abnormality in human neuroblastoma and antifolate-resistant Chinese hamster cell lines in culture. Journal of the National Cancer Institute. 1976 Sep 1;57(3):683-95.

126. Polyplus-transfection. jetPRIME® in vitro DNA & siRNA Transfection Reagent Protocol. 2015 [05.04.2016]; Available from http://www.polyplus-transfection.com/wp-content/uploads/2015/08/CPT_114_jetPRIME_vJ.pdf
127. Fan F, Wood KV. Bioluminescent assays for high-throughput screening. Assay and drug development technologies. 2007 Feb 1;5(1):127-36.
128. Promega. Bioluminiscent reactions. 2011 [05.04.2016]; Available from: http://www.promegaconnections.com/dual-luciferase-or-dual-glo-luciferase-assay-system-which-one-should-i-choose-for-my-reporter-assays/
129. Macherey-Nagel. User Manual: Protein Quantification AssayRev. 04, 2014 [05.04.16]; Available from: http://www.mnnet.com/ProductsBioanalysis/DNAandRNApurification/RNA/ProteinQuantificationAssay/tabid/10972/language/en-US/Default.aspx
130. Guastafierro A, Feng H, Thant M, Kirkwood JM, Chang Y, Moore PS, Shuda M. Characterization of an early passage Merkel cell polyomavirus-positive Merkel cell carcinoma cell line, MS-1, and its growth in NOD scid gamma mice. Journal of virological methods. 2013 Jan 31;187(1):6-14.
131. Mishra N, Pereira M, Rhodes RH, An P, Pipas JM, Jain K, Kapoor A, Briese T, Faust PL, Lipkin WI. Identification of a novel polyomavirus in a pancreatic transplant recipient with retinal blindness and vasculitic myopathy. Journal of Infectious Diseases. 2014 May 1: jiu250.
132. Barcena-Panero A, Echevarría JE, Van Ghelue M, Fedele G, Royuela E, Gerits N, Moens U. BK polyomavirus with archetypal and rearranged non-coding control regions is present in cerebrospinal fluids from patients with neurological complications. Journal of General Virology. 2012 Aug 1;93(8):1780-94.
133. Moens U, Van Ghelue M, Ludvigsen M, Korup-Schulz S, Ehlers B. Early and late promoters of BK polyomavirus, Merkel cell polyomavirus, Trichodysplasia spinulosa-associated polyomavirus and human polyomavirus 12 are among the strongest of all known human polyomaviruses in 10 different cell lines. Journal of General Virology. 2015 Aug 1;96(8):2293-303.
134. Church CD, Nghiem P. How does the Merkel Polyomavirus Lead to a Lethal Cancer? Many Answers, Many Questions, and a New Mouse Model. Journal of Investigative Dermatology. 2015 May 1;135(5):1221-4.
135. Paulson KG, Tegeder A, Willmes C, Iyer JG, Afanasiev OK, Schrama D, Koba S, Thibodeau R, Nagase K, Simonson WT, Seo A. Downregulation of MHC-I expression

is prevalent but reversible in Merkel cell carcinoma. Cancer immunology research. 2014 Nov 1;2(11):1071-9.

136. Houben R, Angermeyer S, Haferkamp S, Aue A, Goebeler M, Schrama D, Hesbacher S. Characterization of functional domains in the Merkel cell polyoma virus Large T antigen. International Journal of Cancer. 2015 Mar 1;136(5): E290-300.

137. Kim SY, Choi EC, Jo YW, Henson JW, Kim HS. Transcriptional activation of JC virus early promoter by phorbol ester and interleukin-1β: critical role of nuclear factor-1. Virology. 2004 Sep 15;327(1):60-9.

138. Espel E, Fromental C, Reichenbach P, Nabholz M. Activity and interleukin 1 responsiveness of SV40 enhancer motifs in a rodent immature T cell line. The EMBO journal. 1990 Mar;9(3):929.

139. Nukuzuma S, Nakamichi K, Kameoka M, Sugiura S, Nukuzuma C, Tasaki T, Takegami T. TNF-α stimulates efficient JC virus replication in neuroblastoma cells. Journal of medical virology. 2014 Dec 1;86(12):2026-32.

140. Wollebo HS, Melis S, Khalili K, Safak M, White MK. Cooperative Roles of NF-κB and NFAT4 in polyomavirus JC regulation at the KB control element. Virology. 2012 Oct 10;432(1):146-54.

141. Shuda M, Arora R, Kwun HJ, Feng H, Sarid R, Fernández-Figueras MT, Tolstov Y, Gjoerup O, Mansukhani MM, Swerdlow SH, Chaudhary PM. Human Merkel cell polyomavirus infection I. MCV T antigen expression in Merkel cell carcinoma, lymphoid tissues and lymphoid tumors. International journal of cancer. 2009 Sep 15;125(6):1243-9.

142. Rodig SJ, Cheng J, Wardzala J, DoRosario A, Scanlon JJ, Laga AC, Martinez-Fernandez A, Barletta JA, Bellizzi AM, Sadasivam S, Holloway DT. Improved detection suggests all Merkel cell carcinomas harbor Merkel polyomavirus. The Journal of clinical investigation. 2012 Dec 3;122(12):4645-53.

143. Sastre-Garau X, Peter M, Avril MF, Laude H, Couturier J, Rozenberg F, Almeida A, Boitier F, Carlotti A, Couturaud B, Dupin N. Merkel cell carcinoma of the skin: pathological and molecular evidence for a causative role of MCV in oncogenesis. The Journal of pathology. 2009 May 1;218(1):48-56.

144. Schowalter RM, Reinhold WC, Buck CB. Entry tropism of BK and Merkel cell polyomaviruses in cell culture. PLoS One. 2012 Jul 31;7(7): e42181.

145. Gosert R, Kardas P, Major EO, Hirsch HH. Rearranged JC virus noncoding control regions found in progressive multifocal leukoencephalopathy patient samples increase

virus early gene expression and replication rate. Journal of virology. 2010 Oct 15;84(20):10448-56.

146. Salehi-Vaziri M, Sadeghi F, Alamsi-Hashiani A, Haeri H, Monavari SH, Keyvani H. Merkel cell polyomavirus and human papillomavirus infections in cervical disease in Iranian women. Archives of virology. 2015 May 1;160(5):1181-7.

147. Del Valle L, White MK, Khalili K. Potential mechanisms of the human polyomavirus JC in neural oncogenesis. Journal of Neuropathology & Experimental Neurology. 2008 Aug 1;67(8):729-40.

148. White MK, Khalili K. Polyomaviruses and human cancer: molecular mechanisms underlying patterns of tumorigenesis. Virology. 2004 Jun 20;324(1):1-6.

149. White MK, Khalili K. Signaling pathways and polyomavirus oncoproteins: Importance in malignant transformation. Gene Ther Mol Biol. 2004; 8:19-30.

150. Moens U, Rekvig OP. Molecular biology of BK virus and clinical and basic aspects of BK virus renal infection. Human Polyomaviruses: Molecular and Clinical Perspectives. 2001 Oct 11:359-408.

151. Hashida Y, Imajoh M, Kamioka M, Taniguchi A, Kuroda N, Hayashi K, Nakajima H, Sano S, Daibata M. Phylogenetic analysis of Merkel cell polyomavirus based on full-length LT and VP1 gene sequences derived from neoplastic tumours in Japanese patients. Journal of General Virology. 2014 Jan 1;95(1):135-41.

152. Messeguer X, Escudero R, Farré D, Núñez O, Martínez J, Albà MM. PROMO: detection of known transcription regulatory elements using species-tailored searches. Bioinformatics. 2002 Feb 1;18(2):333-4.

153. Asselin CL, Vass-Marengo J, Bastin MA. Mutation in the polyomavirus genome that activates the properties of large T associated with neoplastic transformation. Journal of virology. 1986 Jan 1;57(1):165-72.

154. Noda TE, Satake MA, Yamaguchi YU, Ito YO. Cooperation of middle and small T antigens of polyomavirus in transformation of established fibroblast and epithelial-like cell lines. Journal of virology. 1987 Jul 1;61(7):2253-63.

155. Cubitt CL. Molecular genetics of the BK virus. InPolyomaviruses and Human Diseases 2006 (pp. 85-95). Springer New York.

156. Moens U, Van Ghelue M, Ehlers B. Are human polyomaviruses co-factors for cancers induced by other oncoviruses? Reviews in medical virology. 2014 Sep 1;24(5):343-60.

157. Erickson KD, Garcea RL, Tsai B. Ganglioside GT1b is a putative host cell receptor for the Merkel cell polyomavirus. Journal of virology. 2009 Oct 1;83(19):10275-9.

158. Low JA, Magnuson B, Tsai B, Imperiale MJ. Identification of gangliosides GD1b and GT1b as receptors for BK virus. Journal of virology. 2006 Feb 1;80(3):1361-6.
159. Bukowski JF, Roncarolo MG, Spits H, Krangel MS, Morita CT, Brenner MB, Band H. T cell receptor-dependent activation of human lymphocytes through cell surface ganglioside GT1b: implications for innate immunity. European journal of immunology. 2000 Nov 1;30(11):3199-206.
160. Sheikh KA, Deerinck TJ, Ellisman MH, Griffin JW. The distribution of ganglioside-like moieties in peripheral nerves. Brain. 1999 Mar 1;122(3):449-60.
161. Sung CC, O'Toole EA, Lannutti BJ, Hunt J, O'Gorman M, Woodley DT, Paller AS. Integrin α5β1 expression is required for inhibition of keratinocyte migration by ganglioside GT1b. Experimental cell research. 1998 Mar 15;239(2):311-9.
162. Hong S, Laimins LA. Regulation of the life cycle of HPVs by differentiation and the DNA damage response. Future microbiology. 2013 Dec;8(12):1547-57.

Appendix

Supplementary Figure 1: Nucleotide and amino acid sequences of MCPyV small t-antigen

GAGCATCCACGCTGTTTTGACCTCCATAGAAGACACCGGGACCGATCCAGCCTCCGGACTCTAGCGTTTAA
ACTTAAGCTTGGTACCGAGCTCGGATCCACTAGTAACGGCCGCCAGTGTGCTGGAATTCAGGGGGGGTACC
ATGGATTTAGTCCTAAATAGGAAAGAAAGAGAGGCTCTCTGCAAGCTTTTAGAGATTGCTCCTAATTGTTA
TGGCAACATCCCTCTGATGAAAGCTGCTTTCAAAAGAAGCTGCTTAAAGCATCACCCTGATAAAGGGGGAA
ATCCTGTTATAATGATGGAATTGAACACCCTTTGGAGCAAATTCCAGCAAAATATCCACAAGCTCAGAAGT
GACTTCTCTATGTTTGATGAGGTCAGTACAAAATTTCCTTGGGAAGAATATGGAACTTTAAAGGATTATAT
GCAAAGTGGATATAATGCTAGATTTTGCAGAGGTCCTGGGTGCATGCTTAAGCAACTTAGAGATTCTAAGT
GCGCTTGTATTAGCTGTAAGTTGTCTCGCCAGCATTGTAGTCTAAAAACTTTAAAGCAAAAAAACTGTCTG
ACGTGGGGAGAGTGTTTTTGCTATCAGTGCTTTATTCTTTGGTTTGGATTTCCTCCTACTTGGGAAAGTTT
TGACTGGTGGCAAAAAACTTTAGAAGAAACTGACTACTGCTTACTGCATCTGCACCTTTTCGATCATGATT
ACAAGGATGACGACGATAAGTGAGCGGCCCGCCCTGAATTCTGCAGATATCCATCACACTGGCGGCCGCTC
GAGTCTAGAGGGCCCGTTTAAACCCGCTGATCAGCCTCGACTGTGCCTTCTAGTTGCCAGCCATCTGTTGT
TTGCCCCTCCCCCCGTGCCTTCCTTGACCCTGGAAGGTGCCACTCCCACTGTCCTTTCCTATAAAATGAAG
GAAGTGCGCATCCGCATTGTCTGAATAGGTGTCATTGAATTCTGGGGGGGTGGGTGAGAC

MDLVLNRKEREALCKLLEIAPNCYGNIPLMKAAFKRSCLKHHPDKGGNPVIMMELNTLWSKFQQNIHKLRSDFSM
FDEVSTKFPWEEYGTLKDYMQSGYNARFCRGPGCMLKQLRDSKCACISCKLSRQHCSLKTLKQKNCLTWGECFCY
QCFILWFGFPPTWESFDWWQKTLEETDYCLLHLHLFDHDYKDDDDK

Flag tag

>gi|733573633|ref|YP_009111422.1| small T antigen [Merkel cell
polyomavirus]
MDLVLNRKEREALCKLLEIAPNCYGNIPLMKAAFKRSCLKHHPDKGGNPVIMMELNTLWSKFQQNIHKLRSDFSM
FDEVSTKFPWEEYGTLKDYMQSGYNARFCRGPGCMLKQLRDSKCACISCKLSRQHCSLKTLKQKNCLTWGECFCY
QCFILWFGFPPTWESFDWWQKTLEETDYCLLHLHLF

Clustal Omega (http://www.ebi.ac.uk/Tools/msa/clustalo/)

```
Ibr        MDLVLNRKEREALCKLLEIAPNCYGNIPLMKAAFKRSCLKHHPDKGGNPVIMMELNTLWS
stag       MDLVLNRKEREALCKLLEIAPNCYGNIPLMKAAFKRSCLKHHPDKGGNPVIMMELNTLWS
           ************************************************************

Ibr        KFQQNIHKLRSDFSMFDEVSTKFPWEEYGTLKDYMQSGYNARFCRGPGCMLKQLRDSKCA
stag       KFQQNIHKLRSDFSMFDEVSTKFPWEEYGTLKDYMQSGYNARFCRGPGCMLKQLRDSKCA
           ************************************************************

Ibr        CISCKLSRQHCSLKTLKQKNCLTWGECFCYQCFILWFGFPPTWESFDWWQKTLEETDYCL
stag       CISCKLSRQHCSLKTLKQKNCLTWGECFCYQCFILWFGFPPTWESFDWWQKTLEETDYCL
           ************************************************************

Ibr        LHLHLFDHDYKDDDDK
stag       LHLHLF----------
           ******


Ibr        MDLVLNRKEREALCKLLEIAPNCYGNIPLMKAAFKRSCLKHHPDKGGNPVIMMELNTLWS
stag       MDLVLNRKEREALCKLLEIAPNCYGNIPLMKAAFKRSCLKHHPDKGGNPVIMMELNTLWS
           ************************************************************

Ibr        KFQQNIHKLRSDFSMFDEVSTKFPWEEYGTLKDYMQSGYNARFCRGPGCMLKQLRDSKCA
stag       KFQQNIHKLRSDFSMFDEVSTKFPWEEYGTLKDYMQSGYNARFCRGPGCMLKQLRDSKCA
           ************************************************************

Ibr        CISCKLSRQHCSLKTLKQKNCLTWGECFCYQCFILWFGFPPTWESFDWWQKTLEETDYCL
stag       CISCKLSRQHCSLKTLKQKNCLTWGECFCYQCFILWFGFPPTWESFDWWQKTLEETDYCL
           ************************************************************

Ibr        LHLHLFDHDYKDDDDK
stag       LHLHLF----------
```

******

NB: the pink, yellow ,green and magenta colours are multiple cloning sites in the vector sequences.
There is a flag tag at the C-terminal end, which enables the use of flag antibody to confirm via WB.

Supplementary Figure 2: Amino acid sequence of Full-length MCPyV large T-antigen. The amino acids marked in red represent the last amino acid of the truncated LTag in MS-1 (N), MKL-1 (Y), and MKL-2 (F)

The underlined amino acids corresponds to the sequences obtained by sequencing with the forward and reverse MCV LTag primers.

>gi|531990549|dbj|BAN78688.1| large T antigen [Merkel cell polyomavirus]
MDLVLNRKEREALCKLLEIAPNCYGNIPLMKAAFKRSCLKHHPDKGGNPVIMMELNTLWSKFQQNIHKLRSDFSM
FDEVDEAPIYGTTKFKEWWRSGGFSFGKAYEYGPNPHGTNSRSRKPSSNASRGAPSGSSPPHSQSSSSGYGSFSA
SQTSDSQSRGPDIPPEHHEEPTSSSGSSSREETTNSGRESSTPNGTSVPRNSSRTDGTWEDLFCDESLSSPEPPS
SSEEPEEPPSSRSSPRQPPSSSAEEASSSQFTDEECRSSSFTTPKTPPPFSRKRKFGGSRSSASSASSASFTSTP
PKPKKNRETPVPTDFPIDLSDYLSHAVYSNKTVSCFAIYTTSDKAIELYDKIEKFKVDFKSRHACELGCILLFIT
LSKHRVSAIKNFCSTFCTISFLICKGVNKMPEMYNNLCKPPYKLLQENKPLLNYEFQEKEKEASCNWNLVAEFAC
EYELDDHFIILAHYLDFAKPFPCQKCENRSRLKPHKAHEAHHSNAKLFYESKSQKTICQQAADTVLAKRRLEMLE
MTRTEMLCKKFKKHLERLRDLDTIDLLYYMGGVAWYCCLFEEFEKKLQKIIQLLTENIPKHRNIWFKGPINSGKT
SFAAALIDLLEGKALNINCPSDKLPFELGCALDKFMVVFEDVKGQNSLNKDLQPGQGINNLDNLRDHLDGAVAVS
LEKKHVNKKHQIFPPCIVTANDYFIPKTLIARFSYTLHFSPKANLRDSLDQNMEIRKRRILQSGTTLLLCLIWCL
PDTTFKPCLQEEIKNWKQILQSEISYGKFCQMIENVEAGQDPLLNILVEEEGPEETEETQDSGTFSQ

AYEYGPNPHGTNSRSRKPSSNASRGAPSGSSPPHSQSSSSGYGSFSASQASDPQSRGPDIPPEHHEEPTSSSGSS
SREETTNSGRESSTPNGTSVPRNSSRTDGTWEDLFCDESLSSPEPPSSSEEPEEPPSSRSSPRQPPSSSAEEASS
SQFTDEEYRSSSFTTPKTPPPFSRKRKFGGSRSSASSASSASFTSTPPKPKKNRETPVPTDFPIDLSDYLSHAVY
SNKTVSCFAIYTTSDKAIELYDKIEKFKVDFKSRHACELGCILLFITLSKHRVSAIKNFCSTFCTISFLICKGVN

KMPEMYNNLCKPPYKLLQENKPLLNYD

Supplementary Figure 3: Amino acid and Nucleotide sequence of MS-1 truncated Large T – antigen. The underlined amino acids represent the end of LT-ag of MKL-1 and MKL-2 LT-ag. The red amino acids are residues that differ in MKL-2 LT-ag.

MDLVLNRKEREALCKLLEIAPNCYGNIPLMKAAFKRSCLKHHPDKGGNPVIMMELNTLWSKFQQNIHKLRSDFSM
FDEVDEAPIYGTTKFKEWWRSGGFSFGKAYEYGPNPHGTNSRSRKPSSNASRGAPSGSSPPHSQSSSSGYGSFSA
SQASDSQSRGPDIPPEHHEEPTSSSGSSSREETTNSGRESSTPNGTSVPRNSSRTDGTWEDLFCDESLSSPEPPS
SSEEPEEPPSSRSSPRQPPSSSAEEASSSQFTDEEYRSSSFTTPKTPPPFSRKRKFGGSRSSASSASSASFTSTP
PKPKKNRETPVPTDFPIDLSDYLSHAVYSNKTVSCFAIYTTSDKAIELYDKIEKFKVDFKSRHACELGCILLFIT
LSKHRVSAIKNFCSTFCTISFLICKGVNKMPEMYNNLCKPPYKLLQENKPLLN

atggatttagtcctaaataggaaagaaagagaggctctctgcaagcttttagagattgctcctaattgttatggc
aacatccctctgatgaaagctgctttcaaaagaagctgcttaaagcatcaccctgataaaggggaaatcctgtt
ataatgatggaattgaacacccttggagcaaattccagcaaaatatccacaagctcagaagtgacttctctatg
tttgatgaggttgacgaggcccctatatatgggaccactaaattcaaagaatggtggagatcaggaggattcagc
ttcgggaaggcatacgaatatgggcccaatccacacgggaccaactcaagatccagaaagccttcctccaatgca
tccaggggagcccccagtggaagctcaccaccccacagccagagctcttcctctgggtatgggtccttctcagcg
tcccaggcttcagactcccagtccagaggacccgatatacctcccgaacaccatgaggaacccacctcatcctct
ggatccagtagcagagaggagaccaccaattcaggaagagaatccagcacacccaatggaaccagtgtacctaga
aattcttccagaacggatggcacctgggaggatctcttctgcgatgaatcactttcctcccctgagcctccctcg
tcctctgaggagcctgaggagcccccctcctcaagaagctcgccccggcagcccccgtcttcctctgccgaggag
gcctcgtcatctcagtttacagatgaggaatacagatcctcctccttcaccaccccgaagacccctcctccattc
tcaagaaagcgaaaatttgggggtcccgaagctctgcaagctctgctagttcagcaagttttacaagcactcca
ccaaagccaaaaaagaacagagaaactcctgttcctactgattttcctattgatctttctgattatcttagccat
gctgtatatagtaataaaacagtaagttgttttgccatttatactacttctgataaagctatagagttatatgat
aagattgagaaatttaaagttgattttaaaagcaggcatgcctgtgaattaggatgtattttattgtttataact
ttatcaaagcatagagtatctgctattaagaatttttgctctaccttctgcactataagctttttaatttgtaaa
ggagtgaataagatgcctgaaatgtataataatttatgcaagccccttacaaattactgcaagagaataagcca
ctgctcaattgaatttagttgctgaatttgcttgtgaatatgagctaga
cgaccactttattatcttagcccattatct

Supplementary Figure 4: Amino acid and Nucleotide sequence of MKL-1 truncated Large T –antigen. The underlined amino acids represent the end of MKL-2 LT-ag. The red amino acids are residues that differ in MKL-2 LT-ag.

MDLVLNRKEREALCKLLEIAPNCYGNIPLMKAAFKRSCLKHHPDKGGNPVIMMELNTLWSKFQQNIHKLRSDFSM
FDEVDEAPIYGTTKFKEWWRSGGFSFGKAYEYGPNPHGTNSRSRKPSSNASRGAPSGSSPPHSQSSSSGYGSFSA
SQASDSQSRGPDIPPEHHEEPTSSSGSSSREETTNSGRESSTPNGTSVPRNSSRTDGTWEDLFCDESLSSPEPPS
SSEEPEEPPSSRSSPRQPPSSSAEEASSSQFTDEEYRSSSFTTPKTPPP**F**SRKRKFGGSRSSASSASSASFTSTP
PKPKKNRETPVPTDFPIDLSDYLSHAVYKL

atggatttagtcctaaataggaaagaaagagaggctctctgcaagcttttagagattgctcctaattgttatggc
aacatccctctgatgaaagctgctttcaaaagaagctgcttaaagcatcaccctgataaaggggaaatcctgtt
ataatgatggaattgaacacccttggagcaaattccagcaaaatatccacaagctcagaagtgacttctctatg
tttgatgaggttgacgaggcccctatatatgggaccactaaattcaaagaatggtggagatcaggaggattcagc
ttcgggaaggcatacgaatatgggcccaatccacacgggaccaactcaagatccagaaagccttcctccaatgca
tccaggggagcccccagtggaagctcaccaccccacagccagagctcttcctctgggtatgggtccttctcagcg
tcccaggcttcagactcccagtccagaggacccgatatacctcccgaacaccatgaggaacccacctcatcctct
ggatccagtagcagagaggagaccaccaattcaggaagagaatccagcacacccaatggaaccagtgtacctaga
aattcttccagaacggatggcacctgggaggatctcttctgcgatgaatcactttcctcccctgagcctccctcg
tcctctgaggagcctgaggagcccccctcctcaagaagctcgccccggcagcccccgtcttcctctgccgaggag
gcctcgtcatctcagtttacagatgaggaatacagatcctcctccttcaccaccccgaagacccctcctccattc
tcaagaaagcgaaaatttgggggtcccgaagctctgcaagctctgctagttcagcaagttttacaagcactcca
ccaaagccaaaaaagaacagagaaactcctgttcctactgattttcctattgatctttctgattatcttagccat
gctgtatataagctatagagttatatgataagattgagaaatttaaagttgattttaaaagcaggcatgcctgtg
aatt

Supplementary Figure 5: Amino acid and Nucleotide sequence of MKL-2 truncated Large T –antigen

MDLVLNRKEREALCKLLEISPNCYGNIPLMKAAFKRSCLKHHPDKGGNPVIMMELNTLWSKFQQNIHKLRSDFSM
FDEVDEAPIYGTTKFKEWWRSGGFSFGKAYEYGPNPHGTNSRSRKPSSNASRGAPSGSSPPHSQSSSSGYGSFSA
SQASDSQSRGPDIPPEHHEEPTSSSGSSSREETTNSGRESSTPNGTSVPRNSSRTDGTWEDLFCDESLSSPEPPS
SSEEPEEPPSSRSSPRQPPSSSAEEASSSQFTDEEYRFSSFTTPKTPPAF

atggatttagtcctaaataggaaagaaagagaggctctctgcaagcttttagagatttctcctaattgttatggc
aacatccctctgatgaaagctgctttcaaaagaagctgcttaaagcatcaccctgataaaggggaaatcctgtt
ataatgatggaattgaacacccttggagcaaattccagcaaaatatccacaagctcagaagtgacttctctatg
tttgatgaggttgacgaggcccctatatatgggaccactaaattcaaagaatggtggagatcaggaggattcagc
ttcgggaaggcatacgaatatgggcccaatccacacgggaccaactcaagatccagaaagccttcctccaatgca
tccaggggagcccccagtggaagctcaccaccccacagccagagctcttcctctgggtatgggtccttctcagcg
tcccaggcttcagactcccagtccagaggacccgatatacctcccgaacaccatgaggaacccacctcatcctct
ggatccagtagcagagaggagaccaccaattcaggaagagaatccagcacacccaatggaaccagtgtacctaga
aattcttccagaacggatggcacctgggaggatctcttctgcgatgaatcactttcctcccctgagcctccctcg
tcctctgaggagcctgaggagcccccctcctcaagaagctcgccccggcagcccccgtcttcctctgccgaggag
gcctcgtcatctcagtttacagatgaggaatacagattctcctccttcaccaccccgaagacccctcctgcattc
taaagaaagcgaaaatttgggggtcccgaagctctgcaagctgtgctagtttagcaagttttat

Supplementary Figure 6: Alignment of MCPyV NCCRs available in GenBank.

```
AmePI          CCTGAAAAATAAATAGGGATACTTACTCTTTTAATGTCCTCCTCCCT-------------
FraMerk20      CCTGAAAAATAAATAAGGATACTTACTCTTTTAATGTCCTCCTCCCT-------------
MKT-26         CCTGAAAAATAAATAAGGATACTTACTCTCTTAATGTCCTCCTCCCT-------------
MCVw156        CCTGAAAAATAAATAAGGATACTTACTCTTTTAATGTCCTCCTCCCT-------------
MKT-22         CCTGAAAAATAAATAATGATACTTACTCTTTTAATGTCCTCCTCCCT-------------
MKT-32         CCTGAAAAATAAATAAGGATACTTACTCTTTTAATGTCCTCCTCCCT-------------
R26b           CCTGAAAAATAAATAAGGATACTTACTCTTTTAATGTCCTCCTCCCT-------------
R12b           CCTGAAAAATAAATAAGGATACTTACTCTTTTAATGTCCTCCTCCCT-------------
MKT-33         CCTGAAAAATAAATAAGGATACTTACTCTTTTAATGTCCTCCTCCCT-------------
R15a           CCTGAAAAATAAATAAGGATACTTACTCTTTTAATGTCCTCCTCCCT-------------
R13a           CCTGAAAAATAAATAAGGATACTTACTCTTTTAATGTCCTCCTCCCT-------------
FraMerk2       CCTGAAAAATAAATAAGGATACTTACTCTTTTAATGTCCTCCTCCCT-------------
MCC352         CCTGAAAAATAAATAAGGATACTTACTCTTTTAATGTCCTCCTCCCT-------------
R17a           CCTGAAAAATAAATAAGGATACTTACTCTTTTAATGTCCTCCTCCCT-------------
R09b           CCTGAAAAATAAATAAGGATACTTACTCTTTTAATGTCCTCCTCCCT-------------
FraMerk22      CCTGAAAAATAAATAAGGATACTTACTCTTTTAATGTCCTCCTCCCT-------------
BroLi          CCTGAAAAATAAATAAGGATACTTACTCTTTTAATGTCCTCCTCCCT-------------
FraMerk24      CCTGAAAAATAAATAAGGATACTTACTCTTTTAATGTCCTCCTCCCT-------------
MCC350         CCTGAAAAATAAATAAGGATACTTACTCTTTTAATGTCCTCCTCCCT-------------
MCC85          CCTGAAAAATAAATAAGGATACTTACTCTTTTAATGTCCTCCTCCCT-------------
MKL-1          CCTGAAAAATAAATAAGGATACTTACTCTTTTAATGTCCTCCTCCCT-------------
BG1            CCTGAAAAATAAATAAGGATACTTACTCTTTTAATGTCCTCCTCCCT-------------
MKT-31         CCTGAAAAATAAATAAGGATACTTACTCTTTTAATGTCCTCCTCCCT-------------
EurCauC1       CCTGAAAAATAAATAAGGATACTTACTCTTTTAATGTCCTCCTCCCT-------------
AlDo           CCTGAAAAATAAATAAGGATACTTACTCTTTTAATGTCCTCCTCCCT-------------
R17b           CCTGAAAAATAAATAAGGATACTTACTCTTTTAATGTCCTCCTCCCT-------------
R30b           CCTGAAAAATAAATAAGGATACTTACTCTTTTAATGTCCTCCTCCCT-------------
R12a           CCTGAAAAATAAATAAGGATACTTACTCTTTTAATGTCCTCCTCCCT-------------
LoKe           CCTGAAAAATAAATAAGGATACTTACTCTTTTAATGTCCTCCTCCCT-------------
WoWe           CCTGAAAAATAAATAAGGATACTTACTCTTTTAATGTCCTCCTCCCT-------------
WaGa           CCTGAAAAATAAATAAGGATACTTACTCTTTTAATGTCCTCCTCCCT-------------
PJ2            CCTGAAAAATAAATAAGGATACTTACTCTTTTAATGTCCTCCTCCCT-------------
HF             CCTGAAAAATAAATAAGGATACTTACTCTTTTAATGTCCTCCTCCCT-------------
MCC349         CCTGAAAAATAAATAAGGATACTTACTCTTTTAATGTCCTCCTCCCT-------------
R16b           CCTGAAAAATAAATAGGGATACTTACTCTTTTAATGTCCTCCTCCCTTTGTAAGAG--AA
HB039C         CCTGAAAAATAAATAGGGATACTTACTCTTTTAATGTCCTCCTCCCTTTGTAAGAGAAAA
TKS            CCTGAAAAATAAATAGGGATACTTACTCTTTTAATGTCCTCCTCCCTTTGTAAGAGAAAA
```

```
OcepolW1        CCTGAAAAATAAATAGGGATACTTACTCTTTTAATGT----------------------
R10b            CCTGAAAAATAAATAGGGATACTTACTCTTTTAATGT----------------------
R25b            CCTGAAAAATAAATAAGGATACTTACTCTTTTAATGT----------------------
MCC344          CCTGAAAAATAAATAAGGATACTTACTCTTTTAATGT----------------------
PeTa            CCTGAAAAATAAATAAGGATACTTACTCTTTTAATGT----------------------
MCC339          CCTGAAAAATAAATAAGGATACTTACTCTTTTAATGT----------------------
R14a            CCTGAAAAATAAATAAGGATACTTACTCTTTTAATGT----------------------
R06b            CCTGAAAAATAAATAAGGATACTTACTCTTTTAATGT----------------------
MKT-21          CCTGAAAAATAAATAAGGATACTTACTCTTTTAATGT----------------------
MS-1            CCTGAAAAATAAATAAGGATACTTACTCTTTTAATGT----------------------
CG4             CCTGAAAAATAAATAAGGATACTTACTCTTTTAATGT----------------------
KN4             CCTGAAAAATAAATAAGGATACTTACTCTTTTAATGT----------------------
HUN             CCTGAAAAATAAATAAGGATACTTACTCTTTTAATGT----------------------
                ***************  ************ *******

AmePI           --------------TTGTAAGAGAAAAAAAAAGCCTCCGGGCCTCCCTTGT-------TG
FraMerk20       --------------TTGTAAGAGAAAAAAAAGCCTCCGGGCCTCCCTTGTT-------GA
MKT-26          --------------TTGTAAGAGAAAAAAAAGCCTCCGGGCCTCCCTTGTT-------GA
MCVw156         --------------TTGTAAGAGAAAAAAAAGCCTCCGGGCCTCCCTTGTT-------GA
MKT-22          --------------TTGTAAGAGAAAA-AAAGCCTCCGGGCCTCCCTTGTT-------GA
MKT-32          --------------TTGTAAGAGAAAAAAAAGCCTCCGGGCCTCCCTTGTT-------GA
R26b            --------------TTGTAAGAGAAAAAAAAGCCTCC-GGCCTCCCTTGTT-------GA
R12b            --------------TTGTAAGAGAAAAAAAAGCCTCCGGGCCTCCCTTGTT-------GA
MKT-33          --------------TTGTAAGAGAAAAAAAAGCCTCCGGGCCTCCCTTGTT-------GA
R15a            --------------TTGTAAGAGAAAAAAAAGCCTCCGGGCCTCCCTTGTT-------GA
R13a            --------------TTGTAAGAGAAAAAAAAGCCTCCGGGCCTCCCTTGTT-------GA
FraMerk2        --------------TTGTAAGAGAAAAAAAAGCCTCCGGGCCTCCCTTGTT-------GA
MCC352          --------------TTGTAAGAGAAAAAAAAGCCTCCGGGCCTCCCTTGTT-------GA
R17a            --------------TTGTAAGAGAAAAAAAAGCCTCCGGGCCTCCCTTGTT-------GA
R09b            --------------TTGTAAGAGAAAAAAAAGCCTCCGGGCCTCCCTTGTT-------GA
FraMerk22       --------------TTGTAAGAGAAAAAAAAGCCTCCGGGCCTCCCTTGTT-------GA
BroLi           --------------TTGTAAGAGAAAAAAAAGCCTCCGGGCCTCCCTTGTT-------GA
FraMerk24       --------------TTGTAAGAGAAAAAAAAGCCTCCGGGCCTCCCTTGTT-------GA
MCC350          --------------TTGTAAGAGAAAAAAAAGCCTCCGGGCCTCCCTTGTT-------GA
MCC85           --------------TTGTAAGAGAAAAAAAAGCCTCCGGGCCTCCCTTGTT-------GA
MKL-1           --------------TTGTAAGAGAAAAAAAAGCCTCCGGGCCTCCCTTGTT-------GA
BG1             --------------TTGTAAGAGAAAAAAAAGCCTCCGGGCCTCCCTTGTT-------GA
MKT-31          --------------TTGTAAGAGAAAAAAAAGCCTCCGGGCCTCCCTTGTT-------GA
EurCauC1        --------------TTGTAAGAGAAAAAAAAGCCTCCGGGCCTCCCTTGTT-------GA
AlDo            --------------TTGTAAGAGAAAAAAAAGCCTCCGGGCCTCCCTTGTT-------GA
R17b            --------------TTGTAAGAGAAAAAAAAGCCTCCGGGCCTCCCTTGTT-------GA
R30b            --------------TTGTAAGAGAAAAAAAAGCCTCCGGGCCTCCCTTGTT-------GA
R12a            --------------TTGTAAGAGAAAAAAAAGCCTCCGGGCCTCCCTTGTT-------GA
LoKe            --------------TTGTAAGAGAAAAAAAAGCCTCCGGGCCTCCCTTGTT-------GA
WoWe            --------------TTGTAAGAGAAAAAAAAGCCTCCGGGCCTCCCTTGTT-------GA
WaGa            --------------TTGTAAGAGAAAAAAAAGCCTCCGGGCCTCCCTTGTT-------GA
PJ2             --------------TTGTAAGAGAAAAAAAAGCCTCCGGGCCTCCCTTGTT-------GA
HF              --------------TTGTAAGAGAAAAAAAAGCCTCCGGGCCTCCCTTGTT-------GA
MCC349          --------------TTGTAAGAGAAAAAAAAGCCTCCGGGCCTCCCTTGTT-------GA
R16b            ATGTCCTCCTCCCTTTGTAAGAGAAAAAAAAGCCTCCGGGCCTCCCTTTTGTTGAAAAAA
HB039C          ATGTCCTCCTCCCTTTGTAAGAGAAAAAAAAGCCTCCGGGCCTCCCTTTTGTTGAAAAAA
TKS             ATGTCCTCCTCCCTTTGTAAGAGAAAAAAAAGCCTCCGGGCCTCCCTTTTGTTGAAAAAA
OcepolW1        ----CCTCCTCCCTTTGTAAGAGAAAAAAAAGCCTCCGAGCCT------------CGAAA
R10b            ----CCTCCTCCCTTTGTAAGAGAAAAAAAAGCCTCCGGGCCT---------CGAAAAAA
R25b            ----CCTCCTCCCTTTGTAAGAGAAAAAAAAGCCTCCGGGCCTC--CCTTGTTGAAAAAA
MCC344          ----CCTCCTCCCTTTGTAAGAGAAAAAAAAGCCTCCGGGCCTC--CCTTGTTGAAAAAA
PeTa            ----CCTCCTCCCTTTGTAAGAGAAAAAAAAGCCTCCGGGCCTC--CCTTGTTGAAAAAA
MCC339          ----CCTCCTCCCTTTGTAAGAGAAAAAAAAGCCTCCGGGCCTC--CCTTGTTGAAAAAA
R14a            ----CCTCCTCCCTTTGTAAGAGAAAAAAAAGCCTCCGGGCCTC--CCTTGTTGAAAAAA
R06b            ----CCTCCTCCCTTTGTAAGAGAAAAAAAAGCCTCCGGGCCTC--CCTTGTTGAAAAAA
MKT-21          ----CCTCCTCCCTTTGTAAGAGAAAAAAAAGCCTCCGGGCCTC--CCTTGTTGAAAAAA
MS-1            ----CCTCCTCCCTTTGTAAGAGAAAAAAAAGCCTCCGGGCCTC--CCTTGTTGAAAAAA
CG4             ----CCTCCTCCCTTTGTAAGAGAAAAAAAAGCCTCCGGGCCTC--CCTTGTTGAAAAAA
KN4             ----CCTCCTCCCTTTGTAAGAGAAAAAAAAGCCTCCGGGCCTC--CCTTGTTGAAAAAA
HUN             ----CCTCCTCCCTTTGTAAGAGAAAAAAAAGCCTCCGGGCCTC--CCTTGTTGAAAAAA
                             ************* ***  *  *  * *

AmePI           AAAAAAGTTAAGAGTCTTCCGTCTCCCTCCCAAACAGAAAGAAAAAAAGTTTTGTTTATC
```

```
FraMerk20       AAAAAAGTTAAGAGTTTTCCGTCTCCCTCCCAAACAGAAAGAAAAAAAGTTTTGTTTATC
MKT-26          AAAAAAGTTAAGAGTCTTCCGTCTCCCTCCCAAACAGAAAGAAAAAAAGTTTTGTTTATC
MCVw156         AAAAAAGTTAAGAGTCTTCCGTCTCCCTCCCAAACAGAAAGAAAAAAAGTTTTGTTTATC
MKT-22          AAAAAAGTTAAGAGTCTTCCGTCTCCCTCCCAAACAGAAAGAAAAAAAGTTTTGTTTATC
MKT-32          AAAAAAGTTAAGAGTCTTCCGTCTCCCTCCCAAACAGAAAGAAAAAAAGTTTTGTTTATC
R26b             AAAAAAGTTAAGAGTCTTCCGTCTCCCTCCCAAACAGAAAGAAAAAAAGTTTTGTTTATC
R12b             AAAAAAGTTAAGAGTCTTCCGTCTCCCTCCCAAACAGAAAGAAAAAAAGTTTTGTTTATC
MKT-33          AAAAAAGTTAAGAGTCTTCCGTCTCCCTCCCAAACAGAAAGAAAAAAAGTTTTGTTTATC
R15a             AAAAAAGTTAAGAGTCTTCCGTCTCCCTCCCAAACAGAAAGAAAAAAAGTTTTGTTTATC
R13a             AAAAAAGTTAAGAGTCTTCCGTCTCCCTCCCAAACAGAAAGAAAAAAAGTTTTGTTTATC
FraMerk2        AAAAAAGTTAAGAGTCTTCCGTCTCCCTCCCAAACAGAAAGAAAAAAAGTTTTGTTTATC
MCC352          AAAAAAGTTAAGAGTCTTCCGTCTCCCTCCCAAACAGAAAGAAAAAAAGTTTTGTTTATC
R17a             AAAAAAGTTAAGAGTCTTCCGTCTCCCTCCCAAACAGAAAGAAAAAAAGTTTTGTTTATC
R09b             AAAAAAGTTAAGAGTCTTCCGTCTCCCTCCCAAACAGAAAGAAAAAAAGTTTTGTTTATC
FraMerk22       AAAAAAGTTAAGAGTTTTCCGTCTCCCTCCCAAACAGAAAGAAAAAAAGTTTTGTTTATC
BroLi           AAAAAAGTTAAGAGTCTTCCGTCTCCCTCCCAAACAGAAAGAAAAAAAGTTTTGTTTATC
FraMerk24       AAAAAAGTTAAGAGTCTTCCGTCTCCCTCCCAAACAGAAAGAAAAAAAGTTTTGTTTATC
MCC350          AAAAAAGTTAAGAGTTTTCCGTCTCCCTCCCAAACAGAAAGAAAAAAAGTTTTGTTTATC
MCC85           AAAAAACTTAAGAGTCTTCCGTCTCCCTCCCAAACAGAAAGAAAAAAAGTTTTGTTTATC
MKL-1           AAAAAAGTTAAGAGTCTTCCGTCTCCCTCCCAAACAGAAAGAAAAAAAGTTTTGTTTATC
BG1             AAAAAAGTTAAGAGTCTTCCGTCTCCCTCCCAAACAGAAAGAAAAAAAGTTTTGTTTATC
MKT-31          AAAAAAGTTAAGAGTCTTCCGTCTCCCTCCCAAACAGAAAGAAAAAAAGTTTTGTTTATC
EurCauC1        AAAAAAGTTAAGAGTTTTCCGTCTCCCTCCCAAACAGAAAGAAAAAAAGTTTTGTTTATC
AlDo            AAAAAAGTTAAGAGTCTTCCGTCTCCCTCCCAAACAGAAAGAAAAAAAGTTTTGTTTATC
R17b             AAAAAAGTTAAGAGTCTTCCGTCTCCCTCCCAAACAGAAAGAAAAAAAGTTTTGTTTATC
R30b             AAAAAAGTTAAGAGTCTTCCGTCTCCCTCCCAAACAGAAAGAAAAAAAGTTTTGTTTATC
R12a             AAAAAAGTTAAGAGTCTTCCGTCTCCCTCCCAAACAGAAAGAAAAAAAGTTTTGTTTATC
LoKe             AAAAAAGTTAAGAGTCTTCCGTCTCCCTCCCAAACAGAAAGAAAAAAAGTTTTGTTTATC
WoWe             AAAAAAGTTAAGAGTCTTCCGTCTCCCTCCCAAACAGAAAGAAAAAAAGTTTTGTTTATC
WaGa             AAAAAAGTTAAGAGTCTTCCGTCTCCCTCCCAAACAGAAAGAAAAAAAGTTTTGTTTATC
PJ2              AAAAAAGTTAAGAGTCTTCCGTCTCCCTCCCAAACAGAAAGAAAAAAAGTTTTGTTTATC
HF              AAAAAAGTTAAGAGTCTTCCGTCTCCCTCCCAAACAGAAAGAAAAAAAGTTTTGTTTATC
MCC349          AAAAAAGTTAAGAGTCTTCCGTCTCCCTCCCAAACAGAAAGAAAAAAAGTTTTGTTTATC
R16b             AGTTGAGTTAAGAGTCTTCCGTCTCCCTCCCAAACAGAAAGAAAAAAAGTTTTGTTTATC
HB039C          AGTTGAGTTAAGAGTCTTCCGTCTCCCTCCCAAACAGAAAGAAAAAAAGTTTTGTTTATC
TKS             AGTTGAGTTAAGAGTCTTCCGTCTCCCTCCCAAACAGAAAGAAAAAAAGTTTTGTTTATC
OcepolW1        AATTGTGTTAAGAGTCTTCCGTCTCCCTCCCAAACAGAAAGAAAAAAAGTTTTGTTTATC
R10b             AGTTGTGTTAAGAGTCTTCCGTCTCCCTCCCAAACAGAAAGAAAAAAAGTTTTGTTTATC
R25b             AGTT--GTTAAGAGTCTTCCGTCTCCCTCCCAAACAGAAAGAAAAAAAGTTTTGTTTATC
MCC344          AGTT--GTTAAGAGTCTTCCGTCTCCCTCCCAAACAGAAAGAAAAAAAGTTTTGTTTATC
PeTa            AGTTGAGTTAAGAGTCTTCCGTCTCCCTCCCAAACAGAAAGAAAAAAAGTTTTGTTTATC
MCC339          AGTTGAGTTAAGAGTCTTCCGTCTCCCTCCCAAACAGAAAGAAAAAAAGTTTTGTTTATC
R14a             AGTTGAGTTAAGAGTCTTCCGTCTCCCTCCCAAACAGAAAGAAAAAAAGTTTTGTTTATC
R06b             AGTTGAGTTAAGAGTCTTCCGTCTCCCTCCCAAACAGAAAGAAAAAAAGTTTTGTTTATC
MKT-21          AGTTGAGTTAAGAGTCTTCCGTCTCCCTCCCAAACAGAAAGAAAAAAAGTTTTGTTTATC
MS-1            AGTTGAGTTAAGAGTCTTCCGTCTCCCTCCCAAACAGAAAGAAAAAAAGTTTTGTTTATC
CG4             AGTTGAGTTAAGAGTCTTCCGTCTCCCTCCCAAACAGAAAGAAAAAAAGTTTTGTTTATC
KN4             AGTTGAGTTAAGAGTCTTCCGTCTCCCTCCCAAACAGAAAGAAAAAAAGTTTTGTTTATC
HUN             AATTGAGTTAAGAGTCTTCCGTCTCCCTCCCAAACAGAAAGAAAAAAAGTTTTGTTTATC
                *      ******** ****************************************

AmePI           AGTCAAACTCCGCCTCTCCAGGAAATGAGTCAATGCCAGAAACCCTGCAGCAATAAAAGT
FraMerk20       AGTCAAACTTCGCCC-TTCAGGAAATGAGTCAATGCCAGAAACCCTGCAGCAATAAAAGT
MKT-26          AGTCAAACTCCGCCTCTCCAGGAAATGAGTCAATGCCAGAAACCCTGCAGCAATAAAAGT
MCVw156         AGTCAAACTCCGCCTCTCCAGGAAATGAGTCAATGCCAGAAACCCTGCAGCAATAAAAGT
MKT-22          AGTCAAACTCCGCCTCTCCAGGAAATGAGTCAATGCCAGAAACCCTGCAGCAATAAAAGT
MKT-32          AGTCAAACTCCGCCTCTCCAGGAAATGAGTCAATGCCAGAAA-CCTGCAGCAATAAAAGT
R26b             AGTCAAACTCCGCCTCTCCAGGAAATGAGTCAATGCCAGAAACCCTACAGCAATAAAAGT
R12b             AGTCAAACTCCGCCTCTCCAGGAAATGAGTCAATGCCAGAAACCCTGCAGCAATAAAAGT
MKT-33          AGTCAAACTCCGCCTCTCCAGGAAATGAGTCAATGCCAGAAACCCTGCAGCAATAAAAGT
R15a             AGTCAAACTCCGCCTCTCCAGGAAATGAGTCAATGCCAGAAACCCTGCAGCAATAAAAGT
R13a             AGTCAAACTCCGCCTCTCCAGGAAATGAGTCAATGCCAGAAACCCTGCAGCAATAAAAGT
FraMerk2        AGTCAAACTCCGCCTCTC-AGGAAATGAGTCAATGCCAGAAACCCTGCAGCAATAAAAGT
MCC352          AGTCAAACTCCGCCTCTCCAGGAAATGAGTCAATGCCAGAAACCCTGCAGCAATAAAAGT
R17a             AGTCAAACTCCGCCTCTCCAGGAAATGAGTCAATGCCAGAAACCCTGCAGCAATAAAAGT
R09b             AGTCAAACTCCGCCTCTCCAGGAAATGAGTCAATGCCAGAAACCCTGCAGCAATAAAAGT
FraMerk22       AGTCAAACTCCGCCTCTCCAGGAAATGAGTCAATGCCAGAAACCCTGCAGCAATAAAAGT
BroLi           AGTCAAACTCCGCCTCTCCAGGAAATGAGTCAATGCCAGAAACCCTGCAGCAATAAAAGT
```

```
FraMerk24       AGTCAAACTCCGCCTCTCAAGGAAATGAGTCAATGCCAGAAACCCTGCAGCAATAAAAGT
MCC350          AGTCAAACTCCGCCTCTCCAGGAAATGAGTCAATGCCAGAAACCCTGCAGCAATAAAAGT
MCC85           AGTCAAACTCCGCCTCTCCAGGAAATGAGTCAATGCCAGAAACCCTGCAGCAATAAAAGT
MKL-1           AGTCAAACTCCGCCTCTCCAGGAAATGAGTCAATGCCAGAAACCCTGCAGCAATAAAAGT
BG1             AGTCAAACTCCGCCTCTCCAGGAAATGAGTCAATGCCAGAAACCCTGCAGCAATAAAAGT
MKT-31          AGTCAAACTCCGCCTCTCCAGGAAATGAGTCAATGCCAGAAACCCTGCAGCAATAAAAGT
EurCauC1        AGTCAAACTCCGCCTCTCCAGGAAATGAGTCAATGCCAGAAACCCTGCAGCAATAAAAGT
AlDo            AGTCAAACTCCGCCTCTCCAGGAAATGAGTCAATGCCAGAAACCCTGCAGCAATAAAAGT
R17b            AGTCAAACTCCGCCTCTCCAGGAAATGAGTCAATGCCAGAAACCCTGCAGCAATAAAAGT
R30b            AGTCAAACTCCGCCTCTCCAGGAAATGAGTCAATGCCAGAAACCCTGCAGCAATAAAAGT
R12a            AGTCAAACTCCGCCTCTCCAGGAAATGAGTCAATGCCAGAAACCCTGCAGCAATAAAAGT
LoKe            AGTCAAACTCCGCCTCTCCAGGAAATGAGTCAATGCCAGAAACCCTGCAGCAATAAAAGT
WoWe            AGTCAAACTCCGCCTCTCCAGGAAATGAGTCAATGCCAGAAACCCTGCAGCAATAAAAGT
WaGa            AGTCAAACTCCGCCTCTCCAGGAAATGAGTCAATGCCAGAAACCCTGCAGCAATAAAAGT
PJ2             AGTCAAACTCCGCCTCTCCAGGAAATGAGTCAATGCCAGAAACCCTGCAGCAATAAAAGT
HF              AGTCAAACTCCGCCTCTCCAGGAAATGAGTCAATGCCAGAAACCCTGCAGCAATAAAAGT
MCC349          AGTCAAACTCCGCCTCTCCAGGAAATGAGTCAATGCCAGAAACCCTGCAGCAATAAAAGT
R16b            AGTCAAACTCCGCCTCTCCAGGAAATGAGTCAATGCCAGAAACCCTGCAGCAATAAAAGT
HB039C          AGTCAAACTCCGCCTCTCCAGGAAATGAGTCAATGCCAGAAACCCTGCAGCAATAAAAGT
TKS             AGTCAAACTCCGCCTCTCCAGGAAATGAGTCAATGCCAGAAACCCTGCAGCAATAAAAGT
OcepolW1        AGTCAAACTCCGCCTCTCCAGGAAATGAGTCAATGCCAGAAACCCTGCAGCAATAAAAGT
R10b            AGTCAAACTCCGCCTCTCCAGGAAATGAGTCAATGCCAGAAACCCTGCAGCAATAAAAGT
R25b            AGTCAAACTCCGCCTCTCCAGGAAATGAGTCAATGCCAGAAACCCTGCAGCAATAAAAGT
MCC344          AGTCAAACTCCGCCTCTCCAGGAAATGAGTCAATGCCAGAAACCCTGCAGCAATAAAAGT
PeTa            AGTCAAACTCCGCCTCTCCAGGAAATGAGTCAATGCCAGAAACCCTGCAGCAATAAAAGT
MCC339          AGTCAAACTCCGCCTCTCCAGGAAATGAGTCAATGCCAGAAACCCTGCAGCAATAAAAGT
R14a            AGTCAAACTCCGCCTCTCCAGGAAATGAGTCAATGCCAGAAACCCTGCAGCAATAAAAGT
R06b            AGTCAAACTCCGCCTCTCCAGGAAATGAGTCAATGCCAGAAACCCTGCAGCAATAAAAGT
MKT-21          AGTCAAACTCCGCCTCTCCAGGAAATGAGTCAATGCCAGAAACCCTGCAGCAATAAAAGT
MS-1            AGTCAAACTCCGCCTCTCCAGGAAATGAGTCAATGCCAGAAACCCTGCAGCAATAAAAGT
CG4             AGTCAAACTCCGCCTCTCCAGGAAATGAGTCAATGCCAGAAACCCTGCAGCAATAAAAGT
KN4             AGTCAAACTCCGCCTCTCCAGGAAATGAGTCAATGCCAGAAACCCTGCAGCAATAAAAGT
HUN             AGTCAAACTCCGCCTCTCCAGGAAATGAGTCAATGCCAGAAACCCTGCAGCAATAAAAGT
                ********* ****  *  ********************** *** ************

AmePI           TCAATCATGTAACCACAACTTGGCTGCCTAGGTGACTTTTTT-TTTTCAAGTTGGCAGAG
FraMerk20       TCAATCATGTAACCACAACTTGGCTGCCTAGGTGACTTTTTTTTTTTCAAGTTGGCAGAG
MKT-26          TCAATCATGTAACCACAACTTGGCTGCCTAGGTGACTTTTT--TTTTCAGGTTGGCAGAG
MCVw156         TCAATCATGTAACCACAACTTGGCTGCCTAGGTGACTTTTT--TTTTCAAGTTGGCAGAG
MKT-22          TCAATCATGTAACCACAACTTGGCTGCCTAGGTGACTTTTTT-TTTTCAAGTTGGCAGAG
MKT-32          TCAATCATGTAACCACAACTTGGCTGCCTAGGTGACTTTTTT-TTTTCAAGTTGGCAGAG
R26b            TCAATCATGTAACCACAACTTGGCTGCCTAGGTGACTTTTTT-TTTTCAAGTTGGCAGAG
R12b            TCAATCATGTAACCACAACTTGGCTGCCTAGGTGACTTTTTTTTTTTCAAGTTGGCAGAG
MKT-33          TCAATCATGTAACCACAACTTGGCTGCCTAGGTGACTTTTTTTTTTTCAAGTTGGCAGAG
R15a            TCAATCATGTAACCACAACTTGGCTGCCTAGGTGACTTTTTT-TTTTCAAGTTGGCAGAG
R13a            TCAATCATGTAACCACAACTTGGCTGCCTAGGTGACTTTT---TTTTCAAGTTGGCAGAG
FraMerk2        TCAATCATGTAACCACAACTTGGCTGCCTAGGTGACTTTTTT-TTTTCAAGTTGGCAGAG
MCC352          TCAATCATGTAACCACAACTTGGCTGCCTAGGTGACTTTTTT-TTTTCAAGTTGGCAGAG
R17a            TCAATCATGTAACCACAACTTGGCTGCCTAGGTGACTTTTTT-TTTTCAAGTTGGCAGAG
R09b            TCAATCATGTAACCACAACTTGGCTGCCTAGGTGACTTTTTT-TTTTCAAGTTGGCAGAG
FraMerk22       TCAATCATGTAACCACAACTTGGCTGCCTAGGTGACTTTTTT-TTTTCAAGTTGGCAGAG
BroLi           TCAATCATGTAACCACAACTTGGCTGCCTAGGTGACTTTTTT-TTTTCAAGTTGGCAGAG
FraMerk24       TCAATCATGTAACCACAACTTGGCTGCCTAGGTGACTTTTTT-TTTTCAAGTTGGCAGAG
MCC350          TCAATCATGTAACCACAACTTGGCTGCCTAGGTGACTTTTTT-TTTTCAAGTTGGCAGAG
MCC85           TCAATCATGTAACCACAACTTGGCTGCCTAGGTGACTTTTTT-TTTTCAAGTTGGCAGAG
MKL-1           TCAATCATGTAACCACAACTTGGCTGCCTAGGTGACTTTTTT-TTTTCAAGTTGGCAGAG
BG1             TCAATCATGTAACCACAACTTGGCTGCCTAGGTGACTTTTTT-TTTTCAAGTTGGCAGAG
MKT-31          TCAATCATGTAACCACAACTTGGCTGCCTAGGTGACTTTTTT-TTTTCAAGTTGGCAGAG
EurCauC1        TCAATCATGTAACCACAACTTGGCTGCCTAGGTGACTTTTTT-TTTTCAAGTTGGCAGAG
AlDo            TCAATCATGTAACCACAACTTGGCTGCCTAGGTGACTTTTTT-TTTTCAAGTTGGCAGAG
R17b            TCAATCATGTAACCACAACTTGGCTGCCTAGGTGACTTTTTT-TTTTCAAGTTGGCAGAG
R30b            TCAATCATGTAACCACAACTTGGCTGCCTAGGTGACTTTTTT-TTTTCAAGTTGGCAGAG
R12a            TCAATCATGTAACCACAACTTGGCTGCCTAGGTGACTTTTTT-TTTTCAAGTTGGCAGAG
LoKe            TCAATCATGTAACCACAACTTGGCTGCCTAGGTGACTTTTTT-TTTTCAAGTTGGCAGAG
WoWe            TCAATCATGTAACCACAACTTGGCTGCCTAGGTGACTTTTTT-TTTTCAAGTTGGCAGAG
WaGa            TCAATCATGTAACCACAACTTGGCTGCCTAGGTGACTTTTTT-TTTTCAAGTTGGCAGAG
PJ2             TCAATCATGTAACCACAACTTGGCTGCCTAGGTGACTTTTTT-TTTTCAAGTTGGCAGAG
HF              TCAATCATGTAACCACAACTTGGCTGCCTAGGTGACTTTTTT-TTTTCAAGTTGGCAGAG
```

```
MCC349          TCAATCATGTAACCACAACTTGGCTGCCTAGGTGACTTTTTT-TTTTCAAGTTGGCAGAG
R16b            TCAATCATGTAACCACAACTTGGCAGCCTAGGTGACTTTTTT-TTTTCAAGTTGGCAGAG
HB039C          TCAATCATGTAACCACAACTTGGCAGCCTAGGTGACTTTTTT-TTTTCAAGTTGGCAGAG
TKS             TCAATCATGTAACCACAACTTGGCAGCCTAGGTGACTTTTTT-TTTTCAAGTTGGCAGAG
OcepolW1        TCAATCATGTAACCACAACTTGGCTGCCTAGGTGACTTTTTT-TTTTCAAGTTGGCAGAG
R10b            TCAATCAGGTAACCACAACTTGGCTGCCTAGGTGACTTTTTT-TTTTCAAGTTGGCAGAG
R25b            TCAATCATGTAACCACAACTTGGCTGCCTAGGTGACTTTTTT-TTTTCAAGTTGGCAGAG
MCC344          TCAATCATGTAACCACAACTTGGCTGCCTAGGTGACTTTTTT-TTTTCAAGTTGGCAGAG
PeTa            TCAATCATGTAACCACAACTTGGCTGCCTAGGTGACTTTTTT-TTTTCAAGTTGGCAGAG
MCC339          TCAATCATGTAACCACAACTTGGCTGCCTAGGTGACTTTTTT-TTTTCAAGTTGGCAGAG
R14a            TCAATCATGTAACCACAACTTGGCTGCCTAGGTGACTTTTTT-TTTTCAAGTTGGCAGAG
R06b            TCAATCATGTAACCACAACTTGGCTGCCTAGGTGACTTTTTT-TTTTCAAGTTGGCAGAG
MKT-21          TCAATCATGTAACCACAACTTGGCTGCCTAGGTGACTTTTTT-TTTTCAAGTTGGCAGAG
MS-1            TCAATCATGTAACCACAACTTGGCTGCCTAGGTGACTTTTTT-TTTTCAAGTTGGCAGAG
CG4             TCAATCATGTAACCACAACTTGGCTGCCTAGGTGACTTTTTT-TTTTCAAGTTGGCAGAG
KN4             TCAATCATGTAACCACAACTTGGCTGCCTAGGTGACTTTTTT-TTTTCAAGTTGGCAGAG
HUN             TCAATCATGTAACCACAACTTGGCTGCCTAGGTGACTTTTTT-TTTTCAAGTTGGCAGAG
                ******* ********************** ***************   ****** **********

AmePI           GCTTGGGGCTCCTAGCCTCCGAGGCCTCTGGAAAAAAAAGAGAGAGGCCTCTGAGGCTTA
FraMerk20       GCTTGGGGCTCCTAGCCTCCGAGGCCTCTGGAAAAAAAAGAGAGAGGCCTCTGAGGCTTA
MKT-26          GCTTGGGGCTCCTAGCCTCCGAGGCCTCTGGAAAAAAAAGAGAGAGGCCTCTGAGGCTTA
MCVw156         GCTTGGGGCTCCTAGCCTCCGAGGCCTCTGGAAAAAAAAGAGAGAGGCCTCTGAGGCTTA
MKT-22          GCTTGGGGCTCCTAGCCTCCGAGGCCTCTGGAAAAAAAAGAGAGAGGCCTCTGAGGCTTA
MKT-32          GCTTGGGGCTCCTAGCCTCCGAGGCCTCTGGAAAAAAAAGAGAGAGGCCTCTGGGGCTTA
R26b             GCTTGGGGCTCCTAGCCTCCGAGGCCTCTGGAAAAAAAAGAGAGAGGCCTCTGAGGCTTA
R12b             GCTTGGGGCTCCTAGCCTCCGAGGCCTCTGGAAAAAAAAGAGAGAGGCCTCTGAGGCTTA
MKT-33          GCTTGGGGCTCCTAGCCTCCGAGGCCTCTGGAAAAAAAAGAGAGAGGCCTCTGAGGCTTA
R15a             GCTTGGGGCTCCTAGCCTCCGAGGCCTCTGGAAAAAAAAGAGAGAGGCCTCTGAGGCTTA
R13a             GCTTGGGGCTCCTAGCCTCCGAGGCCTCTGGAAAAAAAAGAGAGAGGCCTCTGAGGCTTA
FraMerk2        GCTTGGGGCTCCTAGCCTCCGAGGCCTCTGGAAAAAAAAGAGAGAGGCCTCTGAGGCTTA
MCC352          GCTTGGGGCTCCTAGCCTCCGAGGCCTCTGGAAAAAAAAGAGAGAGGCCTCTGAGGCTTA
R17a             GCTTGGGGCTCCTAGCCTCCGAGGCCTCTGGAAA-AAAAGAGAGAGGCCTCTGAGGCTTA
R09b             GCTTGGGGCTCCTAGCCTCCGAGGCCTCTGGAAA-AAAAGAGAGAGGCCTCTGAGGCTTA
FraMerk22       GCTTGGGGCTCTTAGCCTCCGAGACCTCTAGAAAAAAAAGAGAGAGGCCTCTGAGGATTA
BroLi           GCTTGGGGCTCCTAGCCTCCGAGGCCTCTGGAAAAACAAGAGAGAGGCCTCTGAGGCTTA
FraMerk24       GCTTGGGGCTCCTAGCCTCCGAGGCCTCTGGAAAAAAAAGAGAGAGGCCTCTGAGGCTTA
MCC350          GCTTGGGGCTCCTAGCCTCCGAGGCCTCTGGAAAAAAAAGAGAGAGGACTCTGAGGCTTA
MCC85           GCTTGGGGCTCCTAGCCTCCGAGGCCTCTGGAAAAAAAAGAGAGAGGCCTCTGAGGCTTA
MKL-1           GCTTGGGGCTCCTAGCCTCCGAGGCCTCTGGAAAAAAAAGAGAGAGGCCTCTGAGGCTTA
BG1             GCTTGGGGCTCCTAGCCTCCGAGGCCTCTGGAAAAAAAAGAGAGAGGCCTCTGAGGCTTA
MKT-31          GCTTGGGGCTCCTAGCCTCCGGGGCCTCTGGAAAAAAAAGAGAGAGGCCTCTGAGGCTTA
EurCauC1        GCTTGGGGCTCCTAGCCTCCGAGGCCTCTGGAAAAAAAAGAGAGAGGCCTCTGAGGCTTA
AlDo            GCTTGGGGCTCCTAGCCTCCGAGGCCTCTGGAAAAAAAAGAGAGAGGCCTCTGAGGCTTA
R17b             GCTTGGGGCTCCTAGCCTCCGAGGCCTCTGGAAAAAAAAGAGAGAGGCCTCTGAGGCTTA
R30b             GCTTGGGGCTCCTAGCCTCCGAGGCCTCTGGAAAAAAAAGAGAGAGGCCTCTGAGGCTTA
R12a             GCTTGGGGCTCCTAGCCTCCGAGGCCTCTGGAAAAAAAAGAGAGAGGCCTCTGAGGCTTA
LoKe             GCTTGGGGCTCCTAGCCTCCGAGGCCTCTGGAAAAAAAAGAGAGAGGCCTCTGAGGCTTA
WoWe             GCTTGGGGCTCCTAGCCTCCGAGGCCTCTGGAAAAAAAAGAGAGAGGCCTCTGAGGCTTA
WaGa             GCTTGGGGCTCCTAGCCTCCGAGGCCTCTGGAAAAAAAAGAGAGAGGCCTCTGAGGCTTA
PJ2             GCTTGGGGCTCCTAGCCTCCGAGGCCTCTGGAAAAAAAAGAGAGAGGCCTCTGAGGCTTA
HF              GCTTGGGGCTCCTAGCCTCCGAGGCCTCTGGAAAAAAAAGAGAGAGGCCTCTGAGGCTTA
MCC349          GCTTGGGGCTCCTAGCCTCCGAGGCCTCTGGAAAAAAAAGAGAGAGGCCTCTGAGGCTTA
R16b             GCTTGGGGCTCCTAGCCTCCGAGGCCTCTGGAAAAAAAAGAGAGAGGCCTCTGAGGCTTA
HB039C          GCTTGGGGCTCCTAGCCTCCGAGGCCTCTGGAAAAAAAAGAGAGAGGCCTCTGAGGCTTA
TKS             GCTTGGGGCTCCTAGCCTCCGAGGCCTCTGGAAAAAAAAGAGAGAGGCCTCTGAGGCTTA
OcepolW1        GCTTGGGGCTCCTAGCCTCCGAGGCCTCTGGAAAAAAAAGAGAGAGGCCTCTGAGGCTTA
R10b             GCTTGGGGCTCCTAGCCTCCGAGGCCTCTGGAAAAAAAAGAGAGAGGCCTCTGAGGCTTA
R25b             GCTTGGGGCTCCTAGCCTCCGAGGCCTCTGGAAAAAAAAGAGAGAGGCCTCTGAGGCTTA
MCC344          GCTTGGGGCTCCTAGCCTCCGAGGCCTCTGGAAAAAAAAGAGAGAGGCCTCTGAGGCTTA
PeTa            GCTTGGGGCTCCTAGCCTCCGAGGCCTCTGGAAAAAAAAGAGAGAGGCCTCTGAGGCTTA
MCC339          GCTTGGGGCTCCTAGCCTCCGAGGCCTCTGGAAAAAAAAGAGAGAGGCCTCTGAGGCTTA
R14a             GCTTGGGGCTCCTAGCCTCCGAGGCCTCTGGAAAAAAAAGAGAGAGGCCTCTGAGGCTTA
R06b             GCTTGGGGCTCCTAGCCTCCGAGGCCTCTGGAAAAAAAAGAGAGAGGCCTCTGAGGCTTA
MKT-21          GCTTGGGGCTCCTAGCCTCCGAGGCCTCTGGAAAAAAAAGAGAGAGGCCTCTGAGGCTTA
MS-1            GCTTGGGGCTCCTAGCCTCCGAGGCCTCTGGAAAAAAAAGAGAGAGGCCTCTGAGGCTTA
CG4             GCTTGGGGCTCCTAGCCTCCGAGGCCTCTGGAAAAAAAAGAGAGAGGCCTCTGAGGCTTA
KN4             GCTTGGGGCTCCTAGCCTCCGAGGCCTCTGGAAAAAAAAGAGAGAGGCCTCTGAGGCTTA
```

```
HUN             GCTTGGGGCTCCTAGCCTCCGAGGCCTCTGGAAAAAAAAGAGAGAGGCCTCTGAGGCTTA
                ********** ********* * ***** **** * ********** ***** ** ***

AmePI           AGAGGCTTAATTAGCAAAAAAGGCAGTATCTAAGGGCAGATCCCAAGGGCGGGAAACTGC
FraMerk20       AGAGGCTTAATTAGCAAAAAAGGCAGTATCTAAGGGCAGATCCCAAGGGCGGGAAACTGC
MKT-26          AGAGGCTTAATTAGCAAAAAAGGCAGTATCTAAGGGCAGATCCCAAGGGCGGGGAACTGC
MCVw156         AGAGGCTTAATTAGCAAAAAAGGCAGTATCTAAGGGCAGATCCCAAGGGCGGGAAACTGC
MKT-22          AGAGGCTTAATTAGCAAAAAAGGCAGTATCTAAGGGCAGATCCCAGGGGCGGGAAACTGC
MKT-32          AGAGGCTTAATTAGCAAAAAAGGCAGTATCTAAGGGCAGATCCCAAGGGCGGGAAACTGC
R26b             AGAGGCTTAATTAGCAAAAAAGGCAGTATCTAAGGGCAGATCCCAAGGGCGGGAAACTGC
R12b             AGAGGCTTAATTAGCAAAAAAGGCAGTATCTAAGGGCAGATCCCAAGGGCGGGAAACTGC
MKT-33          AGAGGCTTAATTAGCAGAAAAGGCAGTATCTAAGGGCAGATCCCAAGGGCGGGAAACTGC
R15a             AGAGGCTTAATTAGCAAAAAAGGCAG--------TGCAGATCCCAAGGGCGGGAAACTGC
R13a             AGAGGCTTAATTAGCAAAAAAGGCAGTATCTAAGGGCAGATCCCAAGGGCGGGAAACTGC
FraMerk2        AGAGGCTTAATTAGCAAAAAAGGCAGTATCTAAGGGCAGATCCCAAGGGCGGGAAACTGC
MCC352          AGAG-CTTAATTAGCAAAAAAGGCAGTATCTAAGGGCAGATCCCAAGGGCGGGAAACTGC
R17a             AGAGGCTTAATTAGCAAAAAAGGCAGTATCTAAGGGCAGATCCCAAGGGCGGGAAACTGC
R09b             AGAGGCTTAATTAGCAAAAAAGGCAGTATCTAAGGGCAGATCCCAAGGGCGGGAAACTGC
FraMerk22       AGAGGCTTAATTAGCAAAAAAGGCAGTATCTAAGGGCAGATCCCAAGGGCGGGAAACTGC
BroLi           AGAGGCTTAATTAGCAAAAAAGGCAGTATCTAAGGGCAAATCCCAAGGGCGGGAAACTGC
FraMerk24       AGAGGCTTAATTAGCAAAAAAGGCAGTATCTAAGGGCAGATCCTAAGGGCGGGAAACTGC
MCC350          AGAGGCTTAATTAGCAAAAAAGGCAGTATCTAAGGGCAGATCCCAAGGGCGGGAAACTGC
MCC85           AGAGGCTTAATTAGCAAAAAAGGCAGTATCTAAGGGCAGATCCCAAGGGCGGGAAACTGC
MKL-1           AGAGGCTTAATTAGCAAAAAAGGCAGTATCTAAGGGCAGATCCCAAGGGCGGGAAACTGC
BG1             AGAGGCTTAATTAGCAAAAAAGGCAGTATCTAAGGGCAGATCCCAAGGGCGGGAAACTGC
MKT-31          AGAGGCTTAATTAGCAAAAAAGGCAGTATCTAAGGGCAGATCCCAAGGGCGGGAAACTGC
EurCauC1        AGAGGCTTAATTAGCAAAAAAGGCAGTATCTAAGGGCAGATCCCAAGGGCGGGAAACTGC
AlDo            AGAGGCTTAATTAGCAAAAAAGGCAGTATCTAAGGGCAGATCCCAAGGGCGGGAAACTGC
R17b             AGAGGCTTAATTAGCAAAAAAGGCAGTATCTAAGGGCAGATCCCAAGGGCGGGAAACTGC
R30b             AGAGGCTTAATTAGCAAAAAAGGCAGTATCTAAGGGCAGATCCCAAGGGCGGGAAACTGC
R12a             AGAGGCTTAATTAGCAAAAAAGGCAGTATCTAAGGGCAGATCCCAAGGGCGGGAAACTGC
LoKe            AGAGGCTTAATTAGCAAAAAAGGCAGTATCTAAGGGCAGATCCCAAGGGCGGGAAACTGC
WoWe            AGAGGCTTAATTAGCAAAAAAGGCAGTATCTAAGGGCAGATCCCAAGGGCGGGAAACTGC
WaGa            AGAGGCTTAATTAGCAAAAAAGGCAGTATCTAAGGGCAGATCCCAAGGGCGGGAAACTGC
PJ2             AGAGGCTTAATTAGCAAAAAAGGCAGTATCTAAGGGCAGATCCCAAGGGCGGGAAACTGC
HF              AGAGGCTTAATTAGCAAAAAAGGCAGTATCTAAGGGCAGATCCCAAGGGCGGGAAACTGC
MCC349          AGAGGCTTAATTAGCAAAAAAGGCAGTATCTAAGGGCAGATCCCAAGGGCGGGAAACTGC
R16b             AGAGGCTTAATTAGCAAAAAAGGCAGTATCTAAGGGCAGATCCCAAGGGCGGGAAACTGC
HB039C          AGAGGCTTAATTAGCAAAAAAGGCAGTATCTAAGGGCAGATCCCAAGGGCGGGAAACTGC
TKS             AGAGGCTTAATTAGCAAAAAAGGCAGTATCTAAGGGCAGATCCCAAGGGCGGGAAACTGC
OcepolW1        AGAGGCTTAATTAGCAAAAAAGGCAGTATCTCAGGGCAGATCCCAAGGGCGGGAAACTGC
R10b             AGAGGCTTAATTAGCAAAAAAGGCAGTATCTAAGGGCAGATCCCAAGGGCGGGAAACTGC
R25b             AGAGGCTTAATTAGCAAAAAAGGCAGTATCTAAGGGCAGATCCCAAGGGCGGGAAACTGC
MCC344          AGAGGCTTAATTAGCAAAAAAGGCAGTATCTAAGGGCAGATCCCAAGGGCGGGAAACTGC
PeTa            AGAGGCTTAATTAGCAAAAAAGGCAGTATCTAAGGGCAGATCCCAAGGGCGGGAAACTGC
MCC339          AGAGGCTTAATTAGCAAAAAAGGCAGTATCTAAGGGCAGATCCCAAGGGCGGGAAACTGC
R14a             AGAGGCTTAATTAGCAAAAAAGGCAGTATCTAAGGGCAGATCCCAAGGGCGGGAAACTGC
R06b             AGAGGCTTAATTAGCAAAAAAGGCAGTATCTAAGGGCAGATCCCAAGGGCGGGAAACTGC
MKT-21          AGAGGCTTAATTAGCAAAAAAGGCAGTATCTAAGGGCAGATCCCAAGGGCGGGAAACTGC
MS-1            AGAGGCTTAATTAGCAAAAAAGGCAGTATCTAAGGGCAGATCCCAAGGGCGGGAAACTGC
CG4             AGAGGCTTAATTAGCAAAAAAGGCAGTATCTAAGGGCAGATCCCAAGGGCGGGAAACTGC
KN4             AGAGGCTTAATTAGCAAAAAAGGCAGTATCTAAGGGCAGATCCCAAGGGCGGGAAACTGC
HUN             AGAGGCTTAATTAGCAAAAAAGGCAGTATCTAAGGGCTGATCCCAAGGGCGGGAAACTGC
                **** ********** *********         **  **** * ******* ******

AmePI           AGTATAAAAACCACTCCTTAGTGAGGTAGCTCATTTGCTCCTCTGCTCTTTCTGCAAACT
FraMerk20       AGTATAAAAACCACTCCTTAGTGAGGTAGCTCATTTGCTCCTCTGCTCTTTCTGCAAACT
MKT-26          AGTATAAAAACCACTCCTTAGTGAGGTAGCTCATTTGCTCCTCTGCTCTTTCTGCAAACT
MCVw156         AGTATAAAAACCACTCCTTAGTGAGGTAGCTCATTTGCTCCTCTGCTGTTTCTGCAAACT
MKT-22          AGTATAAAAACCACTCCTTAGTGAGGTAGCTCATTTGCTCCTCTGCTCTTTCTGCAAACT
MKT-32          AGTATAAAAACCACTCCTTAGTGAGGTAGCTCATTTGCTCCTCTGCTCTTTCTGCAAACT
R26b             AGTATAAAAACCACTCCTTAGTGAGGTAGCTCATTTGCTCCTCTGCTCTTTCTGCAAACT
R12b             AGTATAAAAACCACTCCTTAGTGAGGTAGCTCATTTGCTCCTCTGCTCTTTCTGCAAACT
MKT-33          AGTATAAAAACCACTCCTTAGTGAGGTAGCTCATTTGCTCCTCTGCTCTTTCTGCAAACT
R15a             AGTATAAAAACCACTCCTTAGTGAGGTAGCTCATTTGCTCCTCTGCTCTTTCTGCAAACT
R13a             AGTATAAAAACCACTCCTTAGTGAGGTAGCTCATTTGCTCCTCTGCTCTTTCTGCAAACT
FraMerk2        AGTATAAAAACCACTCCTTAGTGAGGTAGCTCATTTGCTCCTCTGCTCTTTCTGCAAACT
MCC352          AGTATAAAAACCACTCCTTAGTGAGGTAGCTCATTTGCTCCTCTGCTCTTTCTGCAAACT
```

```
R17a            AGTATAAAAACCACTCCTTAGTGAGGTAGCTCATTTGCTCCTCTGCTCTTTCTGCAAACT
R09b            AGTATAAAAACCACTCCTTAGTGAGGTAGCTCATTTGCTCCTCTGCTCTTTCTGCAAACT
FraMerk22       AGTATAAAAACCACTCCTTAGTGAGGTAGCTCATTTGCTCCTCTGCTCTTTCTGCAAACT
BroLi           ATTATAAAAACCACTCCTTAGGGAGGTAGCTCATTTGCTCCTCTGCTCTTTCTGCAAACT
FraMerk24       AGTATAAAAACCACTCCTTAGTGAGGTAGCTCATTTGCTCCTCTGCTCTTTCTGCAAACT
MCC350          AGTATAAAAACCACTCCTTAGTGAGGTAGCTCATTTGCTCCTCTGCTGTTTCTGCAAACT
MCC85           AGTATAAAAACCACTCCTTAGTGAGGTAGCTCATTTGCTCCTCTGCTCTTTCTGCAAACT
MKL-1           AGTATAAAAACCACTCCTTAGTGAGGTGGCTCATTTGCTCCTCTGCTCTTTCTGCAAACT
BG1             AGTATAAAAACCACTCCTTAGTGAGGTAGCTCATTTGCTCCTCTGCTCTTTCTGCAAACT
MKT-31          AGTATAAAAACCACTCCTTAGTGAGGTAGCTCATTTGCTCCTCTGCTCTTTCTGCAAACT
EurCauC1        AGTATAAAAACCACTCCTTAGTGAGGTAGCTCATTTGCTCCTCTGCTCTTTCTGCAAACT
AlDo            AGTATAAAAACCACTCCTTAGTGAGGTAGCTCATTTGCTCCTCTGCTCTTTCTGCAAACT
R17b            AGTATAAAAACCACTCCTTAGTGAGGTAGCTCATTTGCTCCTCTGCTCTTTCTGCAAACT
R30b            AGTATAAAAACCACTCCTTAGTGAGGTAGCTCATTTGCTCCTCTGCTCTTTCTGCAAACT
R12a            AGTATAAAAACCACTCCTTAGTGAGGTAGCTCATTTGCTCCTCTGCTCTTTCTGCAAACT
LoKe            AGTATAAAAACCACTCCTTAGTGAGGTAGCTCATTTGCTCCTCTGCTCTTTCTGCAAACT
WoWe            AGTATAAAAACCACTCCTTAGTGAGGTAGCTCATTTGCTCCTCTGCTCTTTCTGCAAACT
WaGa            AGTATAAAAACCACTCCTTAGTGAGGTAGCTCATTTGCTCCTCTGCTCTTTCTGCAAACT
PJ2             AGTATAAAAACCACTCCTTAGTGAGGTAGCTCATTTGCTCCTCTGCTCTTTCTGCAAACT
HF              AGTATAAAAACCACTCCTTAGTGAGGTAGCTCATTTGCTCCTCTGCTCTTTCTGCAAACT
MCC349          AGTATAAAAACCACTCCTTAGTGAGGTAGCTCATTTGCTCCTCTGCTCTTTCTGCAAACT
R16b            AGTATAAAAACCACTCCTTAGTGAGGTAGCTCATTTGCTCCTCTGCTCTTTCTGCAAACT
HB039C          AGTATAAAAACCACTCCTTAGTGAGGTAGCTCATTTGCTCCTCTGCTCTTTCTGCAAACT
TKS             AGTATAAAAACCACTCCTTAGTGAGGTAGCTCATTTGCTCCTCTGCTCTTTCTGCAAACT
OcepolW1        AGTATAAAAACCACTCCTTAGTGAGGTAGCTCATTTGCTTCTCTGCTCTTTCTTCAAACT
R10b            AGTATAAAAACCACTCCTTAGTGAGGTAACTCATTTGCTCCTCTGCTCTTTCTGCAAACT
R25b            AGTATAAAAACCACTCCTTAGTGAGGTAGCTCATTTGCTCCTCTGCTCTTTCTGCAAACT
MCC344          AGTATAAAAACCACTCCTTAGTGAGGTAGCTCATTTGCTCCTCTGCTCTTTCTGCAAACT
PeTa            AGTATAAAAACCACTCCTTAGTGAGGTAGCTCATTTGCTCCTCTGCTCTTTCTGCAAACT
MCC339          AGTATAAAAACCACTCCTTAGTGAGGTAGCTCATTTGCTCCTCTGCTCTTTCTGCAAACT
R14a            AGTATAAAAACCACTCCTTAGTGAGGTAGCTCATTTGCTCCTCTGCTCTTTCTGCAAACT
R06b            AGTATAAAAACCACTCCTTAGTGAGGTAGCTCATTTGCTCCTCTGCTCTTTCTGCAAACT
MKT-21          AGTATAAAAACCACTCCTTAGTGAGGTAGCTCATTTGCTCCTCTGCTCTTTCTGCAAACT
MS-1            AGTATAAAAACCACTCCTTAGTGAGGTAGCTCATTTGCTCCTCTGCTCTTTCTGCAAACT
CG4             AGTATAAAAACCACTCCTTAGTGAGGTAGCTCATTTGCTCCTCTGCTCTTTCTGCAAACT
KN4             AGTATAAAAACCACTCCTTAGTGAGGTAGCTCATTTGCTCCTCTGCTCTTTCTGCAAACT
HUN             AGTATAAAAACCACTCCTTAGTGAGGTAGCTCATTTGCTCCTCTGCTCTTTCTGCAAACT
                * ******************** *****  ********** ******* ***** ******

AmePI           CCTTCTGCATATAGACAAG
FraMerk20       CCTTCTGCATATAGACAAG
MKT-26          CCTTCTGCATATAGACAAG
MCVw156         CCTTCTGCATATAGACAAG
MKT-22          CCTTCTGCATATAGACAAG
MKT-32          CCTTCTGCATATAGACAAG
R26b            CCTTCTGCATATAGACAAG
R12b            CCTTCTGCATATAGACAAG
MKT-33          CCTTCTGCATATAGACAAG
R15a            CCTTCTGCATATAGACAAG
R13a            CCTTCTGCATATAGACAAG
FraMerk2        CCTTCTGCATATAGACAAG
MCC352          CCTTCTGCATATAGACAAG
R17a            CCTTCTGCATATAGACAAG
R09b            CCTTCTGCATATAGACAAG
FraMerk22       CCTTCTGCATATAGACAAG
BroLi           CCTTCTGCATATAGACAAG
FraMerk24       CCTTCTGCATATAGACAAG
MCC350          CCTTCTGCATATAGACAAG
MCC85           CCTTCTGCATATAGACAAG
MKL-1           CCTTCTGCATATAGACAAG
BG1             CCTTCTGCATATACACAAG
MKT-31          CCTTCTGCATATAGACAAG
EurCauC1        CCTTCTGCATATAGACAAG
AlDo            CCTTCTGCATATAGACAAG
R17b            CCTTCTGCATATAGACAAG
R30b            CCTTCTGCATATAGACAAG
R12a            CCTTCTGCATATAGACAAG
LoKe            CCTTCTGCATATAGACAAG
```

```
WoWe            CCTTCTGCATATAGACAAG
WaGa            CCTTCTGCATATAGACAAG
PJ2             CCTTCTGCATATAGACAAG
HF              CCTTCTGCATATAGACAAG
MCC349          CCTTCTGCATATAGACAAG
R16b            CCTTCTGCATATAGACAAG
HB039C          CCTTCTGCATATAGACAAG
TKS             CCTTCTGCATATAGACAAG
OcepolW1        CCTTCTGCATATAGCCAAG
R10b            CCTTCTGCATATAGACAAG
R25b            CCTTCTACATATAGACAAG
MCC344          CCTTCTGCATATAGACAAG
PeTa            CCTTCTGCATATAGACAAG
MCC339          CCTTCTGCATATAGACAAG
R14a            CCTTCTGCATATAGACAAG
R06b            CCTTCTGCATATAGACAAG
MKT-21          CCTTCTGCATATAGACAAG
MS-1            CCTTCTGCATATAGACAAG
CG4             CCTTCTGCATATAGACAAG
KN4             CCTTCTGCATATAGACAAG
HUN             CCTTCTGCATATAGACAAG
                ****** ******  ****
```

Supplementary Table 1: NCCR sizes and sources of various MCPyV strains

strain	Size NCCR (bp)	source
MCC350	464	MCC
EurCauC1	464	Skin
AlDo	464	MCC
17b	464	skin
30b	464	skin
12a	464	skin
12b	465	skin
MKT-31	464	MCC
17a	463	skin
09b	463	skin
MKT-33	465	MCC
26b	463	skin
13a	462	skin
MKT-32	463	MCC
AmePI	464	skin
MKT-22	463	MCC
25b	467	skin
BroLi	464	MCC
PeTa	469	MCC
MCC339	469	MCC
14a	469	skin
6b	469	skin
MKT-26	463	MCC
MKT-21	469	MCC
15a	456	skin
10b	462	skin
16b	496	skin
Ocepol W1	459	skin
FraMerk 22	464	MCC
Loke	464	MCC
WoWe	464	MCC
WaGa	464	MCC
915F 06 004 BG1	464	skin

915F 06 001 PJ2	464	skin
HF	464	consensus genome based on 7 full-length genomes isolated from MCC
MCV352	463	MCC
MCV349	464	MCC
MKL-1	464	MCC
FraMerk 24	464	MCC
MCC85	464	MCC
FraMerk 2	463	MCC
MCVw156	463	MCC
MCC344	467	MCC
FraMerk 20	464	MCC
7673/2011/HUN	469	metastatic cervical lymph node
MS-1	469	MCC
915F 06 008 CG4	469	skin
915F 06 002 KN4	469	skin
HB039C	498	feces
TKS	498	Kaposi’s sarcoma